2017

# Biophysical And Biomolecular Components Of Dendritic Cell Chemokinesis

Amy Chevalier Bendell
*University of Pennsylvania*, amychev22@gmail.com

# Biophysical And Biomolecular Components Of Dendritic Cell Chemokinesis

**Abstract**
Dendritic cells (DCs) are important regulators of the adaptive immune response. Integral to their antigen-presenting capability is their ability to travel from sites of antigen capture in peripheral tissues to the T cell rich zones of the lymph node. Along the way, they encounter many different environments and are presented with a variety of chemical and biophysical cues. However, the response of DC migration to these extracellular cues is not fully characterized. My first goal was to establish an in vitro culture system for studying DC chemokinesis. I chose to use PDMS surfaces due to their biocompatibility and easy functionalization. I determined that DC chemokinesis is a diffusive process modeled well by a persistent random walk. In addition, I used micropost array detectors (mPADs) to quantify the forces of chemokinesis. Next, I sought to identify biophysical and biomolecular characteristics that contribute to DC chemokinesis. Despite the diversity of microenvironments that DCs encounter, there is a paucity of information about how DCs respond to the physical characteristics of their surroundings. I addressed this question by examining differences in DC migration on surfaces with different stiffness, 2D geometry and ligand patterning. I show that DCs are insensitive to differences in substrate stiffness but are sensitive to the spatial organization of ligand. In addition, I investigated signaling pathways involved in environmental sensing. To my knowledge, this is the first investigation of DC response to substrate stiffness and geometry. Finally, I quantified random motility and force generation in HS1 -/- and WASP -/- DCs. I determined that both proteins are required for random migration, through their regulation of cellular speed. In addition, I determined that both proteins are involved in force generation. This study provides the first description of the influence of HS1 on DC random migration as well as the first measurements for traction forces from HS1 and WASP deficient DCs. In this thesis, I build upon the current knowledge of DC chemokinesis by identifying critical biophysical and biomolecular components.

**Degree Type**
Dissertation

**Degree Name**
Doctor of Philosophy (PhD)

**Graduate Group**
Chemical and Biomolecular Engineering

**First Advisor**
Daniel A. Hammer

**Subject Categories**
Chemical Engineering

# BIOPHYSICAL AND BIOMOLECULAR COMPONENTS OF DENDRITIC CELL CHEMOKINESIS

Amy C. Bendell

A DISSERTATION

in

Chemical and Biomolecular Engineering

Presented to the Faculties of the University of Pennsylvania in Partial Fulfillment of the Requirements for the Degree of Doctor of Philosophy

2017

Professor Daniel A. Hammer
Supervisor of Dissertation

Professor John C. Crocker
Graduate Group Chairperson

Dissertation Committee:
Dr. Janis K. Burkhardt, Dept. of Pathology and Laboratory Medicine, CHOP
Professor John C. Crocker, CBE
Professor Kathleen J. Stebe, CBE

BIOPHYSICAL AND BIOMOLECULAR COMPONENTS OF DENDRITIC CHEMOKINESIS

# ACKNOWLEDGEMENTS

I would first like to thank my advisor, Daniel A. Hammer, who has given me the opportunity to grow as a scientist. I am a very different person from the first-year graduate student that joined the lab in 2011. Thank you for providing guidance and encouragement and for giving me the independence to explore interesting problems. I would also like to thank the members of my thesis committee: Dr. John Crocker, Dr. Kathleen Stebe and Dr. Janis Burkhardt for dedicating your time and for providing useful insight and advice. To my collaborators in the Burkhardt laboratory—Janis K. Burkhart, Edward K. Williamson, Nathan Roy, Daniel Blumenthal—thank you for all of your help planning and executing experiments, for all the mice and reagents you have provided over the years and for your invaluable insight. I would also like to thank past and present lab members for making the lab such a welcome environment and for providing a useful sounding board for planning new experiments and troubleshooting problems. In addition, thank you to all of the mice who dedicated their lives to science and made my PhD work possible.

I would like to send a huge thank you to my parents for their unwavering love and support over the past 28 years. I was very fortunate to have parents who invested so much time in fostering my education—from reading to me every night as a child, to helping me with homework, taking me to music lessons and encouraging me to pursue my dreams. To my dad, you always believed in me, and I wish more than anything you were here today to see me. To my mom, I know you were very upset when I got a "needs improvement" in skipping on my kindergarten report card. I hope that this thesis more

than makes up for that. I would not be the person I am today without both of you and all the opportunities you gave me.

I would also like to thank my sister, Katie who has been my best friend for 26 years. Thank you for always being there to share my triumphs and pick me up when I am down. You have grown up so much in the past six years, and your determination and hard work have been an inspiration to me. I am also grateful for all my other family members, both here and across the pond, who have shown me unconditional love and support over the years. I feel truly blessed to be surrounded by so many wonderful people.

To my husband, David, who has been by my side through most of my PhD. You supported me during many personal hardships over the past five years, and without you I do not know how I would have made it through this period in my life. You have taught me how to be strong and how to persevere in the face of adversity. Thank you for letting me talk to you about my research and for letting me bounce ideas off you. And most of all, thank you for being my biggest supporter and for believing in me, even when I did not believe in myself.

I would also like to thank my friends—Nicole, Julie and Susan—for all the smiles, laughter and memories over the past six years. My time together has made me enjoy life while working on my PhD. Thank you all for your love and support. To Nicole in particular, thank you for always being there for me. You have been an important part of my life for two decades and have always been one of my biggest cheerleaders, from suffering through classical musical concerts when we were younger, to proofreading papers as I wrapped up my PhD. Your support means the world to me.

# ABSTRACT

BIOPHYSICAL AND BIOMOLECULAR COMPONENTS OF DENDRITIC CELL CHEMOKINESIS ON PDMS SURFACES

Amy C. Bendell

Daniel A. Hammer

Dendritic cells (DCs) are important regulators of the adaptive immune response. Integral to their antigen-presenting capability is their ability to travel from sites of antigen capture in peripheral tissues to the T cell rich zones of the lymph node. Along the way, they encounter many different environments and are presented with a variety of chemical and biophysical cues. However, the response of DC migration to these extracellular cues is not fully characterized. My first goal was to establish an in vitro culture system for studying DC chemokinesis. I chose to use PDMS surfaces due to their biocompatibility and easy functionalization. I determined that DC chemokinesis is a diffusive process modeled well by a persistent random walk. In addition, I used micropost array detectors (mPADs) to quantify the forces of chemokinesis. Next, I sought to identify biophysical and biomolecular characteristics that contribute to DC chemokinesis. Despite the diversity of microenvironments that DCs encounter, there is a paucity of information about how DCs respond to the physical characteristics of their surroundings. I addressed this question by examining differences in DC migration on surfaces with different stiffness, 2D geometry and ligand patterning. I show that DCs are insensitive to differences in substrate stiffness but are sensitive to the spatial organization of ligand. In

addition, I investigated signaling pathways involved in environmental sensing. To my knowledge, this is the first investigation of DC response to substrate stiffness and geometry. Finally, I quantified random motility and force generation in HS1 $^{-/-}$ and WASP $^{-/-}$ DCs. I determined that both proteins are required for random migration, through their regulation of cellular speed. In addition, I determined that both proteins are involved in force generation. This study provides the first description of the influence of HS1 on DC random migration as well as the first measurements for traction forces from HS1 and WASP deficient DCs. In this thesis, I build upon the current knowledge of DC chemokinesis by identifying critical biophysical and biomolecular components.

# TABLE OF CONTENTS

# LIST OF FIGURES

# LIST OF TABLES

# CHAPTER 1 : INTRODUCTION

## MOTIVATION

The immune system is responsible for protecting the body from a variety of infections and diseases. An important constituent of the immune response is the dendritic cell (DC). DCs are the most potent antigen presenting cell (APC) in the body, and have the unique role of linking the innate and adaptive immune responses (1). As immature cells, they circulate in peripheral tissues searching for signs of infection (2). Upon encountering a danger signal, DCs capture and process antigen and present peptide fragments on surface-bound major histocompatibility complexes (3). Antigen capture coincides with maturation, a series of phenotypical and functional changes, including down-regulation of endocytosis, increased migration and increased expression of CCR7 and various costimulatory molecules (4). Mature DCs are fully primed to transmit their antigenic signal to T cells and launch an adaptive immune response (4). Essential to their role as APCs is their ability to migrate from sites of antigen capture in peripheral tissues to site of antigen presentation in lymph nodes. As such, understanding all the nuances of DC migration is extremely important.

While DC chemotaxis and haptotaxis have been studied extensively (some examples include (5–7)), DC chemokinesis has been an infrequent focus. The canonical picture of DC migration is that these cells travel up a chemokine gradient towards the lymph node (2). While this is indeed an important process, DCs also spend time migrating randomly during various stages of their life cycle, such as before entry into lymphatic vessels and once they reach the saturated environment of the lymph node (7,8). The goal of this thesis is to gain a better understanding of DC random migration through identification of important biophysical and biomolecular parameters

## THESIS ORGANIZATION

This thesis contains six chapters. Chapters 1 and 6 provide an introduction and conclusion, respectively. Chapter 2 provides detailed background information on dendritic cells, their role in the immune response and approaches for studying them in vitro. Chapter 3 lays the groundwork for the characterization of DC chemokinesis and introduces my analysis methods. In this chapter, I quantify a variety of motility metrics and traction forces, and highlight the usefulness of PDMS. In the next two chapters, I explore a variety of biophysical and biomolecular factors that play a role in DC migration. I first focus on the biophysical aspects of migration and examine the influence of substrate stiffness and geometry in chapter 4. I then move on to an analysis of two different cytoskeletal proteins in chapter 5, and how they affect motility and force production. Collectively, this thesis contributes to the field of DC research by providing a better understanding of how this unique cell navigates a diverse array of environments and modulates subcellular signaling along the way.

### *Specific Aim 1*

In this aim I quantify DC chemokinesis on PDMS-coated coverslips. I hypothesize that DCs will migrate well on these surfaces and that I will find an optimal fibronectin and chemokine combination for random motility. I quantify DC migration using a persistent random walk model and measure traction forces using micropost array detectors (mPADs).

*Specific Aim 2*

In this aim, I seek to determine the influence of biophysical parameters on DC migration. I hypothesize that DC migration will be affected by the physical characteristics of their microenvironment, such as stiffness and geometry. I perform further studies to identify the subcellular signaling pathways responsible for interacting with the external milieu.

*Specific Aim 3*

In my final aim, I identify two biomolecular components of DC random migration. I hypothesize that both proteins are required for efficient random motility and force generation. I perform studies to quantify a variety of motility parameters and further probe cellular signaling through the use of small molecule inhibitors.

# CHAPTER 2 : BACKGROUND

Throughout the next decade, Steinman and others began to characterize the properties and functions of DCs. It was noted that DCs were a very rare cell type, constituting up to 1% of nucleated cells in lymphoid organs and barely detectable in nonlymphoid tissues (1). Through lethal irradiation and reconstitution experiments, it was shown that DCs originated from precursor cells in the bone marrow, and to a lesser extent the spleen (2). It was also shown that DCs are loosely adherent, non-proliferating and viable in cell culture, which helped to pave the way for forty years of in vitro DC research (3). Towards the end of the 1970s, Steinman showed that DCs are highly potent stimulators of the mixed leukocyte reaction (MLR); as few as 300-1000 DCs are capable of inducing a strong response (4). DCs are much more stimulatory than other immune cell types, and in spite of their low numbers, they are the main cell type responsible for carrying out the MLR in lymphoid organs (4). Steinman further identified the presence of major histocompatibility complex (MHC) molecules on all DCs, thus solidifying their role as a highly potent APC (3). For all this seminal work on DC discovery and characterization, Ralph Steinman was honored with the 2011 Nobel Prize.

*DC Ontogeny and Heterogeneity*

DCs can be subdivided into three general classes: classical DCs (cDCs), Langerhans cells (LCs) and plasmacytoid DCs (pDCs), each with different origins and specialized functions (5). Common features of all DCs are expression of CD45, MHC class II and CD11c; absence of lineage markers from T cells, NK cells, B cells, granulocytes and erythrocytes; presence of transcripts for Flt3, c-kit, CCR7 and the zinc

finger transcription factor zbtb46 (5). Figure 2.1 provides a summary of the DC subtypes discussed below.

cDCs develop outside of the bone marrow from circulating, committed pre-cDC progenitors, and can trace their origin to both common lymphoid progenitors (CLPs) and common myeloid progenitors (CMPs) (5). cDCs have a short half-life and develop quickly, with repopulation taking only 2-3 days (6). There are two categories of cDCs—Batf3-dependent/CD8+ or CD103+ cDCs and Irf4-dependent/CD11b+ cDCs (5,7). Batf3 cDCs can be further subdivided into tissue resident CD8+ DCs and migratory CD103+langerin+ DCs (5,7). Development of Batf3 cDCs is dependent on Flt3 ligand and the transcription factors IRF8 and Batf3, and these cells are specialized in cross presentation (7). Irf4 cDCs can be further subdivided into tissue resident CD8-CD11b+ cDCs and migratory CD11b+ cDCs (5,7). Their development depends on Flt3 ligand and the transcription factors RelB and IRF4. These cells are specialized for MHC-II presentation (7).

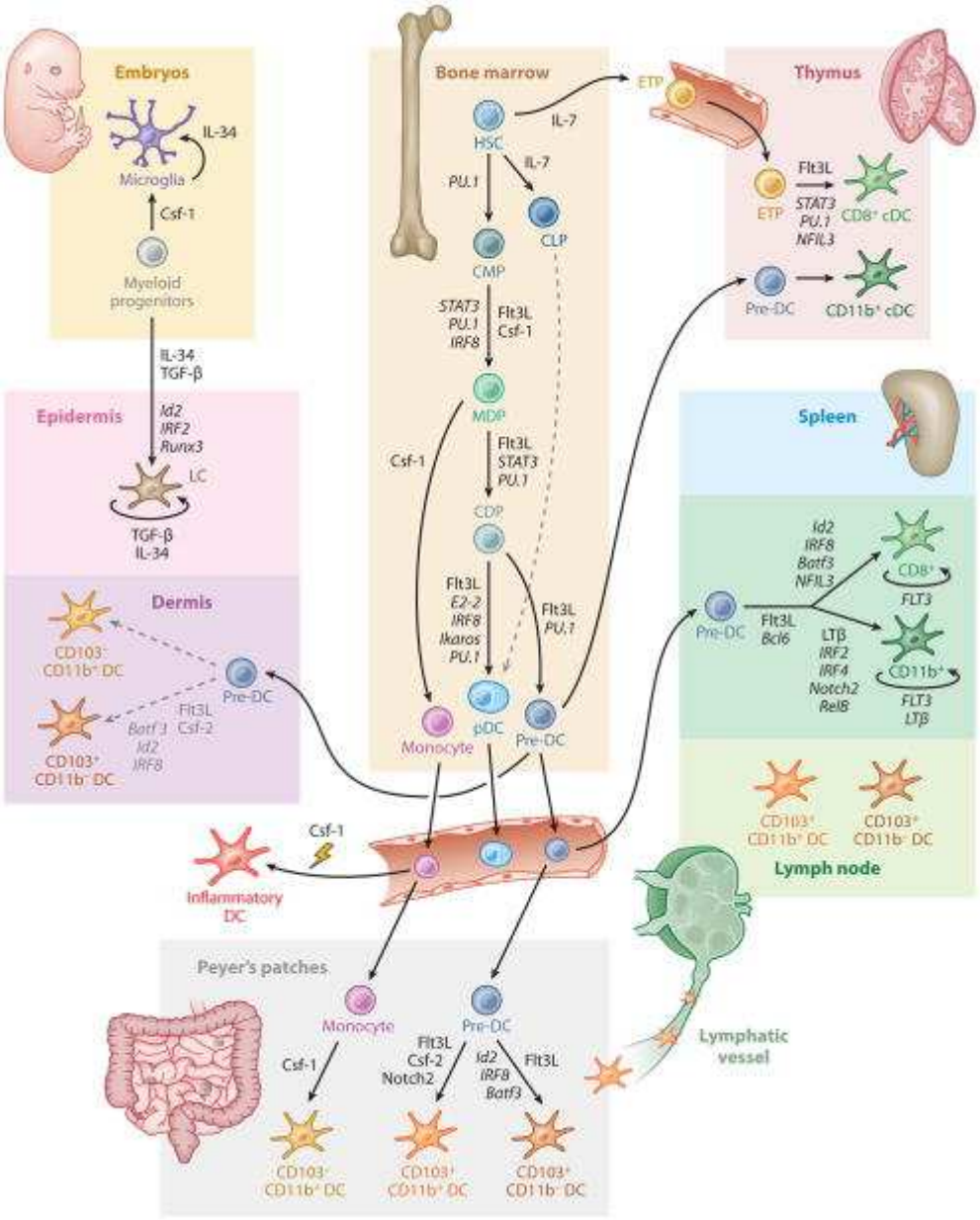


*Figure 2.1. DC origin, development and heterogeneity.*

Arrows indicate a stage of DC development or migration between tissues. Key developmental factors for each DC subset are shown adjacent to the arrows. Adapted from (5).

LCs were discovered in the epidermis by Paul Langerhans in 1868 (6). The true character of the LC went unidentified for many years, as it was initially thought to be a component of the nervous system (with its dendritic morphology resembling that of neurons) (6). It has since been shown that LCs are a type of DC and share many of the functions of their cDC counterparts (8). LCs are located in the epidermis and oral and vaginal mucosa and constitute 3-5% of nucleated cells in these tissues (5,7). Unlike cDCs, LC development does not depend on circulating precursor cells from the bone marrow; rather LCs develop from a source of embryonic monocytes that seed the skin prior to birth (5,6). LC development (repopulation time of several weeks) and turnover (half-life of 53-78 days) are also much slower than cDCs and are dependent on MCSF-R, IL-34 and the chemokine receptors CCR2 and CCR6 (6). Finally, LCs contain a combination of distinguishing features such as high expression of langerin and DEC-205 and the presence of Birbeck granules (6).

pDCs, like LCs, were not immediately recognized as DCs (9). Unlike cDCs, they fully form in the bone marrow before seeding peripheral tissues (10). They can develop from either CLPs or CMPs in a process that depends on Flt3 ligand (7,10). pDCs are most widely known for their ability to recognize and fight viral infections (9). They achieve this through expression of specific toll-like receptors (TLR7 and TLR9) and production of high levels of interferons (10). They can further be differentiated from cDCs by their surface phenotype ($CD11b^{-}CD11c^{low}B220^{+}$ in mice) (10).

An additional subset known as monoctye-derived DCs or "inflammatory DCs" develop directly from monocytes in response to active inflammation (7). These DCs have a phenotype and function similar to cDCs, but are ontogenically distinct and require

MCSF-R for development (7). The DCs that are discussed in the body of this thesis are most similar to these monocyte-derived DCs, and were generated by treating hematopoietic progenitor bone marrow cells with GM-CSF in vitro (11,12). Initially, this method was believed to generate cDCs, but recent studies have highlighted the unique nature of GM-CSF DCs (13,14). Further work needs to be performed to fully characterize this specific DC subset.

The above descriptions pertain to murine DCs, which have been the principal focus of research on DCs for the past few decades. Characterization of human DCs lagged behind murine DCs due to the relative difficulty in obtaining adequate numbers of cells (7). The development of protocols for the generation of DCs from human blood mononuclear cells has facilitated human DC research (15), and recent advances in transcriptome analysis have allowed researchers to match homologous murine and human DCs types (7). The two cDC subsets in humans are BDCA1/CD1c$^+$ and BDCA3/CD141$^+$, which correspond to murine IRF4/CD11b$^+$ and Batf3/CD103$^+$ cDCs, respectively (7).

*DC Maturation*

Dendritic cells exist as a heterogenous population of cells in a variety of developmental stages. The transition from immature DC to mature DC is accompanied by a collection of phenotypical and functional changes termed maturation or activation. The process of maturation can be triggered by a variety of signals, including, but not limited to, whole pathogens and pathogen-derived molecules (i.e. LPS, CpG, dsRNA), mechanical stress, exposure to necrotic cells, heat shock proteins, signs of infection (i.e.

IFN-α, IFN-β, IL-15), degradation of ECM components and CD40 engagement (16–26). Upon encountering one of these signals, DCs down-regulate immature DC markers (i.e. CD1a, CD115, mannose receptor), up-regulate MHC class I and II molecules, costimulatory molecules (i.e. CD80, CD83, CD86, CD40) and adhesion molecules (i.e. VLA-4, CD54/ICAM-1), and produce a variety of cytokines (i.e. IL-1β, TNF-α, IL-8, IL-12, IL-18, IFN- α, IFN-β, IFN-γ, MCP-1, MIP-1α) (18,22,23,27,28). Morphologically, DCs become more irregularly shaped, with an increasing number of dendrites, long veils and sheet-like projections (20,24). DCs lose their podosomes and transition from adherent, tissue-resident cells to highly migratory cells (29,30). Chemokine receptor expression switches from inflammatory receptors (i.e. CCR1, CCR2, CCR5, CXCR1) to constitutive receptors (CCR7, CXCR4, CCR4), facilitating the exit of DCs from sites of inflammation and their entrance into the T cell rich areas of lymph nodes (31). By the time DCs reach T cell rich areas, they have downregulated their capacity to capture and process antigen and are capable of stimulating T cells through stable adhesion and synapse formation (16,22,32).

## DENDRITIC CELL FUNCTIONS

### *Antigen Capture and Processing*

Immature dendritic cells use macropinocytosis and receptor-mediated endocytosis to sample large volumes of soluble and small particulate molecules in their surroundings in search of danger signals (33). Macropinocytosis and endocytosis are regulated by the activities of the Rho GTPases Rac1 and cdc42 (34), respectively, and macropinocytosis is down-regulated upon maturation (33). Dendritic cells are also capable of phagocytosis of

large pathogens (i.e. apoptotic cells, bacteria and yeast) through the activity of various phagocytic receptors (i.e. FcϒT Type I and II, CD36, $\alpha_v\beta_5$ and VLA-5) (35–38). Unlike other phagocytes, such as macrophages, DCs are not involved in complete degradation of pathogens; they have tuned their lysosomal machinery for partial degradation, thus enabling them to retain antigen peptides for presentation to T cells (39). One method in which DCs regulate peptide degradation is through control of lysosomal pH (40,41). Immature DC lysosomes have a weakly acidic pH, which encourages activity of protease inhibitors, impairs proteolytic degradation and provides a stable environment for antigen and MHC class II colocalization (40,41) . Upon maturation, the lysosomal pH drops, which allows for proteolysis and peptide loading onto MHC class II complexes (40,41). This acidification process is rather slow (~24 hours), allowing for highly coordinated antigen/MHC class II movement to the plasma membrane and migration to T cell rich areas of lymph nodes (41).

Another APC function unique to DCs is cross-presentation of exogenous antigens (i.e. apoptotic cells, pathogens, infected cells or tumor cells) on MHC class I molecules (42,43). For cross-presentation to occur successfully, exogenously derived antigens must be partially degraded in endocytic vesicles, exit the endocytic pathway via the cytosol and transit from the cytosol to the endoplasmic reticulum, where the MHC class I molecules reside (43,44). This is an energy intensive process and requires the activity of ATP-dependent translocators (TAP1/2) (44). Once assembled, the peptide/MHC class I molecules travel via the Golgi to the plasma membrane where they can by recognized by CD8+ T cells (44). Through these various methods of antigen capture and processing, DCs are able to colocalize and load antigen peptides onto MHC class I and II molecules

and provide a potent stimulus for cells of the adaptive immune system, a topic which is discussed in detail below (35,37).

*Activation of $CD4^+$ T cells*

Perhaps the most widely studied function of DCs is their ability to activate T cells. Dendritic cells are the most efficient APC, capable of presenting both endogenous and exogenous antigens and eliciting a strong T cell responses (45). Through coordinated random migration and dynamic dendrite extension, DCs actively search for cognate T cells in the lymph node (46). About 5000 T cells can scan a given DC per hour, allowing small numbers of DCs to elicit high levels of T cell activation (46). The exact nature of DC-T cell interactions appears to vary depending on the context. Traditionally, T cell activation was thought to depend on stable, long-lived interactions with dendritic cells. Many have shown that DCs and T cells form aggregates in culture (47). T cells and DCs form stable immunological synapses, consisting of antigen-loaded MHC complex, TCR and a variety of costimulatory molecules (48). DCs are actively involved in this process, through polarization of F-actin and fascin at the site of contact; inhibition of the dendritic cell cytoskeleton leads to their inability to activate T cells (49). DCs can remain tightly associated with T cells for many hours, leading to T cell activation and clonal expansion (50). However, it has also been shown that DCs can activate T cells through a series of successive, short-lived interactions, and it is possible that these interactions lead to a cumulative activation signal (46,47). Regardless of the exact nature of DC-T cell contact, a DC is able to provide three distinct activation signals to T cells: peptide-loaded MHC

complex, costimulatory molecules and soluble cytokines; perturbation of any of these signals can eliminate or significantly alter the T cell response (51,52).

An emerging area of study is the ability of dendritic cells to shape the specific type of immune response through $T_H$ (T helper) cell polarization. The classical view of this process is that different subsets of DCs lead to the different types of $T_H$ cells. In mice, $CD8\alpha^+$ DCs lead to $T_H1$ polarization (IL-2 and IFN-ϒ producing T cells, cell-mediated adaptive immunity), while $CD8\alpha^-$ DCs lead to $T_H2$ polarization (IL-4, IL-5 and IL-10 producing T cells, humoral adaptive immunity); likewise, in humans, monocyte-derived DC1 lead to $T_H1$ polarization and DC2 lead to $T_H2$ polarization (53–55). While this does seem to explain many cases of $T_H$ cell polarization, it is not a hard and fast rule (56). The type of response seems highly dependent on the type of cytokine secreted by a given DC. $CD8\alpha^+$ DCs or DC1 generally produce high levels of IL-12, which appears to be critical for $T_H1$ induction; in fact, $T_H1$ responses can be eliminated with IL-12 inhibition or artificially induced by adding exogenous IL-12 to $CD8\alpha^-$ DCs or DC2 (54,57). A comparable $T_H2$-specific cytokine has not yet been identified, although IL-4 may play a role (53,55,56). Further confounding the picture are reports suggesting that the polarization response may be determined as early as DC maturation, with different maturation stimuli leading to different $T_H$ subsets (56). It has also been suggested that the DC:T cell ratio may affect the type of $T_H$ cells formed, and that pre-existing $T_H$ cells can provide negative feedback and regulate DC numbers and priming ability (55,56). Additionally, DCs can polarize the immune system towards tolerance, through activation of regulatory T cells, preventing aberrant immune cell function and autoimmunity (58).

Through these various activities, dendritic cells garner the status of the most potent antigen-presenting cell in the body.

*Activation of $CD8^+$ T cells*

DCs not only indirectly activate cell-mediated adaptive immunity through $T_H1$ polarization, but also directly activate this branch of the adaptive immune response through their interactions with CD8+ T cells. DCs activate the subset of CD8+ cytotoxic T cells, which are responsible for clearing the body of harmful cells, independently of CD4+ activity (59,60). DCs regulate CD8+ T cell proliferation and effector function through regulation of cytokines (i.e. IL-4 and IL-2), presentation of antigens via MHC class I complexes and direct engagement through costimulatory molecules (60–64). Through their activation of CD8+ T cells, DCs have been implicated in the ability of the immune system to combat viral infections (i.e. HSV-1, influenza A), bacterial infections (i.e. Listeria monocytogenes), parasitic infections (i.e. Plasmodium yoelii) and cancer (62,65,66).

*Activation of B cells*

As discussed above, DCs are able to indirectly induce a humoral immune response through activation of $TH_2$ polarized CD4+ T cells and through the formation of clusters with cognate T cells and B cells in the lymph node (56,67). They were initially thought as nothing more than accessory cells, impacting B cell activation indirectly through the activation of T cells (68). It is now understood that DCs directly interact with B cells through extensive cell-cell contact (69), presentation of intact antigen in

membrane bound immune complexes (70) and release of soluble cytokines (71). Through these physical and chemical cues dendritic cells ensure B cell survival (72), increase B cell retention in the T cell zone (69), promote B cell proliferation and differentiation (71) and induce antibody production and class switching (70,73). A more thorough understanding of the interaction of DCs and B cells may lead to better medical treatments for diseases such as lupus, in which DCs lead to increased levels of B cell proliferation (74).

*Activation of Natural Killer Cells*

While much focus has been placed on the ability of dendritic cells to launch the adaptive immune response, recent studies have shown that dendritic cells are also able to enhance the innate immune response through their interaction with natural killer (NK) cells. Coculture of dendritic cells with natural killer cells leads to increased NK cell activation, as shown by proliferation and expansion of NK cell populations (75), increased $Ca^{2+}$ signaling and IFN-γ secretion (76), upregulation of CD69 (77), de novo expression of CD25 (78) and increased cytolytic activity (79). Direct DC and NK cell contact is necessary (77,80,81), and leads to the formation of actin-rich immunological synapses, enriched in cytosolic cytokines (i.e. IL-12, IL-15) and adhesion molecules (i.e. LFA-1, talin) (76,77,82,83). Due to the interaction of NK cell inhibitory molecules (i.e. KIR, CD94) and MHC class I receptors on mature DCs, dendritic cells are able to remain viable after interacting with NK cells, thus enabling them to launch both an immediate, innate immune response and a delayed, adaptive immune response (75,77,78) While not fully understood, many studies have shown reciprocal activation of DCs and NK cells,

suggesting that feedback loops are in place to amplify specific NK-mediated immune responses (84). Understanding DC and NK cell interactions will be useful in treating a variety of diseases, as impaired DC-mediated NK activation leads to greater susceptibility to infections such as HSV (65) and poorer tumor clearance (85).

## DC MIGRATION

Migration is critical for proper antigen presentation. DCs tune their migration to their maturation state and their stage of antigen presentation (antigen capture vs. active presentation to T cells) (86). Immature DCs express inflammatory chemokine receptors, such as CCR1, CCR5 and CCR6, which allow them to home to sites of infection (87,88). Maturation changes the chemokine receptor expression profile, most notably by down-regulating the inflammatory receptors and up-regulating CXCR4 and CCR7 (87,88). CCR7 is widely regarded as the most important chemokine receptor for DC trafficking, since absence of CCR7 or its ligands leads to impaired homing of DCs to lymph nodes (89,90).

CCR7 interacts with two chemokines—CCL19 (MIP-3β, ELC, exodus-3) and CCL21 (6Ckine, SLC, exodus-2) (88). In mice, there are two different forms of CCL21, CCL21-Leu and CCL21-Ser, which are expressed in the periphery and lymph nodes, respectively (86). CCL19 is found in the lymph node and is also involved in paracrine signaling by mature DCs (86,87,91). While both chemokines interact with CCR7 with similar kinetics (92), there are several notable differences between them. First, CC21 can be expressed in a surface bound state or a soluble state after cleavage of its C-terminus, whereas CCL19 only exists in a soluble form (91,93). CCR7 is rapidly

internalized after binding to CCL19 but not when binding to CCL21, thus leading to receptor desensitization after CCL19 interactions (94). Binding of CCL21 or CCL19 also leads to different downstream signaling; binding of surface bound CCL21 has been shown to regulate integrin-dependent adhesion, polarization and migration, whereas binding of CCL19 has been shown to regulate filopodial extensions and spreading (93,95).

The type of migration employed by DCs is highly dependent on the presentation mode of chemical signals. When DCs encounter a uniform solution of CCL19 or CCL21, they migrate randomly with increased velocity in a process known as chemokinesis (96). When DCs encounter a gradient of soluble CCL19 or CCL21, they migrate in a directional manner in a process known as chemotaxis (96). Similarly, when DCs are exposed to uniformly printed CCL21, they undergo random migration or haptokinesis, and when DCs are exposed to a gradient of printed CCL21, they undergo directed migration or haptotaxis (93). DCs are exposed to a complex array of these signals in the body and must properly interpret them to home to the T-cell rich areas of lymph nodes (97). For example, when DCs exit peripheral tissues and enter the lymphatic system, they need to move directionally toward lymphatic vessels, following gradients of soluble CCL19 and printed CCL21 on the vessel walls (97). At the start of this process, DCs can detect chemokine signals from adjacent vessels, migrating randomly between the vessels until they interpret and commit to a single source (97). Once in the lymph node, chemokine signals become saturated and DCs begin to migrate randomly, dancing around in search of cognate T cells (46,64). An overview of the canonical DC migration

process—from antigen capture in the periphery to T cell homing in the lymph node—is shown in Figure 2.2.

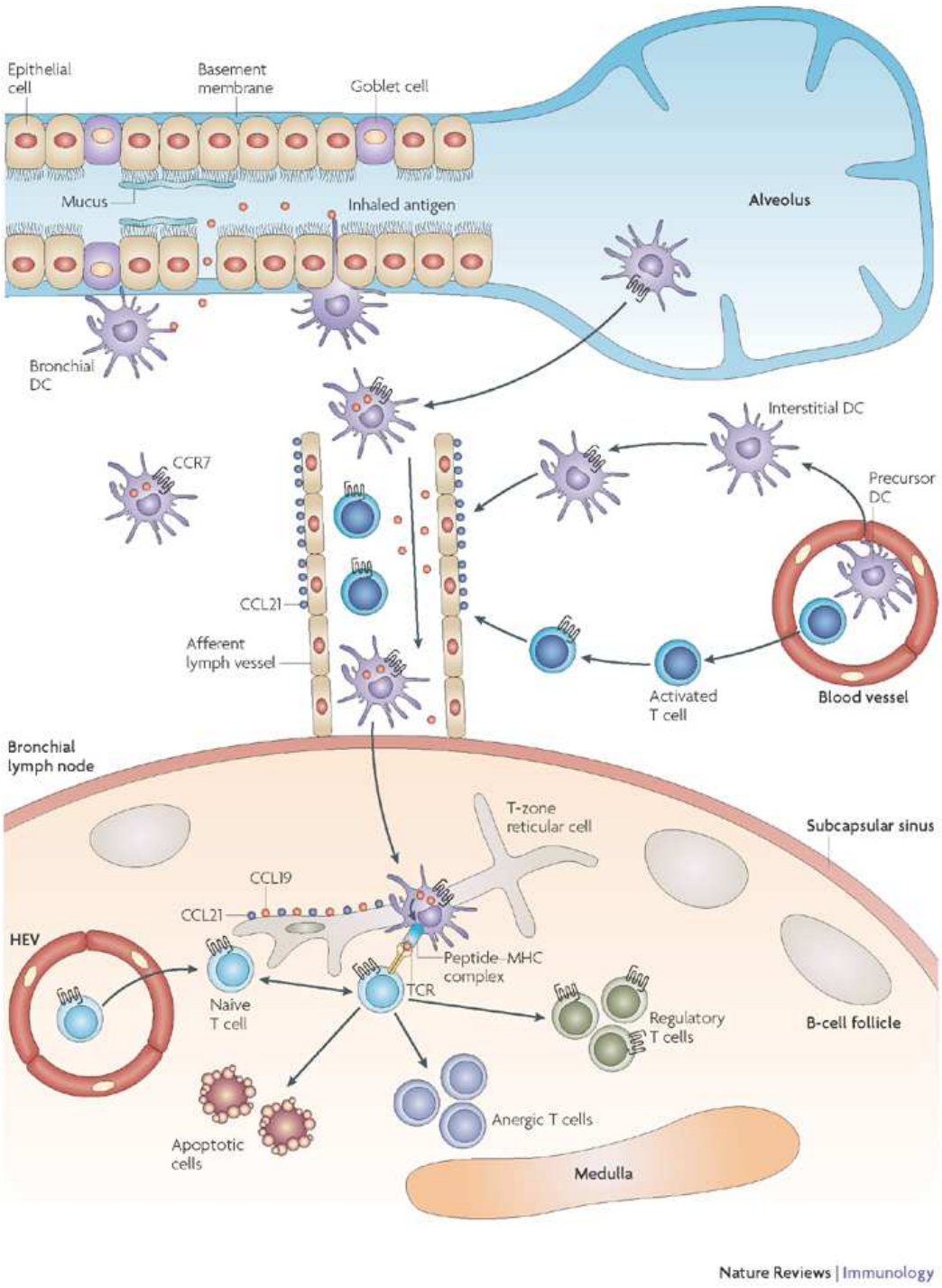


*Figure 2.2. Overview of DC migration from peripheral tissues to the lymph node.* Circulating DC precursors exit the bloodstream and populate bronchial tissue. Upon antigen capture, DCs upregulate CCR7 and follow gradients of CCL19 and CCL21 to the

lymph node. Adapted by permission from Macmillan Publishers Ltd: [Nat Rev Immunol] (89), copyright (2008).

The exact response of DCs to competing chemokine signals is still under investigation. In 2D systems, it has been shown that soluble CCL19 is more potent than soluble CCL21 and that DCs in counter gradients home to a location where the two signals are balanced, displaying random migration in the region where the competing gradients are balanced (92). In contrast, when DCs are exposed to counter-gradients of CCL19 and CCL21 in 3D, CCL21 seems to provide a more potent signal (91). The fact that results in 2D and 3D seem to contradict each other can be reconciled given how different the mechanisms of DC migration are in 2D and 3D (98). In 2D, DC migration is integrin dependent, while in 3D, DCs are able to migrate in an integrin-independent fashion (98). A firm understanding of DC migration in both 2D and 3D is critical. In the following chapters, I have added to the current knowledge, with descriptions of DC chemokinesis and how it is affected by various cytoskeletal proteins and signaling pathways as well as physical characteristics of the environment.

## DENDRITIC CELLS AND DISEASE

Defects in DC function have been shown to contribute to a variety of diseases. As a result, many groups have started to explore the power of harnessing DCs for immunotherapy treatments. Two of the most widely researched diseases for DC immunotherapies are cancer and HIV.

### *Cancer*

Cancer is able to evade the immune system by rendering it ignorant and tolerant (99). Much of the impact cancer has on the immune system is mediated by its effects on

DC function (99). Tumors secrete a variety of soluble factors (i.e. VEGF, M-CSF, IL-6 spermine, IL-10, tumor-derived gangliosides, prostaglandin $E_2$) that inhibit DC development from CD34+ hematopoietic progenitor cells and lead to an accumulation of myeloid precursors in the blood (99,100). In addition to reducing DC development, many of these factors also lead to apoptosis of circulating DCs (101). Collectively this leads to lower numbers of DCs in the peripheral blood of cancer patients (100). Of the DCs that successfully develop and avoid premature death, many are functionally impaired through perturbations in their maturation state (99). DCs in cancer patients express increased levels of the maturation marker CD83 and are inefficient at antigen capture (100). These DCs are further characterized by reduced expression of MHC class II, CD86 and CD40 and decreased production of cytokines such as IL-12 (100,102). Collectively this leads to DCs that mature prematurely and incompletely, fail to capture tumor antigens, are unsuccessful at activating anti-tumor T cell responses and induce immune tolerance (99,102).

Improving DC function in cancer patients could improve the ability of the body to fight off the disease. Many early studies showed that ex vivo generated DCs primed with tumor antigen in vitro were able to induce potent anti-tumor T cell responses when injected back into the host (103). DC cancer research has now progressed to numerous clinical trials in human subjects (104). DC cancer vaccines are considered safe and have minimal side effects (104). One DC immunotherapy, PROVENGE® (Dendreon Corporation; Seattle, WA), has already been approved by the FDA for the treatment of hormone-refractory prostate cancer and has been shown to significantly increase patient survival time (104). In spite of the strong protective immune response imparted by DC

cancer vaccines, migration of ex vivo generated DCs remains rather inefficient, with less than 5% of intradermally injected DCs reaching draining lymph nodes (105). Efforts to improve DC trafficking are ongoing and have included pretreatment of the vaccine injection site with inflammatory cytokines or toll-like receptor ligands and investigations into different modes of delivery (i.e. intravenous, sub-cutaneous, intra-dermal) (105,106). Understanding DC migration is critical to the improvement DC cancer vaccines.

*HIV*

Another major illness that is able to evade the immune system through manipulation of DCs is HIV (107). HIV proteins readily bind to DC receptors such as DC-SIGN (108). Despite this binding affinity, the virus does not rapidly replicate within DCs; rather DCs act as carriers which efficiently spread the virus to $CD4^+$ T cells (107). HIV binding to DC receptors leads to activation of cdc42 and the formation of large numbers of membrane extensions (108,109). This hijacking of the DC cell membrane allows for extensive contact between DCs and target T cells, the formation of an infectious synapse and transfer of HIV proteins (108,109). It has also been shown that DCs from HIV patients are less efficient at stimulating protective T cell responses and often induce tolerance (107).

Collectively, this makes DCs prime targets for HIV vaccines. Both immature and mature DCs are capable of trans-infecting T cells, but only mature DCs are able of eliciting a potent $CD4^+$ T cell response (108–110). To ensure immunity and not tolerance, maturation stimuli need to be added prior to administration (110). Early DC HIV vaccines employed ex vivo generated DCs pulsed with heat-inactivated HIV (111).

These clinical trials were safe, led to significant reductions in viral load and resulted in significant increases in HIV-1 specific CD4+ T cell responses for up to a year post-vaccination (111). Another promising avenue for HIV vaccines is the use of DC-targeted antibodies conjugated with HIV gag proteins (110). Preliminary studies in mice have shown that this method is more effective than other vaccination methods and could provide long-term, broad spectrum, systemic protection against HIV infection (110).

## METHODS OF IN VITRO DC CHARACTERIZATION

### *DC Sources for In Vitro Study*

Historically, DCs and DC precursors have been obtained from a variety of sources for in vitro studies, including the spleen (112), heart and kidney (113), thymus (114), fetal skin cells (115), whole blood (15,116) and bone marrow (117). Thanks to advances in in vitro culture methods, large populations of highly purified DCs can be generated. Today, the most common sources in humans and mice are peripheral blood mononuclear cells (PBMNCs) obtained from the blood and bone marrow progenitors obtained from femurs and tibia, respectively. Critical factors for the in vitro development of DCs include the cytokine GM-CSF, fetal bovine serum (118) and culture dish type and ECM composition (119,120). Additional factors that may enhance DC generation include IL-3, IL-4, IL-7, Flt-3-L, TNF-α, IL-1β, SCF, CSF-1, CD40-L, TGF-β1, although their importance and the nature of their effect on in vitro DC generation is still a matter for debate (114,121–124). Some groups have started to translate these in vitro studies into methods for enhancing DC generation in situ. For example, Maraskovsky et al. have

shown that injection of Flt 3-ligand into healthy human volunteers leads to an increase in DC levels, a result that could be useful in augmenting the natural immune response (125).

*Polydimethylsiloxane*

Traditionally, 2D migration has been studied on glass and tissue culture plastic surfaces. While these surfaces have been very useful in basic characterization of cell behavior, they are not very versatile and have little physiological relevance (i.e. very stiff compared to most tissues) (126). An alternative material for use in cell culture is PDMS (polydimethylsiloxane). PDMS is a silicon-based polymer consisting of methyl groups along a siloxane backbone (127,128). PDMS has many favorable qualities for use in biological research; it is chemical inert, thermally stable, durable, permeable to gases, easy to use, inexpensive, transparent, non-fluorescent and nontoxic (128,129). It is highly biocompatible and is already in use for many medical devices, such as catheters, pacemakers and ear and nose implants (128). PDMS substrates are made by mixing polymer base and cross linker, with the stiffness depending on the ratio of the two components (increase in cross linker leads to decrease in stiffness) (128). The recommended ratio for most applications is 10:1 and this can be spun onto glass coverslips and other surfaces to provide thin and uniform substrates for cell migration (128).

*Soft Lithography*

The use of PDMS to make cellular substrates is known as soft lithography, and was developed in 1993 by Whitesides et al., as an alternative for photolithography (129).

Photolithography has been in use in the semi-conductor industry since the late 1950's, but poses many challenges for biological applications (127). It is complex and expensive, it uses harsh solvents, it is limited to planar surfaces, it does not integrate well with other cell culture materials and it provides little control over the chemistry of surface patterning (127,129). For these reasons, soft lithography has replaced photolithography in many cellular applications.

One of the most widely used soft lithography techniques is microcontact printing, which is used to precisely and gently transfer biologically active proteins to surfaces (129,130). The method involves inking an elastomeric stamp with a protein solution, gently rinsing and drying the stamp and finally transferring the protein monolayer on the stamp to a target substrate through conformal contact (130). Microcontact printing is fast and efficient, and can be used to make patterns on a variety of different materials, such as glass and PDMS (130).

When using PDMS surfaces, it is important to properly treat the substrate prior to printing (131). PDMS is innately hydrophobic due to the presence of methyl groups, which prevents the transfer of protein during stamping (131,132). Treatment of PDMS with UV ozone makes the surface hydrophilic through the replacement of methyl groups with SiOH groups (128,132). This is a transient process, with significant hydrophobic recovery occurring after exposure to air for 30 minutes (128). Once PDMS surfaces are treated with UV ozone, protein is rapidly and preferentially transferred from the stamp (133,134).

Microcontact printing can be used to create a variety of adhesive patterns with micron-sized features (131). Printing small features initially posed problems due to

stamp compliance and collapse (127). This problem is resolved by either coating the top of the stamp with a stiff polymer or by using the stamp off method (which involves making the desired pattern with a planar stamp) (131). Microcontact printed surfaces are often blocked to restrict cell engagement to the printed areas and eliminate nonspecific interactions with the underlying substrate (134). Overall, microcontact printing has proven to be a useful tool for investigating the importance of adhesive signals on processes such as cell shape and migration (131,135).

Another soft lithography method that is very useful for the study of cell migration is replica molding (129). Replica molding involves curing PDMS against a silicon mold and provides a reliable and repeatable method for duplicating complex micron-sized structures (129,130). An example of a replica-molded structure is the micropost array detector (mPAD), shown in Figure 2.3 (136). mPADs are arrays of micron-sized pillars that are used to quantify cellular traction forces (136). They are an attractive alternative to bead-containing hydrogels for traction force microscopy (137), as they are both manufacturally and computationally simple to use and are able to resolve very small forces (138). Forces are readily calculated from post deflections using beam bending theory and a known spring constant for the given array (139). The post dimensions (and consequent geometry and compliance) can be modified to optimize the array for a variety of cell types (140). Both of the soft lithography techniques discussed above have been indispensable for my study of DC migration in 2D.

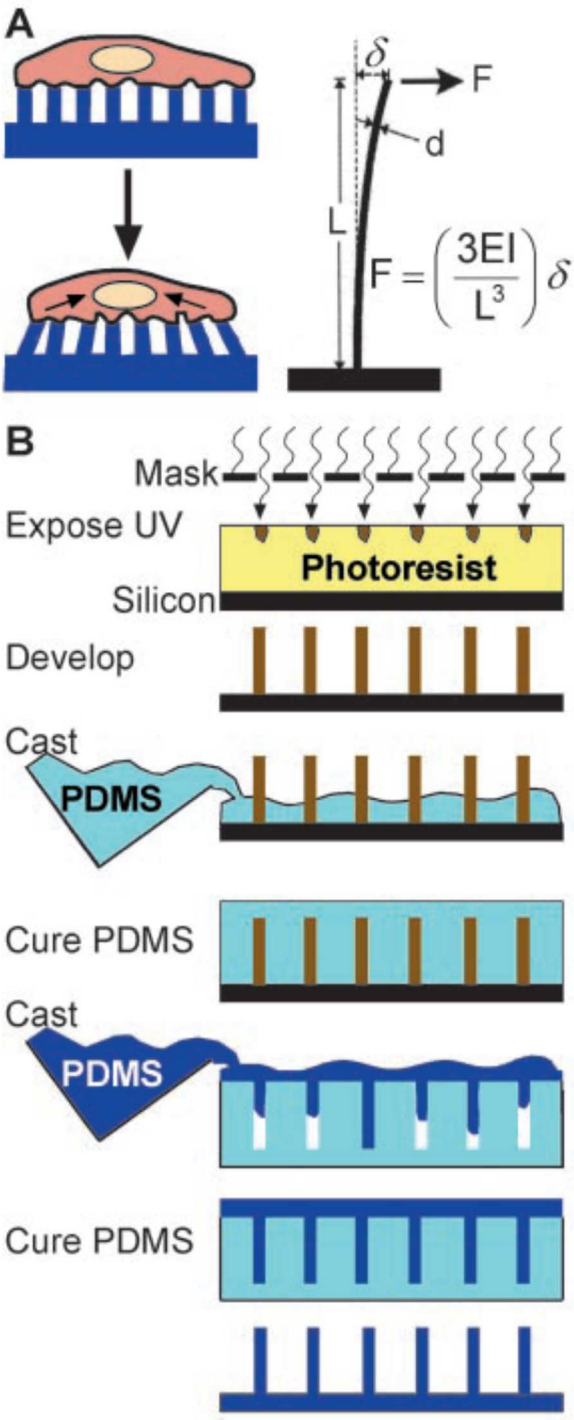


*Figure 2.3. mPAD replica molding.*

mPADs are tools used for measuring cellular traction forces and were made possible by advances in soft lithography. A) Cells engage mPADs and deflect posts. Post deflections

can be computed using beam bending theory and the known elasticity (E), moment of inertia (I) and height (L). B) Schematic of mPAD fabrication. Adapted from (136). 

REFERENCES


1. Steinman RM, Cohn Z a. Identification of a novel cell type in peripheral lymphoid organs of mice. I. Morphology, quantitation, tissue distribution. J Exp Med [Internet]. 1973;137(5):1142–62. Available from: http://www.ncbi.nlm.nih.gov/pmc/articles/PMC2184752/
2. Steinman RM, Lustig DS, Cohn AZA. Identification of a novel cell type in peripheral lymphoid organs of mice III. Functional properties in vivo. J Exp Med. 1974;139(13):1431–45.
3. Steinman RM, Kaplan G, Witmer MD, Cohn ZA. Identification of a novel cell type in peripheral lymphoid organs of mice. V. Purification of spleen dendritic cells, new surface markers, and maintenance in vitro. J Exp Med [Internet]. 1979;149(1):1–16. Available from: /pmc/articles/PMC2184752/?report=abstract%5Cnhttp://www.ncbi.nlm.nih.gov/pubmed/762493%5Cnhttp://www.pubmedcentral.nih.gov/articlerender.fcgi?artid=PMC2184752
4. Steinman RM, Witmer MD. Lymphoid dendritic cells are potent stimulators of the primary mixed leukocyte reaction in mice. PNAS [Internet]. 1978;75(10):5132–6. Available from: http://www.pubmedcentral.nih.gov/articlerender.fcgi?artid=336278&tool=pmcentrez&rendertype=abstract
5. Merad M, Sathe P, Helft J, Miller J, Mortha A. The dendritic cell lineage: ontogeny and function of dendritic cells and their subsets in the steady state and the inflamed setting. Annu Rev Immunol [Internet]. 2013;31:563–604. Available

from:
http://www.pubmedcentral.nih.gov/articlerender.fcgi?artid=3853342&tool=pmcentrez&rendertype=abstract

6. Merad M, Ginhoux F, Collin M. Origin, homeostasis and function of Langerhans cells and other langerin-expressing dendritic cells. Nat Rev Immunol [Internet]. 2008;8(12):935–47. Available from: http://www.ncbi.nlm.nih.gov/pubmed/19029989
7. Segura E. Dendritic Cell Protocols. Methods Mol Biol. 2016;1423:3–15.
8. Schuler G, Romani N, Steinman RM. A comparison of murine epidermal Langerhans cells with spleen dendritic cells. J Invest Dermatol [Internet]. Elsevier Masson SAS; 1985;85(1):99–106. Available from: http://dx.doi.org/10.1111/1523-1747.ep12275566
9. Siegal FP, Kadowaki N, Shodell M, Fitzgerald-bocarsly PA, Shah K, Ho S. The Nature of the Principal Type 1 Interferon – Producing Cells in Human Blood. Science (80- ). 1999;284(June):1835–8.
10. Lande R, Gilliet M. Plasmacytoid dendritic cells: Key players in the initiation and regulation of immune responses. Ann N Y Acad Sci. 2010;1183:89–103.
11. Sixt M, Lämmermann T. In Vitro Analysis of Chemotactic Leukocyte Migration in 3D Environments. Methods Mol Biol [Internet]. 2011;769(4):149–65. Available from: http://link.springer.com/10.1007/978-1-61779-207-6
12. Lutz MB, Inaba K, Schuler G, Romani N. Still Alive and Kicking: In-Vitro-Generated GM-CSF Dendritic Cells! Immunity [Internet]. Elsevier Inc.; 2016;44(1):1–2. Available from: http://dx.doi.org/10.1016/j.immuni.2015.12.013

13. Helft J, Böttcher J, Chakravarty P, Zelenay S, Huotari J, Schraml BU, et al. GM-CSF Mouse Bone Marrow Cultures Comprise a Heterogeneous Population of CD11c+MHCII+ Macrophages and Dendritic Cells. Immunity [Internet]. 2015;42(6):1197–211. Available from: http://linkinghub.elsevier.com/retrieve/pii/S1074761315002162

14. Guilliams M, Malissen B. A Death Notice for In-Vitro-Generated GM-CSF Dendritic Cells? Immunity [Internet]. Elsevier Inc.; 2015;42(6):988–90. Available from: http://dx.doi.org/10.1016/j.immuni.2015.05.020

15. Sallusto F, Lanzavecchia A. Efficient presentation of soluble antigen by cultured human dendritic cells is maintained by granulocyte/macrophage colony-stimulating factor plus interleukin 4 and downregulated by tumor necrosis factor alpha. J Exp Med [Internet]. 1994;179(4):1109–18. Available from: http://jem.rupress.org/content/179/4/1109.abstract

16. De Smedt T, Pajak B, Muraille E, Lespagnard L, Heinen E, De Baetselier P, et al. Regulation of dendritic cell numbers and maturation by lipopolysaccharide in vivo. J Exp Med [Internet]. 1996;184(4):1413–24. Available from: http://www.pubmedcentral.nih.gov/articlerender.fcgi?artid=2192842&tool=pmcentrez&rendertype=abstract

17. Ouaissi A, Guilvard E, Delneste Y, Caron G, Magistrelli G, Herbault N, et al. The Trypanosoma cruzi Tc52-released protein induces human dendritic cell maturation, signals via Toll-like receptor 2, and confers protection against lethal infection. J Immunol. 2002;168(12):6366–74.

18. Cella M, Salio M, Sakakibara Y, Langen H, Julkunen I, Lanzavecchia A.

Maturation, activation, and protection of dendritic cells induced by double-stranded RNA. J Exp Med [Internet]. 1999;189(5):821–9. Available from: http://www.pubmedcentral.nih.gov/articlerender.fcgi?artid=2192946&tool=pmcentrez&rendertype=abstract

19. d'Ostiani CF, Del Sero G, Bacci A, Montagnoli C, Spreca A, Mencacci A, et al. Dendritic cells discriminate between yeasts and hyphae of the fungus Candida albicans. Implications for initiation of T helper cell immunity in vitro and in vivo. J Exp Med. 2000;191(10):1661–74.
20. Hartmann G, Weiner GJ, Krieg a M. CpG DNA: a potent signal for growth, activation, and maturation of human dendritic cells. Proc Natl Acad Sci U S A. 1999;96(16):9305–10.
21. Gallucci S, Lolkema M, Matzinger P. Natural adjuvants: endogenous activators of dendritic cells. Nat Med. 1999;5(11):1249–55.
22. Termeer CC, Hennies J, Voith U, Ahrens T, M. Weiss J, Prehm P, et al. Oligosaccharides of Hyaluronan Are Potent Activators of Dendritic Cells. J Immunol [Internet]. 2000;165(4):1863–70. Available from: http://www.jimmunol.org/content/165/4/1863.full
23. Somersan S, Larsson M, Fonteneau JF, Basu S, Srivastava P, Bhardwaj N. Primary tumor tissue lysates are enriched in heat shock proteins and induce the maturation of human dendritic cells. JImmunol [Internet]. 2001;167(0022–1767 (Print)):4844–52. Available from: http://www.ncbi.nlm.nih.gov/pubmed/11673488
24. Caux BC, Massacrier C, Vanbervliet B, Dubois B, Kooten C Van, Durand I, et al. Activation of Human Dendritic Cells through CD40 Cross-linking. J Exp Med.

1994;180:1263–72.

25. Montoya M, Schiavoni G, Mattei F, Gresser I, Belardelli F, Borrow P, et al. Type I interferons produced by dendritic cells promote their phenotypic and functional activation. Blood. 2002;99(9):3263–71.

26. Mattei F, Schiavoni G, Belardelli F, Tough DF. IL-15 is expressed by dendritic cells in response to type I IFN, double-stranded RNA, or lipopolysaccharide and promotes dendritic cell activation. J Immunol. 2001;167:1179–87.

27. Rescigno M, Citterio S, Thery C, Rittig M, Medaglini D, Pozzi G, et al. Bacteria-induced neo-biosynthesis, stabilization, and surface expression of functional class I molecules in mouse dendritic cells. Proc Natl Acad Sci U S A. 1998;95:5229–34.

28. de Jong EC, Vieira PL, Kalinski P, Schuitemaker JHN, Tanaka Y, Wierenga E a, et al. Microbial compounds selectively induce Th1 cell-promoting or Th2 cell-promoting dendritic cells in vitro with diverse th cell-polarizing signals. J Immunol. 2002;168(4):1704–9.

29. Burns S, Hardy SJ, Buddle J, Yong KL, Jones GE, Thrasher AJ. Maturation of DC Is Associated with Changes in Motile Characteristics and Adherence. Cell Motil Cytoskeleton. 2004;57(October 2003):118–32.

30. Vargas P, Maiuri P, Bretou M, Saez PJ, Pierobon P, Maurin M, et al. Innate control of actin nucleation determines two distinct migration behaviours in dendritic cells. Nat cell Biol. 15AD;18(1):43–53.

31. Sallusto F, Schaerli P, Loetscher P, Schaniel C, Lenig D, Mackay CR, et al. Rapid and coordinated switch in chemokine receptor expression during dendritic cell maturation. Eur J Immunol. 1998;28(9):2760–9.

32. Lantz O, Trautmann SA, Grandjean C, Jancic C, Hivroz AF, Benvenuti C, et al. Dendritic Cell Maturation Controls Adhesion, Synapse Formation, and the Duration of the Interactions with Naive T Lymphocytes. J Immunol J Immunol Bost Univ Lib [Internet]. 2016;172:292–301. Available from: http://www.jimmunol.org/content/172/1/292

33. Sallusto F, Cella M, Danieli C, Lanzavecchia A. Dendritic cells use macropinocytosis and the mannose receptor to concentrate macromolecules in the major histocompatibility complex class II compartment: downregulation by cytokines and bacterial products. J Exp Med. 1995;182:389–400.

34. Garrett WS, Chen L-M, Kroschewski R, Ebersold M, Turley S, Trombetta S, et al. Developmental Control of Endocytosis in Dendritic Cells by Cdc42. Cell [Internet]. 2000;102(3):325–34. Available from: http://www.sciencedirect.com/science/article/pii/S0092867400000386

35. Albert ML, Pearce SF, Francisco LM, Sauter B, Roy P, Silverstein RL, et al. Immature dendritic cells phagocytose apoptotic cells via alphavbeta5 and CD36, and cross-present antigens to cytotoxic T lymphocytes. J Exp Med [Internet]. 1998;188(7):1359–68. Available from: http://www.pubmedcentral.nih.gov/articlerender.fcgi?artid=2212488&tool=pmcentrez&rendertype=abstract

36. Fanger N a, Wardwell K, Shen L, Tedder TF, Guyre PM. Type I (CD64) and type II (CD32) Fc gamma receptor-mediated phagocytosis by human blood dendritic cells. J Immunol. 1996;157:541–8.

37. Filgueira L, Nestlé FO, Rittig M, Joller HI, Groscurth P. Human dendritic cells

phagocytose and process Borrelia burgdorferi. J Immunol [Internet]. 1996;157(7):2998–3005. Available from: http://www.jimmunol.org/content/157/7/2998.short%5Cnhttp://www.ncbi.nlm.nih.gov/entrez/query.fcgi?cmd=Retrieve&db=PubMed&dopt=Citation&list_uids=8816408%5Cnhttp://www.ncbi.nlm.nih.gov/pubmed/8816408

38. Gildea L a, Morris RE, Newman SL. Histoplasma capsulatum yeasts are phagocytosed via very late antigen-5, killed, and processed for antigen presentation by human dendritic cells. J Immunol. 2001;166(2):1049–56.

39. Savina A, Amigorena S. Phagocytosis and antigen presentation in dendritic cells. Immunol Rev. 2007;219(1):143–56.

40. Trombetta ES, Mellman I. Cell Biology of Antigen Processing in Vitro and in Vivo. Annu Rev Immunol [Internet]. 2005;23(1):975–1028. Available from: http://arjournals.annualreviews.org/loi/immunol

41. Lutz M, Rovere P, Kleijmeer M, Rescigno M, Assmann C, Oorschot V, et al. Intracellular routes and selective retention of antigens in mildly acidic cathepsin D/lysosome-associated membrane protein-1/MHC class II-positive vesicles in immature dendritic cells. J Immunol. 1997;159:3707–16.

42. Jancic C, Savina A, Wasmeier C, Tolmachova T, El-Benna J, Dang PM-C, et al. Rab27a regulates phagosomal pH and NADPH oxidase recruitment to dendritic cell phagosomes. Nat Cell Biol. 2007;9(4):367–78.

43. Rodriguez A, Regnault A, Kleijmeer M, Ricciardi-Castagnoli P, Amigorena S. Selective transport of internalized antigens to the cytosol for MHC class I presentation in dendritic cells. Nat Cell Biol [Internet]. 1999;1(6):362–8. Available

from: http://dx.doi.org/10.1038/14058

44. Cresswell P, Ackerman AL, Giodini A, Peaper DR, Wearsch PA. Mechanisms of MHC class I-restricted antigen processing and cross-presentation. Immunol Rev. 2005;207:145–57.

45. Guéry JC, Adorini L. Dendritic cells are the most efficient in presenting endogenous naturally processed self-epitopes to class II-restricted T cells. J Immunol. 1995;154:536–44.

46. Miller MJ, Hejazi AS, Wei SH, Cahalan MD, Parker I. T cell repertoire scanning is promoted by dynamic dendritic cell behavior and random T cell motility in the lymph node. Proc Natl Acad Sci U S A [Internet]. 2004;101(4):998–1003. Available from: http://www.pubmedcentral.nih.gov/articlerender.fcgi?artid=327133&tool=pmcentrez&rendertype=abstract%5Cnhttp://www.ncbi.nlm.nih.gov/pubmed/14722354%5Cnhttp://www.pubmedcentral.nih.gov/articlerender.fcgi?artid=PMC327133

47. Gunzer M, Schäfer a, Borgmann S, Grabbe S, Zänker KS, Bröcker EB, et al. Antigen presentation in extracellular matrix: interactions of T cells with dendritic cells are dynamic, short lived, and sequential. Immunity. 2000;13:323–32.

48. Bromley SK, Burack WR, Kenneth G, Somersalo K, Sims TN, Sumen C, et al. The mmunological synapse. Annu Rev Immunol. 2001;19:375–96.

49. Al-Alwan MM, Rowden G, Lee TD, West KA. The dendritic cell cytoskeleton is critical for the formation of the immunological synapse. J Immunol (Baltimore, Md 1950) [Internet]. 2001;166(3):1452–6. Available from: http://eutils.ncbi.nlm.nih.gov/entrez/eutils/elink.fcgi?dbfrom=pubmed&id=111601

83&retmode=ref&cmd=prlinks%5Cnpapers2://publication/uuid/70BA9022-3A69-488F-BACB-B80464FCD8F1

50. Stoll S, Delon J, Brotz TM, Germain RN. Dynamic Imaging of T Cell – Dendritic Cell Interactions in Lymph Nodes. Science (80- ). 2002;296(June):1873–7.

51. Lanzavecchia a, Sallusto F. Regulation of T cell immunity by dendritic cells. Cell. 2001;106:263–6.

52. Young JW, Koulova L, Soergel SA, Clark EA, Steinman RM, Dupont B. The B7 / BB1 Antigen Provides One of Several Costimulatory Signals for the Activation of CD4 + T Lymphocytes by Human Blood Dendritic Cells In Vitro. JClin Invest. 1992;90(July):229–37.

53. Moser M, Murphy KM. Dendritic cell regulation of TH1-TH2 development. Nat Immunol [Internet]. 2000;1(3):199–205. Available from: http://www.ncbi.nlm.nih.gov/pubmed/10973276

54. Maldonado-López R, De Smedt T, Michel P, Godfroid J, Pajak B, Heirman C, et al. CD8alpha+ and CD8alpha- subclasses of dendritic cells direct the development of distinct T helper cells in vivo. J Exp Med. 1999;189(3):587–92.

55. Rissoan M-C, Soumelis V, Kadowaki N, Grouard G, Briere F, de Waal Malefyt R, et al. Reciprocal Control of T Helper Cell and Dendritic Cell Differentiation. Science (80- ). 1999;283(February):1183–6.

56. Tanaka H, Demeure CE, Rubio M, Delespesse G, Sarfati M. Human monocyte-derived dendritic cells induce naive T cell differentiation into T helper cell type 2 (Th2) or Th1/Th2 effectors. Role of stimulator/responder ratio. J Exp Med [Internet]. 2000;192(3):405–12. Available from:

http://www.pubmedcentral.nih.gov/articlerender.fcgi?artid=2193215&tool=pmcentrez&rendertype=abstract

57. Macatonia SE, Hosken N a, Litton M, Vieira P, Hsieh CS, Culpepper J a, et al. Dendritic cells produce IL-12 and direct the development of Th1 cells from naive CD4+ T cells. J Immunol. 1995;154(10):5071–9.

58. Hawiger D, Inaba K, Dorsett Y, Guo M, Mahnke K, Rivera M, et al. Dendritic cells induce peripheral T cell unresponsiveness under steady state conditions in vivo. J Exp Med. 2001;194(6):769–79.

59. Bhardwaj N, Bender A, Gonzalez N, Bui LK, Garrett MC, Steinman RM. Influenza virus-infected dendritic cells stimulate strong proliferative and cytolytic responses from human CD8+ T cells. J Clin Invest. 1994;94(2):797–807.

60. Inaba K, Young JW, Steinman RM. Direct activation of CD8+ cytotoxic T lymphocytes by dendritic cells. J Exp Med [Internet]. 1987;166(1):182–94. Available from: http://www.pubmedcentral.nih.gov/articlerender.fcgi?artid=2188638&tool=pmcentrez&rendertype=abstract

61. King C, Mueller Hoenger R, Malo Cleary M, Murali-Krishna K, Ahmed R, King E, et al. Interleukin-4 acts at the locus of the antigen-presenting dendritic cell to counter-regulate cytotoxic CD8+ T-cell responses. Nat Med [Internet]. 2001;7(2):206–14. Available from: http://www.nature.com/nm/journal/v7/n2/pdf/nm0201_206.pdf

62. Albert ML, Sauter B, Bhardwaj N. Dendritic cells acquire antigen from apoptotic cells and induce class I-restricted CTLs. Nature [Internet]. 1998;392(6671):86–9.

Available from: http://dx.doi.org/10.1038/32183

63. Carreno BM, Magrini V, Becker-Hapak M, Kaabinejadian S, Hundal J, Petti AA, et al. A dendritic cell vaccine increases the breadth and diversity of melanoma neoantigen-specific T cells. Science (80- ) [Internet]. 2015;348(6236):803–8. Available from: http://www.sciencemag.org/content/348/6236/803.full

64. Bousso P, Robey E. Dynamics of CD8+ T cell priming by dendritic cells in intact lymph nodes. Nat Immunol. 2003;4(6):579–85.

65. Kassim SH, Rajasagi NK, Zhao X, Chervenak R, Jennings SR. In Vivo Ablation of CD11c-Positive Dendritic Cells Increases Susceptibility to Herpes Simplex Virus Type 1 Infection and Diminishes NK and T-Cell Responses. Society. 2006;80(8):3985–93.

66. Jung S, Unutmaz D, Wong P, Sano GI, De Los Santos K, Sparwasser T, et al. In vivo depletion of CD11c+ dendritic cells abrogates priming of CD8+ T cells by exogenous cell-associated antigens. Immunity. 2002;17(2):211–20.

67. Inaba K, Witmer M, Steinman R. Clustering of dendritic cells, helper T lymphocytes, and histocompatible B cells during primary antibody responses in vitro. J Exp … [Internet]. 1984;160(September):858–76. Available from: http://jem.rupress.org/content/160/3/858.abstract

68. Inaba K, Steinman RM, Van Voorhis WC, Muramatsu S. Dendritic cells are critical accessory cells for thymus-dependent antibody responses in mouse and in man. Proc Natl Acad Sci U S A [Internet]. 1983;80(19):6041–5. Available from: http://www.pubmedcentral.nih.gov/articlerender.fcgi?artid=534356&tool=pmcentrez&rendertype=abstract

69. Qi H. Extrafollicular Activation of Lymph Node B Cells by Antigen-Bearing Dendritic Cells. Science (80- ) [Internet]. 2006;312(5780):1672–6. Available from: http://www.sciencemag.org/cgi/doi/10.1126/science.1125703

70. Wykes M, Pombo A, Jenkins C, MacPherson GG. Dendritic cells interact directly with naive B lymphocytes to transfer antigen and initiate class switching in a primary T-dependent response. J Immunol [Internet]. 1998;161(3):1313–9. Available from: http://www.ncbi.nlm.nih.gov/pubmed/9686593

71. Dubois B, Massacrier C, Vanbervliet B, Fayette J, Brière F, Banchereau J, et al. Critical role of IL-12 in dendritic cell-induced differentiation of naive B lymphocytes. J Immunol [Internet]. 1998;161(5):2223–31. Available from: http://www.jimmunol.org/content/161/5/2223.short%5Cnfiles/47/261-Dubois.pdf%5Cnhttp://www.ncbi.nlm.nih.gov/pubmed/9725215

72. Wykes M, Macpherson G. Dendritic cell-B-cell interaction: Dendritic cells provide B cells with CD40-independent proliferation signals and CD40-dependent survival signals. Immunology. 2000;100(1):1–3.

73. Fayette J, Dubois B, Vandenabeele S, Bridon JM, Vanbervliet B, Durand I, et al. Human dendritic cells skew isotype switching of CD40-activated naive B cells towards IgA1 and IgA2. J Exp Med [Internet]. 1997;185(11):1909–18. Available from: http://www.pubmedcentral.nih.gov/articlerender.fcgi?artid=2196343&tool=pmcentrez&rendertype=abstract

74. Wan S, Zhou Z, Duan B, Morel L. Direct B cell stimulation by dendritic cells in a mouse model of lupus. Arthritis Rheum. 2008;58(6):1741–50.

75. Ferlazzo G, Tsang ML, Moretta L, Melioli G, Steinman RM, Münz C. Human dendritic cells activate resting natural killer (NK) cells and are recognized via the NKp30 receptor by activated NK cells. J Exp Med [Internet]. 2002;195(3):343–51. Available from: http://www.pubmedcentral.nih.gov/articlerender.fcgi?artid=2193591&tool=pmcentrez&rendertype=abstract

76. Borg C, Abdelali J, Laderach D, Maruyama K, Wakasugi H, Charrier S, et al. NK Cell Activation by Dendritic Cells (DC) Require The Formation of a Synapse leading to IL-12 Polarization in DC. Blood [Internet]. 2004;104(10):3267–76. Available from: http://www.ncbi.nlm.nih.gov/entrez/query.fcgi?cmd=Retrieve&db=PubMed&dopt=Citation&list_uids=15242871

77. Brilot F, Strowig T, Roberts SM, Arrey F, M??nz C. NK cell survival mediated through the regulatory synapse with human DCs requires IL-15R?? J Clin Invest. 2007;117(11):3316–29.

78. Ferlazzo G, Morandi B, A DA, Meazza R, Melioli G, Moretta A, et al. The interaction between NK cells and dendritic cells in bacterial infections results in rapid induction of NK cell activation and in the lysis of uninfected dendritic cells. Eur J Immunol. 2003;33(2):306–13.

79. Andoniou CE, van Dommelen SLH, Voigt V, Andrews DM, Brizard G, Asselin-Paturel C, et al. Interaction between conventional dendritic cells and natural killer cells is integral to the activation of effective antiviral immunity. Nat Immunol. 2005;6(10):1011–9.

80. Beuneu H, Deguine J, Mandelboim O, Santo JP Di, Bousso P. Dynamic behavior of NK cells during activation in lymph nodes. Blood. 2009;114(15):3227–35.

81. Yu Y, Hagihara M, Ando K, Gansuvd B, Matsuzawa H, Tsuchiya T, et al. Enhancement of human cord blood CD34+ cell-derived NK cell cytotoxicity by dendritic cells. J Immunol [Internet]. 2001;166(3):1590–600. Available from: http://www.ncbi.nlm.nih.gov/pubmed/11160200

82. Barreira da Silva R, Graf C, Münz C, Dc W, Mu C. Cytoskeletal stabilization of inhibitory interactions in immunologic synapses of mature human dendritic cells with natural killer cells Cytoskeletal stabilization of inhibitory interactions in immunologic synapses of mature human dendritic cells with natu. Blood. 2011;118(25):6487–98.

83. Lucas M, Schachterle W, Oberle K, Aichele P, Diefenbach A. Dendritic Cells Prime Natural Killer Cells by trans-Presenting Interleukin 15. Immunity. 2007;26(4):503–17.

84. Piccioli D, Sbrana S, Melandri E, Valiante NM. Contact-dependent Stimulation and Inhibition of Dendritic Cells by Natural Killer Cells. J Exp Med [Internet]. 2002;195(3):335–41. Available from: http://jem.rupress.org/content/195/3/335.abstract

85. Fernandez NC, Lozier a, Flament C, Ricciardi-Castagnoli P, Bellet D, Suter M, et al. Dendritic cells directly trigger NK cell functions: cross-talk relevant in innate anti-tumor immune responses in vivo. Nat Med. 1999;5(4):405–11.

86. Randolph GJ, Angeli V, Swartz M a. Dendritic-cell trafficking to lymph nodes through lymphatic vessels. Nat Rev Immunol [Internet]. 2005;5(8):617–28.

Available from: http://www.ncbi.nlm.nih.gov/pubmed/16056255

87. Sallusto F, Palermo B, Lenig D, Miettinen M, Matikainen S, Julkunen I, et al. Distinct patterns and kinetics of chemokine production regulate dendritic cell function. Eur J Immunol. 1999;29(5):1617–25.

88. Zlotnik a, Yoshie O. Chemokines: a new classification system and their role in immunity. Immunity. 2000;12(2):121–7.

89. Förster R, Davalos-Misslitz AC, Rot A. CCR7 and its ligands: balancing immunity and tolerance. Nat Rev Immunol [Internet]. 2008;8(5):362–71. Available from: http://www.ncbi.nlm.nih.gov/pubmed/18379575

90. Gunn MD, Kyuwa S, Tam C, Kakiuchi T, Matsuzawa A, Williams LT, et al. Mice lacking expression of secondary lymphoid organ chemokine have defects in lymphocyte homing and dendritic cell localization. J Exp Med [Internet]. 1999;189(3):451–60. Available from: http://www.ncbi.nlm.nih.gov/pubmed/9927507%5Cnhttp://www.pubmedcentral.nih.gov/articlerender.fcgi?artid=PMC2192914

91. Haessler U, Pisano M, Wu M, Swartz MA, Rakesh Jain by K. Dendritic cell chemotaxis in 3D under defined chemokine gradients reveals differential response to ligands CCL21 and CCL19. Proc Natl Acad Sci USA. 2011;108(14):5614–9.

92. Ricart BG, John B, Lee D, Hunter CA, Hammer DA. Dendritic cells distinguish individual chemokine signals through CCR7 and CXCR4. J Immunol [Internet]. 2011;186(1):53–61. Available from: http://www.jimmunol.org/cgi/doi/10.4049/jimmunol.1002358

93. Schumann K, Lämmermann T, Bruckner M, Legler DF, Polleux J, Spatz JP, et al.

Immobilized Chemokine Fields and Soluble Chemokine Gradients Cooperatively Shape Migration Patterns of Dendritic Cells. Immunity. 2010;32(5):703–13.

94. Otero C, Groettrup M, Legler DF. Opposite Fate of Endocytosed CCR7 and Its Ligands: Recycling versus Degradation. J Immunol. 2011;

95. Yanagawa Y, Onoé K. CCL19 induces rapid dendritic extension of murine dendritic cells. Blood. 2002;100(6):1948–56.

96. Riol-Blanco L, Sánchez-Sánchez N, Torres A, Tejedor A, Narumiya S, Corbí AL, et al. The Chemokine Receptor CCR7 Activates in Dendritic Cells Two Signaling Modules That Independently Regulate Chemotaxis and Migratory Speed. J Immunol [Internet]. 2005;174:4070–80. Available from: http://www.jimmunol.org/content/174/7/4070

97. Weber M, Hauschild R, Schwarz J, Moussion C, de Vries I, Legler DF, et al. Interstitial dendritic cell guidance by haptotactic chemokine gradients. Sci (New York, NY) [Internet]. 2013;339(6117):328–32. Available from: http://www.sciencemag.org/content/339/6117/328.long%5Cnpapers://99cf836b-0208-4bf7-a35c-5506d5268000/Paper/p18255

98. Lämmermann T, Bader BL, Monkley SJ, Worbs T, Wedlich-Söldner R, Hirsch K, et al. Rapid leukocyte migration by integrin-independent flowing and squeezing. Nature [Internet]. 2008;453(7191):51–5. Available from: http://www.nature.com/doifinder/10.1038/nature06887%5Cnhttp://www.ncbi.nlm.nih.gov/pubmed/18451854

99. Gabrilovich D. Mechanisms and functional significance of tumour-induced dendritic-cell defects. Nat Rev Immunol [Internet]. 2004;4(12):941–52. Available

from: http://www.ncbi.nlm.nih.gov/pubmed/15573129

100. Della Bella S, Gennaro M, Vaccari M, Ferraris C, Nicola S, Riva A, et al. Altered maturation of peripheral blood dendritic cells in patients with breast cancer. Br J Cancer [Internet]. 2003;89(8):1463–72. Available from: http://www.pubmedcentral.nih.gov/articlerender.fcgi?artid=2394334&tool=pmcentrez&rendertype=abstract

101. Pinzon-Charry A, Maxwell T, McGuckin MA, Schmidt C, Furnival C, López JA. Spontaneous apoptosis of blood dendritic cells in patients with breast cancer. Breast Cancer Res [Internet]. 2006;8(1):R5. Available from: http://www.pubmedcentral.nih.gov/articlerender.fcgi?artid=1413992&tool=pmcentrez&rendertype=abstract

102. Satthaporn S, Robins A, Vassanasiri W, El-Sheemy M, Jibril JA, Clark D, et al. Dendritic cells are dysfunctional in patients with operable breast cancer. Cancer Immunol Immunother. 2004;53(6):510–8.

103. Celluzzi CM, Mayordomo JI, Storkus WJ, Lotze MT, Falo LD. Peptide-pulsed dendritic cells induce antigen-specific CTL-mediated protective tumor immunity. J Exp Med [Internet]. 1996;183(1):283–7. Available from: http://www.pubmedcentral.nih.gov/articlerender.fcgi?artid=2192396&tool=pmcentrez&rendertype=abstract

104. Small EJ, Fratesi P, Reese DM, Strang G, Laus R, Peshwa M V, et al. Immunotherapy of hormone refractory prostate cancer with antigen-loaded dendritic cells. J Clin Oncol. 2000;18(23):3894–903.

105. Adema GJ, De Vries IJM, Punt CJA, Figdor CG. Migration of dendritic cell based

cancer vaccines: In vivo veritas? Curr Opin Immunol. 2005;17(2):170–4.

106. Morse MA, Coleman RE, Akabani G, Niehaus N, Coleman D, Lyerly HK. Migration of Human Dendritic Cells after Injection in Patients with. Cancer Res. 1999;59:56–8.

107. Wu L, KewalRamani VN. Dendritic-cell interactions with HIV: infection and viral dissemination. Nat Rev Immunol [Internet]. 2006;6(11):859–68. Available from: http://dx.doi.org/10.1038/nri1960

108. Nikolic DS, Lehmann M, Felts R, Garcia E, Blanchet FP, Subramaniam S, et al. HIV-1 activates Cdc42 and induces membrane extensions in immature dendritic cells to facilitate cell-to-cell virus propagation. Blood. 2011;118(18):4841–52.

109. Felts RL, Narayan K, Estes JD, Shi D, Trubey CM, Fu J, et al. 3D visualization of HIV transfer at the virological synapse between dendritic cells and T cells. Proc Natl Acad Sci U S A [Internet]. 2010;107(30):13336–41. Available from: http://www.scopus.com/inward/record.url?eid=2-s2.0-77955781209&partnerID=tZOtx3y1

110. Trumpfheller C, Finke JS, López CB, Moran TM, Moltedo B, Soares H, et al. Intensified and protective CD4+ T cell immunity in mice with anti-dendritic cell HIV gag fusion antibody vaccine. J Exp Med [Internet]. 2006;203(3):607–17. Available from: http://www.ncbi.nlm.nih.gov/pubmed/16505141%5Cnhttp://www.pubmedcentral.nih.gov/articlerender.fcgi?artid=PMC2118242

111. Lu W, Arraes LC, Ferreira WT, Andrieu J-M. Therapeutic dendritic-cell vaccine for chronic HIV-1 infection. Nat Med [Internet]. 2004;10(12):1359–65. Available

from: http://www.ncbi.nlm.nih.gov/pubmed/15568033

112. Crowley MT, Inaba K, Witmer-Pack MD, Gezelter S, Steinman RM. Use of the fluorescence activated cell sorter to enrich dendritic cells from mouse spleen. J Immunol Methods [Internet]. 1990;133(1):55–66. Available from: http://www.ncbi.nlm.nih.gov/pubmed/2145370

113. Austyn JM, Hankins DF, Larsen CP, Morris PJ, Rao AS, Roake JA. Isolation and characterization of dendritic cells from mouse heart and kidney. J Immunol [Internet]. 1994;152(5):2401–10. Available from: http://dx.doi.org/

114. Saunders D, Lucas K, Ismaili J, Wu L, Maraskovsky E, Dunn A, et al. Dendritic cell development in culture from thymic precursor cells in the absence of granulocyte/macrophage colony-stimulating factor. J Exp Med. 1996;184(6):2185–96.

115. Jakob T, Saitoh a, Udey MC. E-cadherin-mediated adhesion involving Langerhans cell-like dendritic cells expanded from murine fetal skin. J Immunol [Internet]. 1997;159(6):2693–701. Available from: http://www.ncbi.nlm.nih.gov/pubmed/9300689

116. Oehler L, Majdic O, Pickl WF, Stöckl J, Riedl E, Drach J, et al. Neutrophil granulocyte-committed cells can be driven to acquire dendritic cell characteristics. J Exp Med [Internet]. 1998;187(7):1019–28. Available from: http://www.pubmedcentral.nih.gov/articlerender.fcgi?artid=2212207&tool=pmcentrez&rendertype=abstract

117. Sixt M, Lämmermann T. In Vitro Analysis of Chemotactic Leukocyte Migration in 3D Environments. In: Wells CM, Parsons M, editors. Cell Migration [Internet].

Humana Press; 2011. p. 149–65. Available from: http://dx.doi.org/10.1007/978-1-61779-207-6_11

118. Lutz MB, Rößner S. Factors influencing the generation of murine dendritic cells from bone marrow: The special role of fetal calf serum. Immunobiology. 2008;212(9–10):855–62.

119. Brand U, Bellinghausen I, Enk AH, Jonuleit H, Becker D, Knop J, et al. Influence of extracellular matrix proteins on the development of cultured human dendritic cells. Eur J Immunol [Internet]. 1998;28(5):1673–80. Available from: http://www.ncbi.nlm.nih.gov/pubmed/9603474 LA - eng%5Cnhttp://www.ncbi.nlm.nih.gov/pubmed/9603474

120. Sauter A, Mc Duffie Y, Boehm H, Martinez A, Spatz JP, Appel S. Surface-mediated priming during in vitro generation of monocyte-derived dendritic cells. Scand J Immunol. 2015;81(1):56–65.

121. Lutz MB. IL-3 in dendritic cell development and function: A comparison with GM-CSF and IL-4. Immunobiology. 2004;209(1–2):79–87.

122. Takashima A, Edelbaum D, Kitajima T, Shadduck RK, Gilmore GL, Xu S, et al. Colony-stimulating factor-1 secreted by fibroblasts promotes the growth of dendritic cell lines (XS series) derived from murine epidermis. J Immunol. 1995;154(10):5128–35.

123. Grouard G, Rissoan MC, Filgueira L, Durand I, Banchereau J, Liu YJ. The enigmatic plasmacytoid T cells develop into dendritic cells with interleukin (IL)-3 and CD40-ligand. J Exp Med [Internet]. 1997;185(6):1101–11. Available from: http://www.pubmedcentral.nih.gov/articlerender.fcgi?artid=2196227&tool=pmcen

trez&rendertype=abstract

124. Yamaguchi Y, Tsumura H, Miwa M, Inaba K. Contrasting Effects of TGF- β 1 and TNF- α on the Development of Dendritic Cells from Progenitors in Mouse Bone Marrow. Stem Cells. 1997;15:144–53.

125. Maraskovsky E, Daro E, Roux E, Teepe M, Maliszewski CR, Hoek J, et al. In vivo generation of human dendritic cell subsets by Flt3 ligand. Blood. 2000;96(3):878–84.

126. Cox TR, Erler JT. Remodeling and homeostasis of the extracellular matrix: implications for fibrotic diseases and cancer. Dis Model Mech [Internet]. 2011;4(2):165–78. Available from: http://dmm.biologists.org/content/4/2/165

127. James C, Davis R, Kam L. Patterned protein layers on solid substrates by thin stamp microcontact printing. Langmuir [Internet]. 1998;7463(13):741–4. Available from: http://pubs.acs.org/doi/abs/10.1021/la9710482

128. Mata A, Fleischman AJ, Roy S. Characterization of polydimethylsiloxane (PDMS) properties for biomedical micro/nanosystems. Biomed Microdevices. 2005;7(4):281–93.

129. Xia YN, Whitesides GM. Soft lithography. Annu Rev Mater Sci [Internet]. 1998;37(5):551–75. Available from: http://apps.isiknowledge.com/InboundService.do?product=WOS&action=retrieve&SrcApp=Papers&UT=000075395600009&SID=4AeDcEnmon6P1nPEIJo&Init=Yes&SrcAuth=mekentosj&mode=FullRecord&customersID=mekentosj&DestFail=http://access.isiproducts.com/custom_images/wok_f

130. Bernard a, Renault JP, Michel B, Bosshard HR, Delamarche E. Microcontact

printing of proteins. Adv Mater. 2000;12(14):1067–70.

131. Desai R a, Khan MK, Gopal SB, Chen CS. Subcellular spatial segregation of integrin subtypes by patterned multicomponent surfaces. Integr Biol (Camb). 2011;3(5):560–7.

132. Fuard D, Tzvetkova-Chevolleau T, Decossas S, Tracqui P, Schiavone P. Optimization of poly-di-methyl-siloxane (PDMS) substrates for studying cellular adhesion and motility. Microelectron Eng. 2008;85(5–6):1289–93.

133. Tan JL, Tien J, Chen CS. Microcontact Printing of Proteins on Mixed Self-Assembled Monolayers Microcontact Printing of Proteins on Mixed Self-Assembled Monolayers. Langmuir. 2001;18(2):519–23.

134. Tan JL, Liu W, Nelson CM, Raghavan S, Chen CS. Simple approach to micropattern cells on common culture substrates by tuning substrate wettability. Tissue Eng. 2004;10(5–6):865–72.

135. Henry SJ, Crocker JC, Hammer D a. Ligand density elicits a phenotypic switch in human neutrophils. Integr Biol (Camb) [Internet]. 2014;6(3):348–56. Available from: http://www.ncbi.nlm.nih.gov/pubmed/24480897

136. Tan JL, Tien J, Pirone DM, Gray DS, Bhadriraju K, Chen CS. Cells lying on a bed of microneedles: an approach to isolate mechanical force. Proc Natl Acad Sci U S A [Internet]. 2003;100(4):1484–9. Available from: http://www.pnas.org/content/100/4/1484.full

137. Pelham RJ, Wang Y l. High resolution detection of mechanical forces exerted by locomoting fibroblasts on the substrate. Mol Biol Cell [Internet]. 1999;10(4):935–45. Available from:

http://www.pubmedcentral.nih.gov/articlerender.fcgi?artid=25217&tool=pmcentrez&rendertype=abstract

138. Yang MT, Fu J, Wang Y-K, Desai R a, Chen CS. Assaying stem cell mechanobiology on microfabricated elastomeric substrates with geometrically modulated rigidity. Nat Protoc [Internet]. Nature Publishing Group; 2011;6(2):187–213. Available from: http://www.nature.com/doifinder/10.1038/nprot.2010.189

139. Lemmon CA, Sniadecki NJ, Ruiz SA, Tan JL, Romer LH, Chen CS. Shear Force at the Cell-Matrix Interface: Enhanced Analysis for Microfabricated Post Array Detectors. Mech Chem Biosyst. 2005;2(1):1–16.

140. Yang MT, Sniadecki NJ, Chen CS. Geometric considerations of micro- To nanoscale elastomeric post arrays to study cellular traction forces. Adv Mater. 2007;19(20):3119–23.

# CHAPTER 3 : CHARACTERIZING DC RANDOM MIGRATION ON PDMS SURFACES

ABSTRACT

Previous studies of DC chemokinesis were performed on glass surfaces physisorbed with either collagen or fibronectin (1). While glass and plastic tissue culture surfaces have been very useful in initial characterization of many cell types, they are not physiologically relevant and are much less versatile than PDMS. I have used a system consisting of PDMS spin-coated coverslips microcontact printed with fibronectin to characterize DC random migration. This setup allows us to expose DCs to a surface with more relevant compliance and to spatially regulate ligand presentation with great precision. I assayed a variety of fibronectin concentrations and found that while DCs require the presence of fibronectin on the surface to adhere and migrate, they are insensitive to the specific concentration of ligand. Likewise, they migrate robustly in the presence of chemokine, regardless of the concentration present. At each of the ligand and chemokine concentrations tested, I quantified migration in terms of average speed, persistence and the random motility coefficient. In addition to these motility measurements, I used PDMS structures known as mPADs (micropost array detectors) to measure the traction forces of DCs. Collectively, these measurements provide a fundamental understanding of DC chemokinesis on PDMS substrates as well as a basis for comparison in future in-depth studies.

## INTRODUCTION

DCs are critical components of the immune system, responsible for recognizing pathogenic agents in the body and transmitting signals of the infection to T cells in secondary lymphoid organs (2). In order for effective antigen presentation to occur, DCs must be able to travel from sites of antigen detection to T-cell rich areas of the lymph node (3). Along the way, they encounter many different environments and employ many different modes of migration. In this and subsequent chapters, I investigate DC chemokinesis, or random migration in the absence of any chemical gradients. While chemotaxis, or directed migration, is important for guiding DCs from peripheral tissues to the lymph node, DC chemokinesis has been observed in the lymph node itself (3–5).

In my experiments, I use fibronectin, which is a ubiquitously expressed extracellular matrix (ECM) protein, found in many environments encountered by DCs, including the lymph node (6). While it has been shown that DCs can migrate in the absence of integrins in 3D, integrin-mediated adhesion to the ECM is required for migration in 2D (7). Bone marrow-derived DCs (BMDCs) express high levels of $\alpha_5\beta_1$ and can readily bind to fibronectin, thus making it a good choice for studying DCs in vitro (1,7). 2D migration is often thought to have little physiologic relevance, but certain environments in vivo promote this crawling type of migration over integrin-independent, 3D swimming (8). For example, it is believed that once DCs reach the lymph node, they adhere and migrate along the reticular network in their search of T cells (8).

In addition, my experimental setup allows us to study DCs in an environment with a more physiologically relevant stiffness. AFM measurements of my surfaces indicate that the spun layer of PDMS is on the order of $10^2$ kPa. The compliance of healthy

lymph nodes is on the order of 10 kPa (9). While my substrates are still an order of magnitude stiffer than lymph nodes, they provide a much closer approximation to the DCs' native environment than glass or plastic surfaces, which are on the order of $10^6$ kPa (10). Taken together, I believe that characterizing the random migration of mature DCs on PDMS-coated coverslips that have been microcontact printed with fibronectin, will provide a useful and relevant set of information about how DCs might behave in vivo once they reach the lymph node.

In this chapter, I provide a description of the methods used to quantify DC random migration. I begin by assaying a variety of fibronectin and chemokine concentrations in order to determine the optimal parameters for DC chemokinesis. At each set of conditions, I used a persistent random walk model to calculate average speed, persistence and the random motility coefficient. I conclude that while the presence of fibronectin is required for cell adhesion to the substrate, the precise concentration of fibronectin and chemokine does not greatly influence migration. In addition, I used mPADs to resolve and quantify the low magnitude traction forces exerted by migrating DCs. The combination of these measurements provides a thorough biophysical description of DC random migration.

## MATERIALS AND METHODS

### *Mice*

C57BL/6J mice from Jackson Laboratories were housed under pathogen-free conditions in the Children's Hospital of Philadelphia animal facility. All studies involving animals were reviewed and approved by the Children's Hospital of Philadelphia Institutional Animal Care and Use Committee.

### *Generation of Primary BMDCs*

DCs were generated from murine bone marrow following the protocol of Sixt and Lammermann (11). Mice were euthanized with $CO_2$ and cervical dislocation. Femurs and tibias were removed and flushed with sterile PBS. Cells were spun for 10 minutes at 1500 rpm and 4°C and resuspended at 2.5 x $10^6$ cells/mL in R10 media (RPMI 1640 supplemented with 10% FBS and 1% penicillin-streptomycin). Cultures were started in 10 cm Bacterial Petri dishes by combining 1 mL of cell suspension, 9 mL R10 and 100 µL GM-CSF. On day 3, 10 mL fresh media and 100 µL GM-CSF were added to each Petri dish. On day 6, 10 mL of spent media was gently removed from each dish before adding 10 mL fresh media and 100 µL GM-CSF. On day 7 or 8, DCs were spun for 10 minutes at 1500 rpm and 4°C, resuspended in 10 mL R10 per plate and added to 6 cm TC dishes along with 200 ng/mL LPS. After 24 hours, DCs were centrifuged for 10 minutes at 1500 rpm and 4°C, and resuspended at 100,000 cells/mL. Cells were maintained at 37°C and 5% $CO_2$ throughout the entire culture period.

*Preparation of Migration Surfaces*

My standard migration surfaces consisted of glass coverslips spun with PDMS, stamped with fibronectin and adhered to the bottom of a 6 well or 1 well dish. First, a 10:1 solution (base:cure by weight) of PDMS was mixed and degassed. 25 mm round glass coverslips were cleaned of debris with $N_2$ gas. A thin layer of PDMS was evenly spun on the surface of the coverslip using a Laurell spinner (4000 rpm, 1 minute). Spin-coated coverslips were baked overnight at 65°C. Spun coverslips were fixed to the bottom of laser-cut wells with a thin layer of PDMS and cured for 1 hour at 65°C.

Fibronectin was transferred to the PDMS-coated coverslips through microcontact printing. 66 grams of 10:1 PDMS (base: cure, by weight) was mixed and degassed for 1 hour. It was then cast against a clean, flat silicon wafer and baked at 65°C overnight. The following day, the PDMS was carefully pulled away from the wafer and cut into 1 $cm^2$ stamps. Stamps were sonicated for 5 minutes in 200 proof ethanol to clean the surface. The clean stamps were rinsed 2x in di$H_20$, dried with $N_2$ gas and inked with a solution of fibronectin (Sigma-Aldrich), ranging from 1 μg/mL to 100 μg/mL. The inked stamps were incubated for 2 hours, gently rinsed 2x in di$H_20$ and gently dried with $N_2$ gas. The PDMS-coated coverslips were treated with UV ozone for 7 minutes. Fibronectin was printed on the treated coverslips by bringing the stamp into contact with the coverslip surface. The coverslips were blocked with Pluronic F127 for 1 hour at room temperature, rinsed 2x with sterile PBS and stored at 4°C overnight.

*Random Migration Assays*

Mature DCs in RPMI, at a concentration of 100,000 cells/mL were added to the PDMS-coated coverslips along with the desired chemokine. After a brief incubation to allow the cells to adhere to the surface, the plate was moved to a Nikon Eclipse TE300 (Nikon, Melville, NY). DCs were imaged at 10x by phase microscopy using custom-built Labview (National Instruments, Austin, TX) software. A motorized stage was used to capture images at multiple positions. Images were collected every 2 minutes over a period of 2 hours. Cells were maintained at 37°C and 5% $CO_2$ for the duration of the experiments.

Image sequences were opened in ImageJ (NIH; http://rsbweb.nih.gov/ij) and the Manual Tracking plugin was used to track cell position over time. Cells that were apoptotic or completely stationary were excluded, as well as any cells in contact with other cells. I imported the file containing cell tracks to MATLAB (Mathworks, Natick, MA) and used a custom-written code to calculate the MSD. The Dunn equation $\left(\langle MSD(\tau)\rangle = 2S^2P\left[\tau - P\left(1 - exp\left(-{}^{\tau}/_{P}\right)\right)\right]\right)$ was used to fit speed (S) and persistence (P) to the MSD (12). The random motility coefficient was calculated from the speed and persistence as follows: $\mu = \frac{1}{n}S^2P$, where n specifies the dimensionality (12).

*Fabrication of mPADs*

mPADs were created by replica molding of PDMS. Patterned silicon masters were kindly provided by Christopher Chen and were coated with silane by vapor deposition in a vacuum chamber. Negative molds were created by casting 22 grams of

degassed 10:1 PDMS (base: cure by weight) against the silicon mold and curing for 12 minutes at 110°C. The molds were carefully pulled away from the master, plasma etched for 7 seconds and silanized overnight. 2 grams of 10:1 PDMS (base:cure, by weight) was degassed and cast against the silanized negative molds and degassed for a further 30 minutes. 25 mm glass coverslips were cleaned with $N_2$ gas and plasma treated for 90 seconds. The PDMS-coated molds were adhered to the glass coverslips and cured at 110 °C for 20 hours. The mPADs were removed from the oven, cooled to room temperature and gently peeled from the molds. They were then sonicated in 200 proof ethanol and supercritical dried.

mPAD-coated coverslips were fixed to the bottom of one well dishes with a thin layer of PDMS and cured for an hour at 65°C. Fibronectin was added to the post tips by microcontact printing as described above, with minor modifications. After gently stamping fibronectin onto the post tips, 1.4 mL of 200 proof ethanol was added to the mPAD and the stamp was gently flicked away. The ethanol was immediately diluted by adding 1 mL of di$H_2O$, and the mPAD was gently rinsed 3x with di$H_20$, being careful not to completely dewet the surface. The mPADs were incubated with 1 mL of 1x Δ9-DiI (1,1′-dioleyl-3,3,3′,3′-tetramethylindocarbocyanine methanesulfonate; Invitrogen Carlsbad, CA) for one hour, at room temperature. From this point onwards, I minimized mPAD exposure to light. The dye was removed, the mPAD was washed 3x with di$H_2O$ and it was blocked with Pluronic F127 for 1 hour at room temperature. The mPAD was rinsed 3x with di$H_20$ and stored at 4°C overnight.

*Force Measurement Assays*

Mature DCs, at a concentration of 50,000 cells/mL in RPMI were added to the mPAD substrate along with the desired chemokine. They were incubated briefly to allow for cell adhesion prior to imaging. Samples were imaged at 40x by phase and fluorescence microscopy on a Nikon Eclipse TE300 Microscope (Nikon, Melville, NY) with custom-built Labview (National Instruments, Austin, TX) software. A motorized stage was used to capture images every 2 minutes for 30 minutes at multiple positions. Cells were maintained at 37°C and 5% $CO_2$ throughout the duration of the experiment and light exposure was minimized.

Images were imported into MATLAB and a custom-written script was used to compute traction forces. Phase images were used to identify the position of DCs and fluorescent images were used to identify the position of post tips. Deflections from the ideal, hexagonally packed array, were detected and converted into traction forces using Hooke's Law ($F = kx$) and the spring constant of the micropost array (k=1.92 nN/μm). These forces were then used to calculate the total scalar force per cell.

## RESULTS

### *Quantification of Chemokinesis*

I began by quantifying DC random migration under a variety of fibronectin and chemokine concentrations. The $K_D$ of CCR7 for both CCL19 and CCL21 is ~10 nM (13). In my initial experiments, I explored three different chemokine conditions—CCL19 alone, CCL21 alone or no chemokine. I held the level of chemokine constant, at a concentration of twice the $K_D$, which I hypothesized would be close to the optimal concentration. At each of these chemokine conditions, I varied the fibronectin inking concentration over the range of 0.1 μg/mL to 100 μg/mL. As a first step of my analysis, I used the Manual Tracking plug-in from ImageJ to track cell position over time. Figure 3.1A and B show a sample population of DCs and their corresponding trajectories. All trajectories are pseudo-centered at the origin and emanate randomly from the center. There is no directional preference, as one would expect with uniform chemoattractant.

I then used these tracks to compute the mean squared displacement (MSD) as a function of time. When plotted on a log-log scale, the slope of the MSD curve gives a semi-quantitative description of the type of migration. If the slope is less than one, migration is in the subdiffusive regime; if the slope is greater than 1, migration is in the superdiffusive regime; and if the slope is equal to 1, migration is in the diffusive regime. For this sample population of randomly migrating DCs, the MSD curve has a slope of approximately 1, confirming that DCs migrate diffusively or randomly, during chemokinesis (Figure 3.1C).

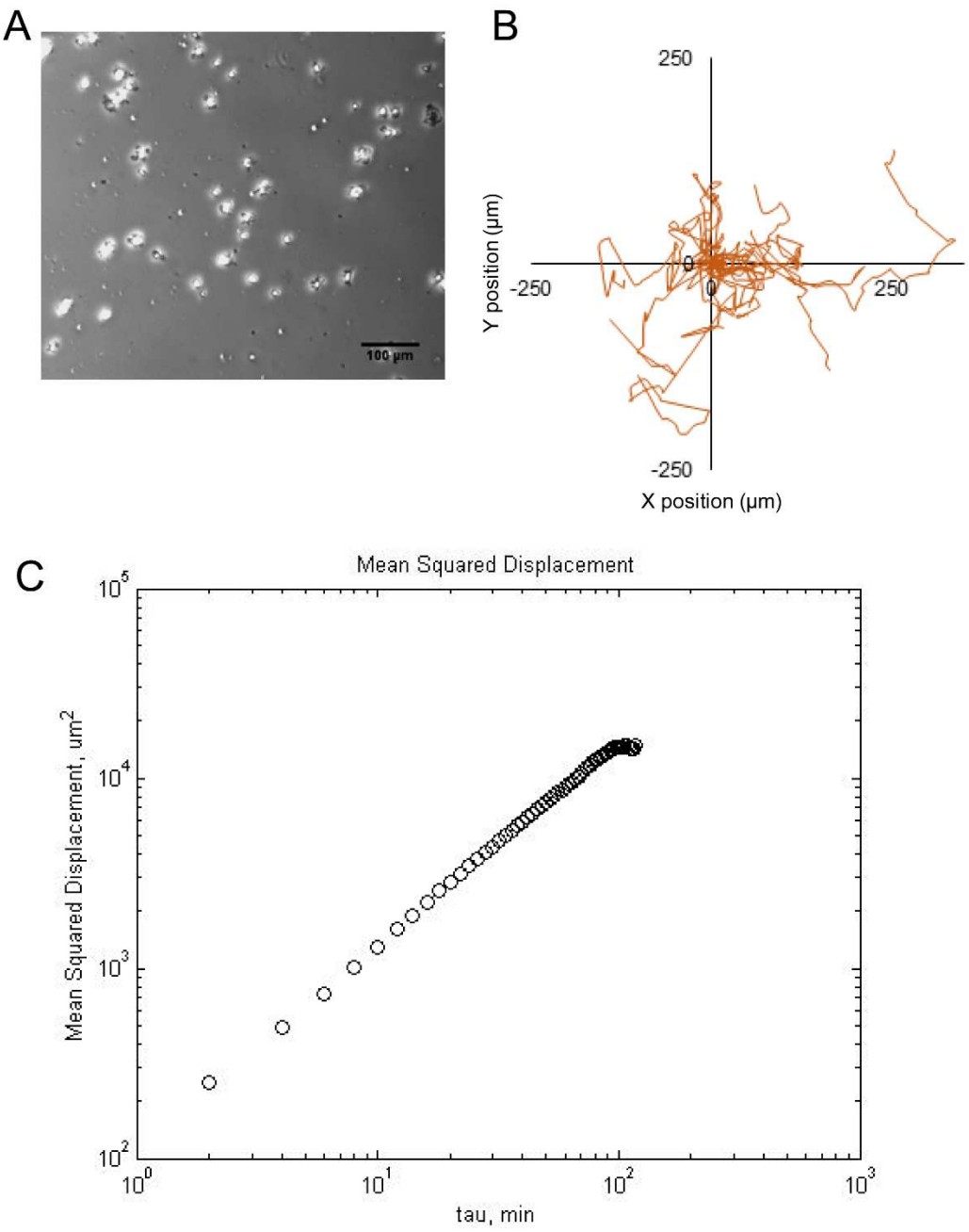


*Figure 3.1. Dendritic cells migrate randomly during chemokinesis.*

A) Sample phase contrast image of mDCs on PDMS-coated coverslips printed with 1 µg/mL fibronectin. The cells have also been exposed to 20 nM CCL19. Scale bar represents 100 µm. B) Cell trajectories for mature DCs shown in A). C) Mean squared

displacement vs. time for the randomly migrating DCs shown in A). Both axes are on a log scale and the slope is approximately equal to 1.

As a final step of the analysis, I fit the MSD to the Dunn Equation (Equation 3.1), which is a model for persistent random walks (12). This allowed us to calculate a variety of useful motility metrics, including average cell speed (S) and persistence time (P; length of time a cell moves in one direction before changing directions). I then used speed and persistence time to calculate persistence length ($P_L$; the distance traveled before changing directions; Equation 3.2) and the random motility coefficient (μ; a measure of cell diffusivity; Equation 3.3). In these equations, n refers to dimensionality, which in my case is 2.

$$\left(\langle MSD(\tau)\rangle = 2S^2P\left[\tau - P\left(1 - exp\left(-{}^{\tau}/_{P}\right)\right)\right]\right)$$

Equation 3.1

$$P_L = (S)(P)$$

Equation 3.2

$$\mu = \frac{1}{n}S^2P$$

Equation 3.3

Figure 3.2 shows the results from these calculations. For optimization purposes, I focused on average speed (Figure 3.2A) and the random motility coefficient (Figure 3.2D), since these give a description of how quickly the cells move and the area swept out by the DCs during chemokinesis, respectively. The presence of chemokine did not affect DC migration at most printed concentrations of fibronectin, although it did impart a significant increase in diffusivity at 10 μg/mL of fibronectin (Figure 3.2D). There was no clear optimal concentration of fibronectin for DC chemokinesis in this range. Despite the

lack of a clear preference for the level of fibronectin, I determined that lowering the level of fibronectin below this range prohibited DC adhesion and migration (data not shown). Collectively, this suggests that during 2D chemokinesis, DCs require the presence of ECM protein and are able to adapt their migration to a variety of concentrations.

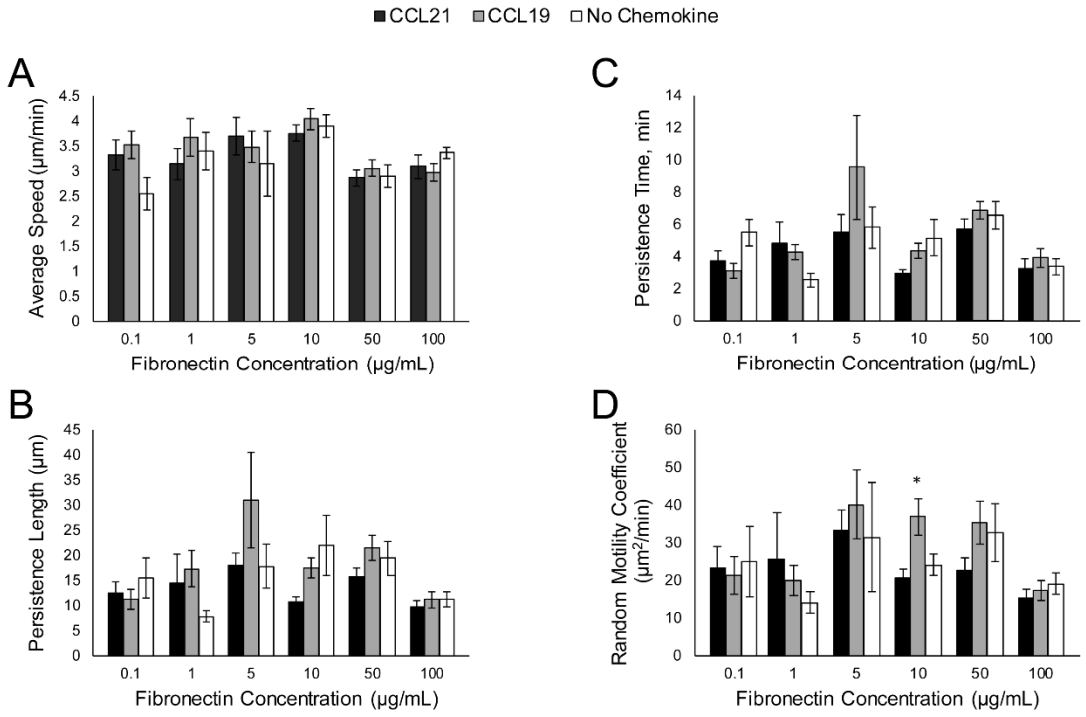


*Figure 3.2. Quantification of DC chemokinesis as a function of fibronectin concentration.* A) Average speed, B) persistence time, C) persistence length and D) random motility coefficient. Concentration of CCL19 and CCL21 was 20 nM. Figures represent average values ± SEM, for > 75 DCs from at least three independent experiments per condition. Statistical significance calculated with single factor ANOVA and post hoc Tukey test. * indicates significant difference compared to No Chemokine condition. *$p<0.05$

I next varied the concentrations of CCL19 and CCL21 over the range of 0 to 100 nM. As I saw with the response to varying surface ligand, variations in soluble chemokine had little effect on DC migration (Figure 3.3). Because DCs migrated well even in the absence of chemokine, I considered the possibility that serum in the media was saturating soluble cues. I tested three conditions, in which DCs were deprived of serum for different amounts of time—serum deprived immediately before running the experiment, 3.5 hour serum starve and 24 hour serum starve. When DCs were deprived of serum for any length of time, their migration was almost completely abrogated. As a result, I continued to use serum in all future experiments.

Despite finding no significant optimal conditions for fibronectin concentration or chemokine concentration, I did show that mature DCs migrate well on microcontact printed PDMS surfaces. Moving forward I chose one set of conditions (10 nM CCL19 and 10 μg/mL fibronectin), for consistency. Table 3.1 shows the values for average speed, persistence time, persistence length and random motility coefficient at these conditions.

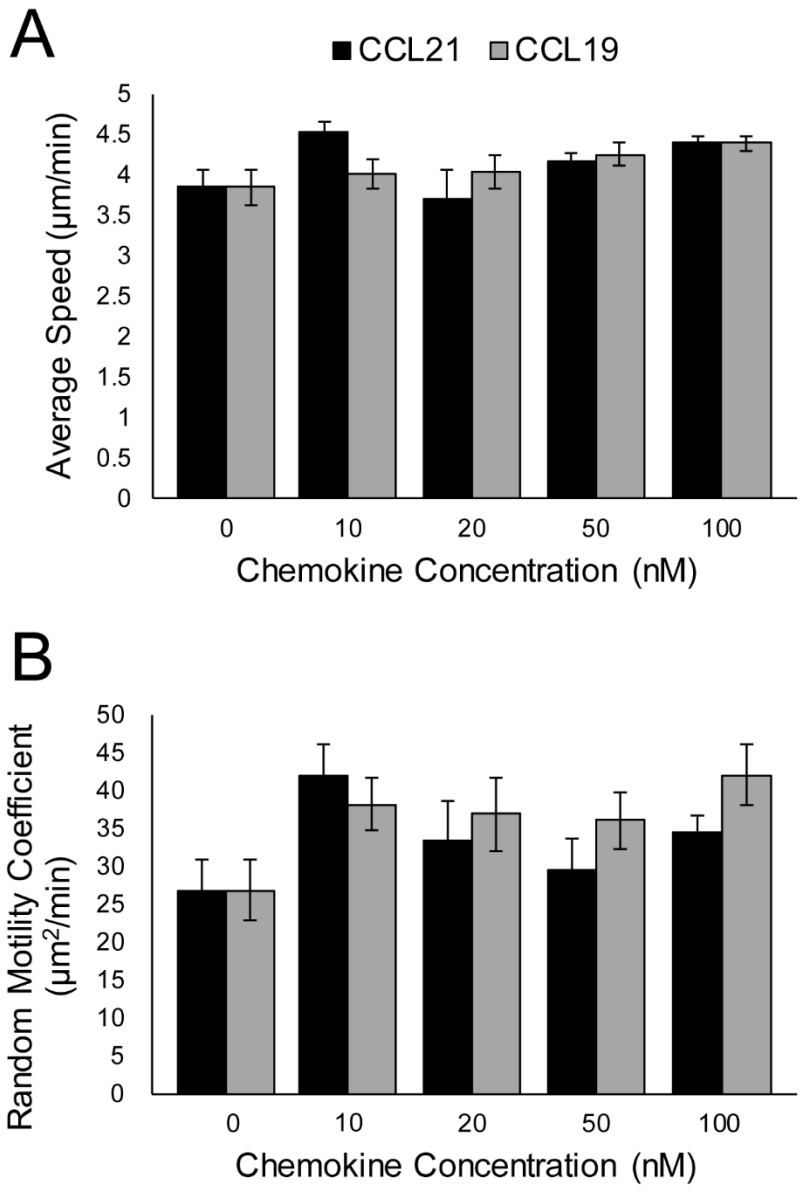


*Figure 3.3. Quantification of DC chemokinesis as a function of chemokine concentration.* A) Average speed and B) the random motility coefficient. Figures represent average values ± SEM, for > 300 DCs from at least three experiments per condition.

*Table 3.1. Values for DC chemokinesis parameters at 10 μg/mL fibronectin and 10 nM CCL19.*

| **Parameter** | **Average Value** |
|---|---|
| Average Speed, μm/min | 4.00 ± 0.18 |
| Persistence Time, min | 4.88 ± 0.46 |
| Persistence Length, μm | 19.00 ± 1.57 |
| Random Motility Coefficient, $\mu m^2$/min | 38.20 ± 3.41 |

*Quantification of Traction Forces*

I also measured traction forces during my initial analysis of DC chemokinesis. mPADs are the best technology available for resolving the small forces exerted by DCs. DC forces during chemotaxis have been previously characterized (14) and I now sought to characterize DC forces of chemokinesis. Randomly migrating DCs are able to adhere to and engage with the micropost tips. For my force measurement experiments I gather two sets of images—phase and fluorescence. A sample of each is shown in Figure 3.4. Post deflections can be readily observed at the periphery of the cell. I converted these post deflections into traction forces and visualized the distribution of forces as a series of vectors overlaid on the appropriate engaged micropost (Figure 3.4C). The sample cell shown in Figure 3.4A exerted strong, tugging forces at the periphery, pulling microposts in towards its center. This is shown by the distribution of relatively large, radially oriented vectors in Figure 3.4C.

After computing the traction forces of many DCs, I computed the total scalar force magnitude as a function of time (Figure 3.4D). While the vector forces of any given cell should sum to zero, the scalar force magnitude is a nonzero, positive value and provides an idea of the overall strength of DC interactions with their substrate. I began taking measurements of forces 15 minutes after addition of DCs to the mPAD, allowing them time to adhere to the microposts tips. Time zero in Figure 3.4D corresponds to the first minute of imaging and laser exposure. At early imaging timepoints, I see an increase in force. This initial rise is followed by a force plateau, although even during the "plateau" regime there is a fair bit of fluctuation. Finally, I computed a time and ensemble average of force per cell. Mature DCs migrating randomly on mPADs generate

a total force of 13.76 ± 0.84 nN. This value is the same order of magnitude as the previously reported value for DC force generation during chemotaxis (14).

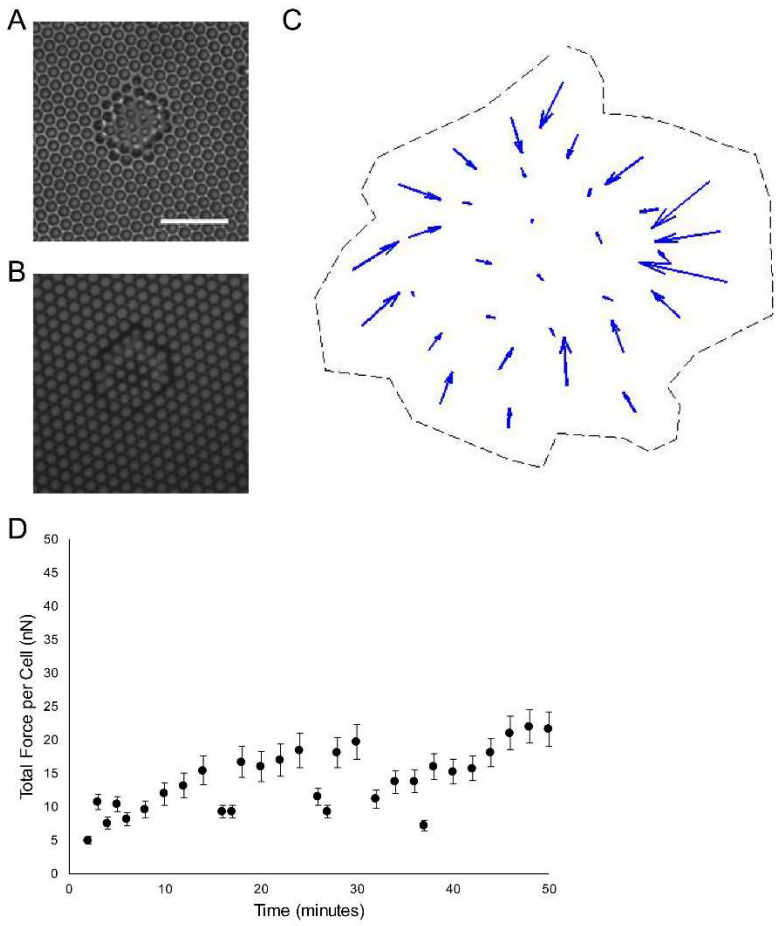


*Figure 3.4. Quantification of DC traction forces during chemokinesis.*

A) Sample phase and B) fluorescent images of a DC on an mPAD printed with 10 μg/mL fibonectin. 10 nM soluble CCL19 was also present. Scale bar represents 20 μm. Post deflections from B) were used to calculate the vector force per post and scalar force magnitude. C) Vector forces produced by the cell shown in A). D) Average traction force as a function of time. The values correspond to the total scalar force magnitude of 29 mature DCs from 3 independent experiments.

## DISCUSSION

The results from this chapter lay the groundwork for my future studies into the biomolecular and biophysical aspects of DC chemokinesis. I selected a set of standard conditions and quantified the speed, persistence and random motility at these conditions. While it may seem counterintuitive that DCs do not respond to fibronectin or chemokines in a biphasic manner, this finding is consistent with previous studies of DCs on glass (1). DCs did respond in a biphasic manner when migrating on collagen, but were unresponsive to differences in concentration on fibronectin (1). This suggests that when studying DC migration, observations might be ligand specific. Attempts to optimize migration by varying the chemokine concentration or removing serum from the solution were unsuccessful. These observations are supported by a recent study by Haessler et al., who compared potencies of CCL19 and CCL21 for DC migration and observed that while both induced very strong chemotaxis, they had little influence in chemokinesis (15).

Overall my quantification of DC random migration on PDMS-coated coverslips fits well with a model for persistent random walk. The slope of the MSD versus time is a linear, with a slope approximately equal to one, indicating pure diffusion. In addition, it has been shown that the speed and persistence time of randomly migrating cells are inversely correlated (Figure 3.5; (16)). My results also follow this relationship (16). Furthermore, the value I calculated for average cell speed agrees well with a variety of in vitro and in vivo measurements (7,17). While DC speed appears to be very robust across a variety of environments, persistence time for DCs in different environments is not well characterized and will be a topic of discussion in the next chapter. Taken together, I

conclude that PDMS-coated coverslips are excellent surfaces to use in the study of DC chemokinesis.

My traction force analysis confirmed the usefulness of mPADs for measuring DC traction forces. In my experiments, I exposed DCs to a uniform concentration of chemokine, whereas previous measurements were made for DCs exposed to a gradient of chemokine (14).

In addition, while fibronectin was printed on the micropost tips in both sets of experiments, the concentration was 5-fold less in my studies. In spite of these differences, I see similar levels of forces generated. DCs during chemokinesis generate 13.76 ± 0.84 nN per cell, whereas DCs during chemotaxis generate 18 ± 1.4 nN/cell (14). It has been shown that DCs migrating up a gradient concentrate strong traction forces at the leading edge (14). Because I studied random motility, in which there is no persistent leading edge, this observation was not as apparent. Further analysis could be performed to correlate force distribution and direction of migration. Collectively, my experiments quantifying random migration parameters and traction forces provides a clear description of how DCs behave during chemokinesis, and lays the groundwork for the results presented in the next two chapters.

REFERENCES


1. Ricart BG. Dendritic Cell Migration and Traction Force Generation in Engineered Microenvironments. University of Pennsylvania Scholarly Commons. 2010.
2. Banchereau J, Briere F, Caux C, Davoust J, Lebecque S, Liu Y, et al. Immunobiology of Dendritic Cells. Annu RevImmunology. 2000;18:767–811.
3. Förster R, Davalos-Misslitz AC, Rot A. CCR7 and its ligands: balancing immunity and tolerance. Nat Rev Immunol [Internet]. 2008;8(5):362–71. Available from: http://www.ncbi.nlm.nih.gov/pubmed/18379575
4. Bousso P, Robey E. Dynamics of CD8+ T cell priming by dendritic cells in intact lymph nodes. Nat Immunol. 2003;4(6):579–85.
5. Miller MJ, Hejazi AS, Wei SH, Cahalan MD, Parker I. T cell repertoire scanning is promoted by dynamic dendritic cell behavior and random T cell motility in the lymph node. Proc Natl Acad Sci U S A [Internet]. 2004;101(4):998–1003. Available from: http://www.pubmedcentral.nih.gov/articlerender.fcgi?artid=327133&tool=pmcentrez&rendertype=abstract%5Cnhttp://www.ncbi.nlm.nih.gov/pubmed/14722354%5Cnhttp://www.pubmedcentral.nih.gov/articlerender.fcgi?artid=PMC327133
6. Sobocinski GP, Toy K, Bobrowski WF, Shaw S, Anderson AO, Kaldjian EP. Ultrastructural localization of extracellular matrix proteins of the lymph node cortex: evidence supporting the reticular network as a pathway for lymphocyte migration. BMC Immunol [Internet]. 2010;11:42. Available from: http://www.ncbi.nlm.nih.gov/pubmed/20716349%5Cnhttp://www.pubmedcentral.nih.gov/articlerender.fcgi?artid=PMC2933709

7. Lämmermann T, Bader BL, Monkley SJ, Worbs T, Wedlich-Söldner R, Hirsch K, et al. Rapid leukocyte migration by integrin-independent flowing and squeezing. Nature [Internet]. 2008;453(7191):51–5. Available from: http://www.nature.com/doifinder/10.1038/nature06887%5Cnhttp://www.ncbi.nlm.nih.gov/pubmed/18451854

8. Gretz JE, Kaldjian EP, Anderson a O, Shaw S. Sophisticated strategies for information encounter in the lymph node: the reticular network as a conduit of soluble information and a highway for cell traffic. J Immunol. 1996;157(2):495–9.

9. Kilic F, Velidedeoglu M, Ozturk T, Kandemirli S, Dikici A, Er M, et al. Ex Vivo Assessment of Sentinel Lymph Nodes in Breast Cancer Using Shear Wave Elastography. J Ultrasound Med. 2016;35(2):271–7.

10. Cox TR, Erler JT. Remodeling and homeostasis of the extracellular matrix: implications for fibrotic diseases and cancer. Dis Model Mech [Internet]. 2011;4(2):165–78. Available from: http://dmm.biologists.org/content/4/2/165

11. Sixt M, Lämmermann T. In Vitro Analysis of Chemotactic Leukocyte Migration in 3D Environments. In: Wells CM, Parsons M, editors. Cell Migration [Internet]. Humana Press; 2011. p. 149–65. Available from: http://dx.doi.org/10.1007/978-1-61779-207-6_11

12. Dunn GA. Characterising a kinesis response: time averaged measures of cell speed and directional persistence. [Internet]. Agents and actions. Supplements. 1983. p. 14–33. Available from: http://www.ncbi.nlm.nih.gov/pubmed/6573115

13. Ricart BG, John B, Lee D, Hunter CA, Hammer DA. Dendritic cells distinguish individual chemokine signals through CCR7 and CXCR4. J Immunol [Internet].

2011;186(1):53–61. Available from: http://www.jimmunol.org/cgi/doi/10.4049/jimmunol.1002358

14. Ricart BG, Yang MT, Hunter C a., Chen CS, Hammer D a. Measuring traction forces of motile dendritic cells on micropost arrays. Biophys J [Internet]. Biophysical Society; 2011;101(11):2620–8. Available from: http://dx.doi.org/10.1016/j.bpj.2011.09.022

15. Haessler U, Pisano M, Wu M, Swartz MA, Rakesh Jain by K. Dendritic cell chemotaxis in 3D under defined chemokine gradients reveals differential response to ligands CCL21 and CCL19. Proc Natl Acad Sci USA. 2011;108(14):5614–9.

16. Lauffenburger DA, Linderman J. Receptors: Models for Binding, Trafficking, and Signaling. Oxford; 1996.

17. Pulecio J, Tagliani E, Scholer A, Prete F, Fetler L, Burrone OR, et al. Expression of Wiskott-Aldrich syndrome protein in dendritic cells regulates synapse formation and activation of naive CD8+ T cells. J Immunol. 2008;181(2):1135–42.

# CHAPTER 4 : BIOPHYSICAL COMPONENTS OF DC RANDOM MIGRATION

Adapted from: **Motile Dendritic Cells Sense and Respond to Substrate Geometry**

Amy C. Bendell, Edward K. Williamson, Christopher S. Chen, Janis K. Burkhardt, Daniel A. Hammer

Submitted to *The Annals of Biomedical Engineering*

ABSTRACT

Dendritic cell (DC) migration is required for efficient presentation of antigen to T cells and the initiation of an adaptive immune response. In spite of the importance of migration for DC function, many aspects of its migration have not yet been characterized. One question in particular that remains unanswered is how DCs respond to differences in their microenvironment. I have previously quantified DC migration on polydimethylsiloxane (PDMS)-coated glass coverslips and measured DC traction forces on micropost array detectors (mPADs) made from PDMS. mPADs differ from spin-coated PDMS in both stiffness and geometry. Since DCs encounter a variety of environments with different stiffness and geometry, but the effect of these parameters on DC migration has not yet been determined, I sought to address this question. I found that DCs migrate well on mPADs printed with fibronectin, with a significant increase in average speed and a significant decrease in persistence time as compared to spin-coated PDMS. To determine whether the geometry or compliance of the post arrays was responsible for these changes in DC migration, I quantified DC migration using several different mPAD geometries. For mPADs with the same geometry but a different stiffness, migration was indistinguishable, indicating that DCs are insensitive to changes in stiffness over the range tested (~1 kPa to 1000 kPa). I tested an additional mPAD with smaller post diameter to determine how sensitive DCs are to post geometry and determined that DCs cannot sense differences in geometry on the micron scale. I further investigated geometry sensing by printing ligands on PDMS-coated coverslips in patterns resembling the geometrical pattern of the tips of mPADs, and determined that the DC response to geometry is due to ligand patterning. Indeed the response was

indistinguishable between printed continuous surfaces and on mPAD arrays. Finally, I used a variety of small molecule inhibitors to determine what pathways are involved in the motile response of DCs to geometry. I saw significant effects in the ability of DCs to sense geometry when I inhibited myosin contractility with blebbistatin and when I blocked adhesion through the integrin $\alpha_5\beta_1$. I also noted significant reorganization of the actin cytoskeleton into dynamic actin rings when DCs were motile on posts. From these experiments, I conclude that DCs are insensitive to substrate compliance but respond to changes in geometry via a mechanism that involves integrin function, myosin contractility, and the remodeling of the actin cytoskeleton.

## INTRODUCTION

Dendritic cells (DCs) are antigen presenting cells, capable of activating naive T cells and launching potent adaptive immune responses (1). As immature cells, DCs are distributed throughout peripheral tissues, where they continuously capture and degrade material from the environment, displaying peptide fragments on surface-bound MHC complexes. When DCs detect molecular signs of infection and inflammation (2), they undergo a series of phenotypic and functional changes, a process termed maturation (3). Mature DCs become highly migratory and travel to T cell-rich areas of lymphoid tissues where they present surface bound antigens to T cells and activate them (4). DC migration is therefore critical to the ability of the body to launch a proper immune response.

One remarkable aspect of DC biology is their ability to migrate robustly through a wide range of body tissues (5). We and others have previously explored the influence of chemokine signals on DC migration and force generation during chemokinesis and chemotaxis (6–8). One of the most important chemokine receptors on DCs is CCR7, which interacts with two separate chemokines - CCL19 and CCL21 (9). The interplay between these chemokine cues is partially responsible for orchestrating the intricate trafficking patterns of DCs in the body (7,10). However, chemical cues are not the only signals that DCs receive. Like all cells, migrating DCs must adjust to the mechanical and geometric characteristics of the microenvironment (11). Geometry, whether physical topography or the spatial patterning of extracellular matrix ligands, has been shown to control cell adhesion, guide cytoskeletal organization, determine cell morphology and regulate migration (12–14). Likewise, stiffness strongly influences the physiology of many cell types, including their differentiation, adhesion, force generation and migration

(15–18). In particular, most immune cells respond to differences in the mechanics of their substrate. Both B cell and T cell activation are regulated by substrate stiffness (19,20). Neutrophil adhesion, directed migration and force generation increase with substrate stiffness, and the magnitude of forces generated by macrophages is dependent on substrate stiffness (21,22). To my knowledge, it is unknown how DCs respond to the biomechanical and topological properties of their surroundings.

Micropost array detectors (mPADs) were developed as tools for probing cellular traction forces (23). The geometry of the mPADs can be finely tuned to yield posts with different shapes, diameters, post-to-post spacing and heights (16,24). The ability to alter the post height independently of the other parameters is particularly useful, as it allows for the generation of a family of substrates with similar topography but differing stiffness (24). In addition, mPADs are more sensitive than other force measurement methods, and thus are better suited for the measurement of weak forces produced by fast moving cells such as DCs. I have used mPADs to measure the forces that DCs exert during chemotaxis and chemokinesis (Chapter 3 and (8,25)). While mPADs are useful tools for measuring forces of migration, I have not considered how switching the substrate from a PDMS-coated coverslip to an mPAD array might affect the ability of the DCs to migrate. It stands to reason that the geometry of the contact points, as presented by the tips of the posts, might influence the ability of the DC to organize its migration machinery. Also, the compliance of those contacts might affect the ability of DCs to push off the substrate.

In the work that follows, I use the terms stiffness, elasticity and compliance to describe how stiff the external environment appears to migrating DCs. Geometry refers to both the physical structure of the substrate as well as the patterning of ligand. I will

specify ligand geometry when I am specifically focusing on that parameter. The word discretization is used to describe a surface with discontinuous geometry. Finally, I use the word topology to describe all of these physical characteristics collectively.

The goal of the present study was to determine how DCs respond to the physical characteristics of their surroundings. I observed that DC migration was unaffected by variations in stiffness over the range of 1 to 1,000 kPa, but was sensitive to the geometry of the substrate. I further confirmed the effect of geometry on the dynamics of motility by testing patterns of ligands printed on PDMS surfaces, and confirmed that the changes in motility are due to changes in the geometry of ligand presentation. Further, I saw that DC responses to geometry are regulated by actomyosin contractility and integrin-based adhesions. Taken together, this work supports the observation that DCs are able to adapt to and migrate in microenvironments of different geometry, which has implications for how DCs maneuver in vivo. A greater understanding of how DCs modulate their migration in different environments can be applied to the development and administration of immunotherapies to optimize treatment efficacy and delivery.

## MATERIALS AND METHODS

### *Reagents*

Recombinant murine CCL19 was purchased from R&D Systems (Minneapolis, MN). Lipopolysaccharide (LPS; L4516), DMSO, Pluronics F127, silane (Trichloro(1H,1H,2H,2H-perfluorooctyl)silane) and bovine fibronectin were obtained from Sigma-Aldrich (St. Louis, MO). PBS was obtained from Thermo Fisher Scientific (Hampton, NH). Poly(dimethylsiloxane) (Sylgard 184 Silicone Elastomer) was purchased from Dow Corning, Midland, MI. Fetal bovine serum was obtained from Atlanta Biologicals (Flowery Branch, GA). Recombinant GM-CSF was produced from the B78Hi/GMCSF.1 cell line provided by T. Laufer (University of Pennsylvania, Philadelphia, PA).

### *Mice*

C57BL/6J mice from Jackson Laboratories and GFP-Lifeact mice bred on the C57BL/6J background (26) were housed under pathogen-free conditions in the Children's Hospital of Philadelphia animal facility. All studies involving animals were reviewed and approved by the Children's Hospital of Philadelphia Institutional Animal Care and Use Committee.

### *Culture of Bone Marrow Derived DCs (BMDCs)*

Primary BMDCs (bone marrow-derived dendritic cells) were prepared following the protocol of Sixt and Lämmermann (27). Mice were euthanized with $CO_2$ gas and cervical dislocation. Leg bones were harvested and bone marrow was flushed with sterile

PBS. Cells were spun at 1500 rpm for 10 minutes at 4°C and resuspended at 2.5 x $10^6$ cell/mL. 1 mL of cells, 9 mL R10 media (RPMI 1640 (1x with L-Glutamine and 25 mM HEPES) + 50 mL heat inactivated FBS + 5 mL pencillin-steptomycin (Thermo Fisher Scientific, final concentration 100 U/mL pen. and 100 µg/mL strep.)) and 100 µL GM-CSF were added to 10 cm Petri dishes. On day three of culture an additional 10 mL R10 and 100 µL GM-CSF were added to each Petri dish. On day six of culture, 10 mL spent media was gently removed from each dish and replaced with 10 mL fresh R10 and 100 µL GM-CSF. Between days seven and nine DCs were transferred to 6 cm tissue culture dishes and matured for 24 hours in the presence of 200 ng/mL LPS. Mature DCs were spun at 1500 rpm for 10 minutes at 4°C and resuspended at 100,000 cells/mL for use in experiments. DCs were maintained at 37°C under 5% $CO_2$ throughout the culture period and experiments.

*PDMS-coated coverslip Preparation*

The following methods were adapted from my previous work (Bendell AC et al, Submitted). Traditional 2D migration experiments were conducted on PDMS-coated coverslips printed with fibronectin. Clean 25 mm round glass coverslips (Thermo Fisher Scientific) were spun with a thin layer of 10:1 PDMS (weight, base:cure) on a Laurell spinner (4000 rpm, 1 minute) and were cured overnight at 65°C. Coverslips were mounted onto the bottom of laser-cut one-well dishes with 10:1 PDMS and cured for at least 3 hours. 60 g of 10:1 PDMS was cast against a flat Silicon wafer in an aluminum weighing dish and cured overnight at 65°C. The weighing dish was cut away and the PDMS was carefully peeled away from the silicon wafer. 1 $cm^2$ stamps were cut from

the flat PDMS. Stamps were sonicated in 200 proof ethanol for 10 minutes, rinsed twice in $DiH_2O$, dried with $N_2$ gas, inked with 10 μg/mL fibronectin and stored at room temperature for 2 hours. The PDMS-coated coverslips were treated with UV/ozone for 7 minutes (UVO Cleaner Model 342, Jelight, Irvine, CA) while the fibronectin-coated stamps were gently rinsed twice in $DiH_2O$ and dried with $N_2$ gas. Fibronectin was transferred from the stamps to the PDMS-coated coverslips through microcontact printing (28) and the PDMS-coated coverslips were blocked with 0.2 w/v% Pluronic F127 for at least one hour. The PDMS-coated coverslips were rinsed 2x with PBS and incubated with PBS at 4°C for at least one hour. Mature DCs were added to the PDMS-coated coverslips at a concentration of 100,000 cells/mL. Any inhibitors were added at this point (for concentrations and incubation times, see below). The cells were incubated at 37°C and 5% $CO_2$ throughout the entirety of the experiment. 10 nM CCL19 was used to stimulate the cells immediately prior to imaging.

*mPAD Preparation*

Micropost array detectors (mPADs) were prepared following the protocol of Yang et al. (24). Micropost arrays were prepared from a silicon master by replica molding. Negative molds were created by casting degassed PDMS (10:1 base to cure) against a silanized silicon master mold and curing for 12 minutes at 110°C. The negative molds were gently peeled away from the silicon master, plasma treated (SPI Supplies Plasma Prep II, West Chester, PA) for 7 seconds, and silanized overnight. PDMS (10:1 base to cure) was added to the negative molds and degassed for 30 minutes to remove any air bubbles. 25 mm round glass coverslips were cleaned with $N_2$ gas and plasma treated for

90 seconds. The molds were placed, fresh PDMS side down, onto the cleaned coverslip and cured at 110°C for 20 hours. The mPADs were gently peeled away from the negative molds, immediately submerged in 200 proof ethanol and supercritical dried (SAMDRI-PVT-3D, Tousimis Corporation, Rockville, MD) in liquid $CO_2$. Circular holes were laser cut from the bottom of one well dishes. mPAD coverslips were secured to the bottom of the one well dishes with 10:1 PDMS and the seal was cured overnight at 65°C.

10 μg/mL fibronectin was microcontact printed onto the post tips, following the same procedure as above with minor modifications. After stamping the mPADs, 1 mL of 200 proof ethanol was added and the stamp was gently flicked off the micropost array. The ethanol was immediately diluted to 60% with di$H_2O$. The mPADs were gently rinsed three times with di$H_2O$. The post tips were blocked with 0.2 % Pluronic F127 for 1 hour at room temperature, rinsed three times with sterile di$H_2O$ and stored at 4°C overnight. The following day, 1 mL of mature DCs (100,000 cells/mL) was added to the mPAD. If inhibitors were being used they were added at this point and cells were incubated at 37°C for the desired amount of time (see below). Motility was stimulated with 10 nM CCL19 immediately before moving the dish to the microscope stage, and cells were allowed to settle on the micropost array before imaging began.

*Ligand Patterning on PDMS-Coated Coverslips*

Patterned stamps were created by casting polymer against a patterned silicon wafer. First, a rigid polymer solution was created by combining 3.4 grams of (7.0-8.0% Vinylmethylsiloxane)-Dimethylsiloxane Copolymer, Trimethylsiloxy Terminated

(Gelest, Inc.); 1.0 grams of (25-35% Methylhydrosiloxane)-(Dimethylsiloxane) Copolymer (Gelest, Inc.); 4 drops of modulator 2,4,6,8-Tetramethyl-2,4,6,8-tetravinylcyclotetrasiloxane (Sigma Aldrich); and 4 drops of catalyst Platinum(0)-2,4,6,8-tetramethyl-2,4,6,8-tetravinylcyclotetrasiloxane complex solution (Sigma Aldrich). The solution was mixed thoroughly and cast against a patterned silicon wafer. Large, surface-trapped air bubbles were removed by gently blowing $N_2$ gas over the layer of polymer and the polymer was baked for 40 minutes at 50°C. A soft PDMS layer (22 grams of 10:1 PDMS (weight, base:cure)) was poured over the rigid polymer and the stamp was baked overnight. The next day, the polymer was gently peeled away from the wafer and the stamps were trimmed. Microcontact printing was performed as described above. The only difference was the use of fluorescently labeled fibronectin (488-conjugated) to visualize stamped patterns.

*Inhibitors and Antibodies*

Inhibitors and antibodies were added to one-well dishes along with mature DCs (at 100,000 cells/mL) prior to imaging. Cells were maintained at 37°C unless otherwise noted. The following concentrations and incubation times were used: blebbistatin (B0560; Sigma-Aldrich, St. Louis, MO) at 2 μM for 1 hour; Y-27632 (68800; Calbiochem, San Diego, CA) at 10 μM for 30 minutes; Exoenzyme C3 Transferase (CT04; Cytoskeleton Inc., San Diego, CA) at 1 μg/mL for 4 hours; LY294002 (99015; Cell Signaling Technology, Danvers, MA) at 50 μM for 1 hour; CK666 (SML006; Sigma-Aldrich, St. Louis, MO) at 10 μM for 1 hour; $\alpha_5$ and $\beta_1$ antibodies (14-0493-85

and 14-0292-85, respectively; eBioscience, San Diego, CA) at 5 μg/mL for 10 minutes at room temperature then 10 minutes at 37°C.

*Live Cell Imaging*

Mature DCs were imaged at 10x by phase microscopy on a Nikon Eclipse TE300 (Nikon, Melville, NY) with MetaMorph software (MetaMorph Inc., Nashville, TN). Images were collected at multiple positions for one hour at one minute intervals using a motorized stage. Cells were maintained at 37°C and 5% $CO_2$ throughout imaging.

*Image Analysis and Quantification*

Cell migration was analyzed with the Manual Tracking plugin in ImageJ (http://rsbweb.nih.gov/ij). Cells were tracked over time by manually specifying their centroid positions in each frame. Cells that were apoptotic or completely stationary were excluded, as well as any cells in contact with other cells. The list of x- and y-coordinates obtained from ImageJ was further analyzed with a custom-written MATLAB (Mathworks, Natick, MA) script. The MATLAB script computed the MSD of the compiled list of cell tracks and used the Dunn equation $\left(\langle MSD(\tau)\rangle = 2S^2P\left[\tau - P\left(1 - exp\left(-{}^{\tau}/_{P}\right)\right)\right]\right)$ to fit speed (S) and persistence (P) (29). The random motility coefficient was calculated from the speed and persistence as follows: $\mu = \frac{1}{n}S^2P$, where n specifies the dimensionality (30).

*Statistical Analysis*

I used a one-way ANOVA along with a Tukey's Post Hoc Test to determine statistical significance. Statistically significant differences at $p < 0.05$ were marked with an asterisk (*) and differences at $p < 0.01$ were marked with a double asterisk (**).

*Atomic Force Microscopy*

All experiments were carried out at room temperature using a Bruker Bioscope Catalyst AFM (Billerica, MA, USA). A spherical tip from Novascan (Boone, IA, USA) was used with a nominal spring constant of 0.06 N/m and a nominal tip radius of 500 nm. The cantilever spring constant was calibrated using Nanoscope software (Bruker). The AFM was operated in the fluid contact mode at a force distance curve acquisition frequency of 2 Hz.

## RESULTS

### *Dendritic Cell Migration is Affected by the Underlying Substrate*

I have previously quantified DC chemokinesis on continuous PDMS surfaces, made by uniformly spin coating PDMS on a glass coverslip, and I have measured force generation by DCs on discrete PDMS microposts (Chapter 3 and (8,25)). Although I have always considered these experiments to be complementary, important differences between the two experimental systems leave open key questions about whether migration is affected by the stiffness and/or the geometry of the underlying substrate. To address these questions, I measured the random migration of DCs on mPADs, and compared the data to my previous results for DCs randomly migrating on PDMS-coated coverslips. In both cases, the surfaces were printed with fibronectin to ensure cell adhesion, and blocked with Pluronic F127 to restrict cell attachment to the printed region. 10 nM CCL19 was also added to DCs to stimulate motility. DCs were able to move and had similar morphologies on the two surfaces (Figure 4.1A and B).

Sample trajectories from DCs on PDMS-coated coverslips and mPADs are shown in Figure 4.1C and D, respectively. As a first step of analysis, I used the trajectories to calculate the mean squared displacement (MSD) as a function of time. When plotted on a log-log scale, the slope of this curve provides a quantitative description of the form of migration. For DCs migrating randomly on either PDMS-coated coverslips or microposts, I found the MSD versus time had a slope of 1 on each surface, indicating purely random migration (Figure 4.1E). I next analyzed this data using the Dunn equation (Equation 4.1) to determine the speed (S) and persistence time (P) (29). I used speed and persistence time to calculate two additional

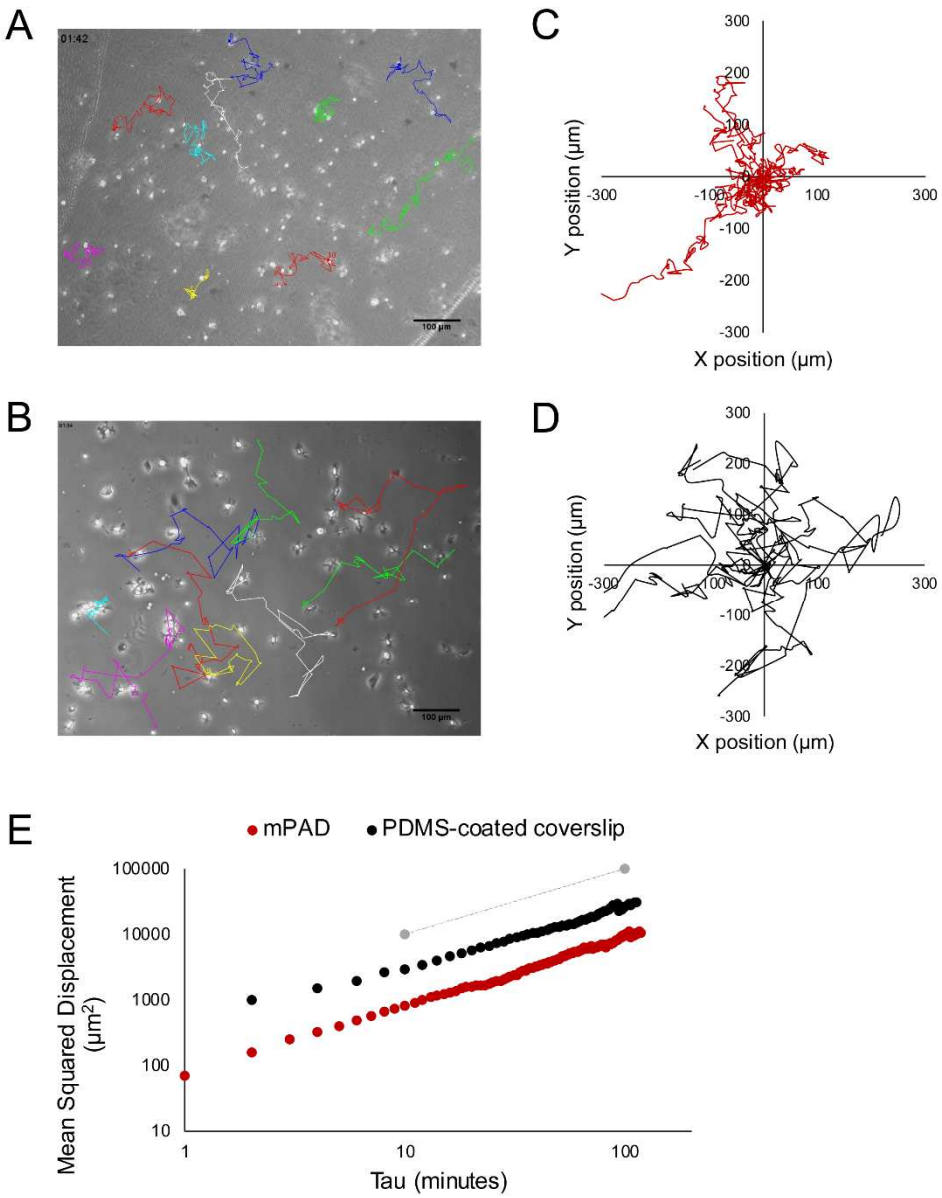


*Figure 4.1. DCs on PDMS-coated coverslips persist in the same direction for longer periods of time.*

A,B) Sample phase contrast images of DCs on mPADs (A) and PDMS-coated coverslips (B). DCs were plated on 10 µg/mL fibronectin and stimulated with 10 nM CCL19. Colored lines show sample cell trajectories at each time point. Trajectories are longer and more linear for DCs on PDMS-coated coverslips than for DCs on mPADs. C,D)

Sample cell tracks for DCs on mPADs (C) and PDMS-coated coverslips (D). In these specific samples, DCs on PDMS-coated coverslips cover a larger area during random migration. Over the entire population of cells tested for each condition, there was no statistically significant difference in this parameter (see random motility coefficient, Figure 4.5D). E) The Mean Squared Displacement of both cell populations shows a linear fit with time, on a log-log scale, with slope approximately equal to 1 (gray dashed line), indicating diffusive migration

quantitative features of motility—the persistence length and random motility coefficient—given by Equations 4.2 and 4.3, respectively.

$$\langle MSD(\tau)\rangle = 2S^2P\left[\tau - P\left(1 - exp\left(-{}^{\tau}/_{P}\right)\right)\right]$$

Equation 4.1

$$P_l = (P)(S)$$

Equation 4.2

$$\mu = \frac{1}{n}S^2P$$

Equation 4.3

The values of these metrics on the two types of materials are shown in Figure 4.2. I previously performed a thorough analysis of WT DCs on PDMS-coated coverslips, and report these values here as reference (8). While the DCs migrated diffusively on mPADs, just as they did on PDMS-coated coverslips, the method by which DCs achieved their random migration was quite different. DCs on PDMS-coated coverslips migrated at a speed of 4.00 ± 0. 18 μm/min and persisted for 4.88 ± 0.46 min before changing directions (Figure 4.2A, B). DCs on mPADs exhibited a modest, but significant increase in speed (4.92 μm/min), and persisted for a significantly shorter time (2.35 min) before changing direction. The significant reduction in persistence time also led to a reduction in persistence length (Figure 4.2C). The decrease in persistence time also contributes to a reduction in the area covered during migration (reflected in a reduced value of the random motility coefficient), although this reduction does not reach significance (Figure 4.2D). By examining the cell trajectories on the PDMS-coated coverslip and mPAD

surfaces, I can see that the majority of DCs on the PDMS-coated coverslips migrate over large distances. In contrast, there appear to be two separate populations of DCs on mPADs, with some DCs exhibiting long trajectories and some DCs exhibiting more circuitous trajectories huddled around the origin. This large variance in the phenotype of DC migration on

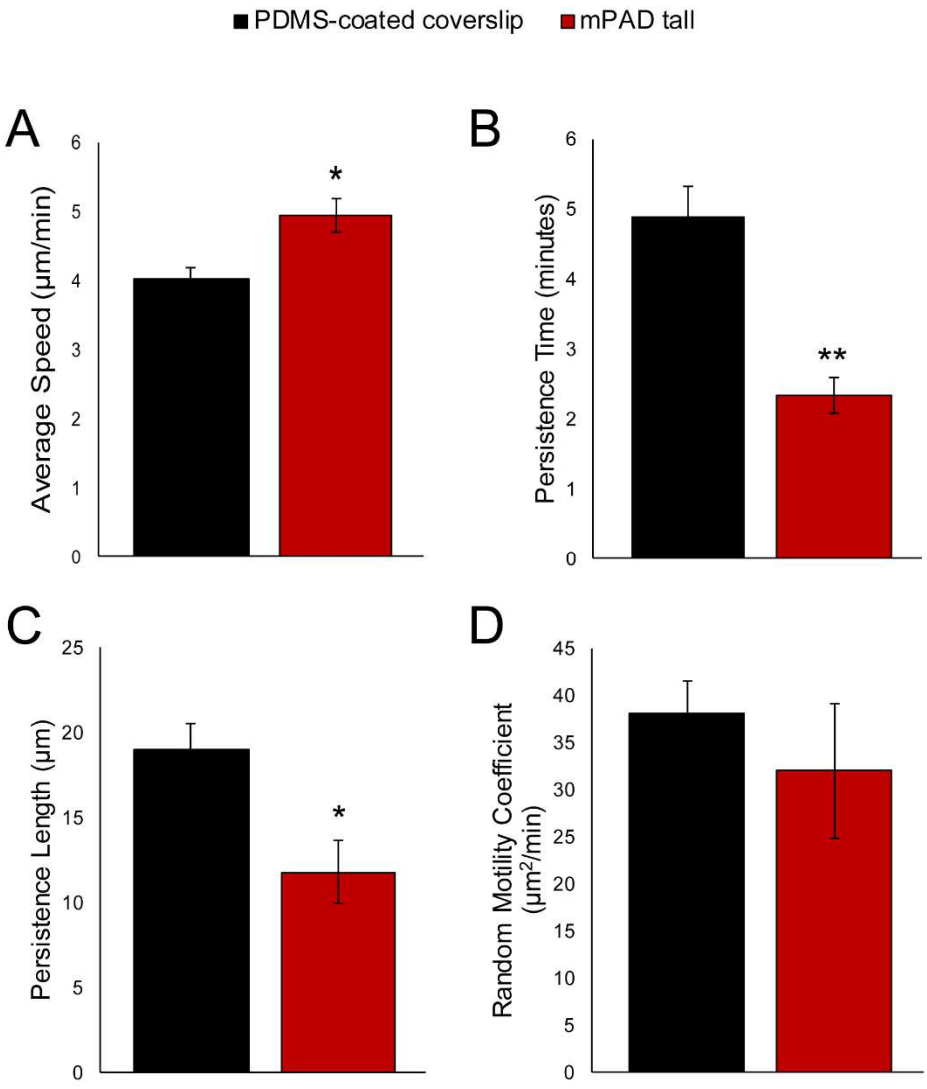


*Figure 4.2. DCs migrated differently on PDMS-coated coverslips and mPADs.*

A) The average speed of DCs on mPADs is significantly greater than that of DCs on PDMS-coated coverslips. B) The persistence time of DCs on mPADs is drastically reduced, as compared to the persistence time of DCs on PDMS-coated coverslips. C) The reduction is persistence time is carried through to a reduction in the persistence length. D) The combination of the increase in average speed and decrease in persistence time, results in a non-significant difference in the overall diffusivity. Figures represent average values ± SEM, for > 650 DCs from at least three independent experiments per

condition. PDMS-coated coverslip values correspond to my previous data on characterizing DC migration on PDMS surfaces (Figure 3.2). Statistical significance calculated with single factor ANOVA and post hoc Tukey test. Indicates significant difference compared to PDMS-coated coverslip. *$p<0.05$, **$p<0.01$

mPADs accounts for the failure of the decrease in random motility coefficient to reach significance. Taken together, these measurements indicate that DCs are able to undergo random migration on mPADs, but the characteristics of their migration are influenced by the geometry of the substrate.

*Dendritic Cells Respond to Geometry and Not Stiffness*

After determining that DC migration is affected by the topology of the substrate, I sought to determine whether the DCs were responding to its geometry or its elasticity. The coverslips are coated with PDMS, the same material used to generate the mPAD surfaces. However, while the coverslip is covered with a continuous layer of PDMS, the mPAD is molded into a discrete array of posts with adjustable geometry (diameter and spacing of posts) and adjustable elasticity (set by the height of the posts) (24). Both substrates present a 2D, fibronectin-printed surface to migrating DCs. However, the stiffness of the PDMS-coated coverslip is two orders of magnitude greater than that of the tall mPAD I generally use, and the ligand-coated surface is discontinuous rather than uniform.

Both the geometry and stiffness of the microenvironment have been known to influence the migration of many different types of cells, making either factor a possible explanation for the changes in DC migration I observe on mPADs (11). Since most immune cells show functional dependence of motility on substrate stiffness, I hypothesized that DCs would also be responsive to this feature of the material (21,22,31). To test whether the elasticity of the mPADs affects the migration of DCs, I repeated the

migration experiments using two additional mPADs, called “short” and “medium.” (Table 4.1). Each mPAD array has the same

*Table 4.1. Dimensions and stiffness of different mPADs.*

| **Large mPADs**<br>**Diameter: 1.83 μm**<br>**Post-to-Post Spacing: ~3 μm** | | | |
|---|---|---|---|
| **Name** | **Post Height (μm)** | **Spring Constant (nN/μm)** | **Effective Stiffness (kPa)** |
| Short | 0.97 | 4523.98 | 1218.44 |
| Medium | 5.70 | 22.30 | 17.21 |
| Tall | 12.90 | 1.92 | 1.49 |
| **Small mPAD**<br>**Diameter: 800 nm**<br>**Post-to-Post Spacing: ~2 μm** | | | |
| Small | 4.77 | 1.39 | 2.49 |

2-dimensional cross sectional geometry, with the same post diameter (1.83 μm) and post spacing (~ 3 μm), but they have different heights which ultimately leads to different stiffnesses (24). The stiffness of "tall" mPADs was approximately 1 kPa, "medium" mPADs were 10 kPa, and "short" mPADs were $10^3$ kPa. In experiments on coverslips, I spun the surface with a layer of 10:1 PDMS (base to cure by weight), which leads to a stiffness on the order of 100 kPa (Figure 4.3). By quantifying DC migration across this range of mPAD stiffnesses, I can effectively tease out the effect of stiffness while keeping substrate geometry constant. If DC migration depends on stiffness, I would expect migration to be different on the different surfaces. As shown in Figure 4.4A, the average speed of DC migration is similar on all three mPAD surfaces. Moreover, there is no difference in the persistence time on the different mPAD surfaces (Figure 4.4B). Consistent with my earlier finding, however, DCs exhibit diminished persistence tiem on all mPADs as compared with PDMS-coated coverslips. These results indicate that DC migratory behavior is unaltered by changes in stiffness over a two-log range.

Next, I wanted to determine if this geometry dependence was due to physical topography of the substrate (i.e. discrete micropillars vs. continuous surface) or the geometry of ligand printed on the surfaces. I addressed this question by spatially patterning ligand on PDMS-coated coverslips (Figure 4.5A). This provided a migration surface in which I can probe ligand geometry independently of the physical structure of the substrate. DC migration on these patterned PDMS-coated coverslips was quantified as described above, and average speed and persistence time were compared to the values for migration on the continuously-printed PDMS-coated coverslips and mPADs (Figure 4.5B, C). DCs migrating on these patterned surfaces migrated significantly faster than

DCs on continuously printed PDMS-coated coverslips, while their speed was indistinguishable from that of DCs on mPADs (Figure 4.5B).

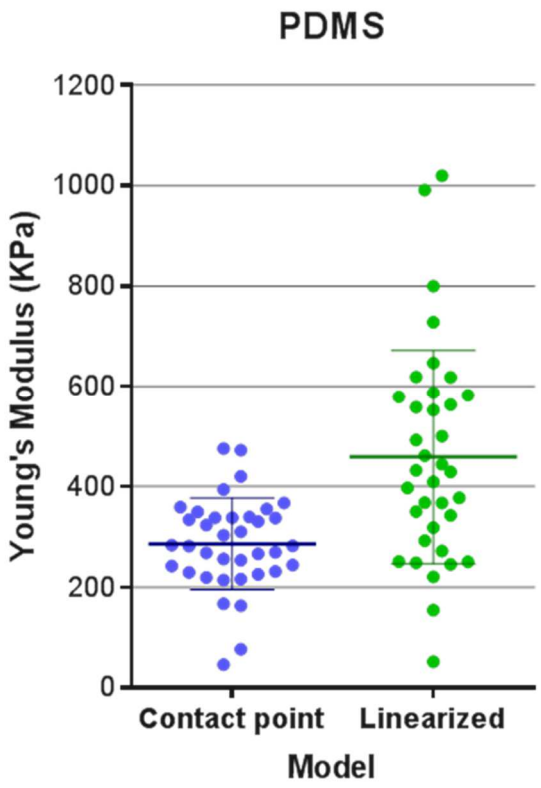


*Figure 4.3. Approximate stiffness of PDMS-coated coverslips.*

Multiple points on two separate spin-coated coverslips were probed with a soft AFM tip. The measurements were fit to two different models. The contact point model is optimal for soft materials measured with a soft tip. The linearized model is optimal for hard materials measured with a hard tip. Due to system limitations (i.e. soft tip), the values reported are only estimates of surface stiffness. Neither model is ideal, but I am confident in reporting an order of magnitude stiffness of 100's of kPa. Figure provided by Daniel Blumenthal.

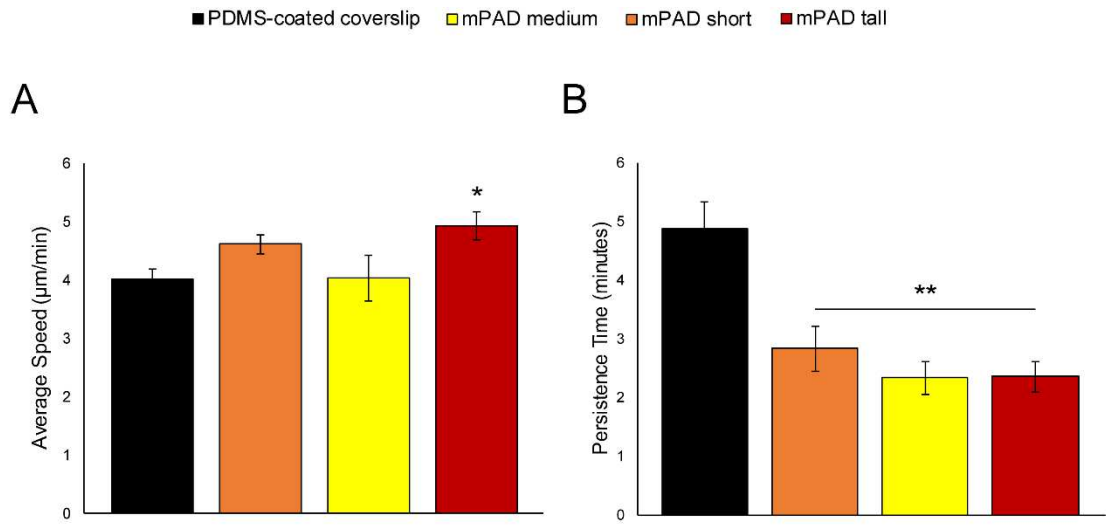


*Figure 4.4. DCs respond to mPAD geometry, not stiffness.*

A) There is no trend in the average speed of DCs on the different mPADs. B) The persistence time of DCs is significantly reduced on all mPADs, regardless of stiffness. Figures represent average values ± SEM, for > 180 DCs from at least three independent experiments per condition. PDMS-coated coverslip values correspond to my previous data on characterizing DC migration on PDMS surfaces (8). Statistical significance calculated with single factor ANOVA and post hoc Tukey test. Asterisks indicate significant difference compared to PDMS-coated coverslip. *$p<0.05$, **$p<0.01$. There is no statistically significant difference between the tall mPAD and the short and medium mPADs.

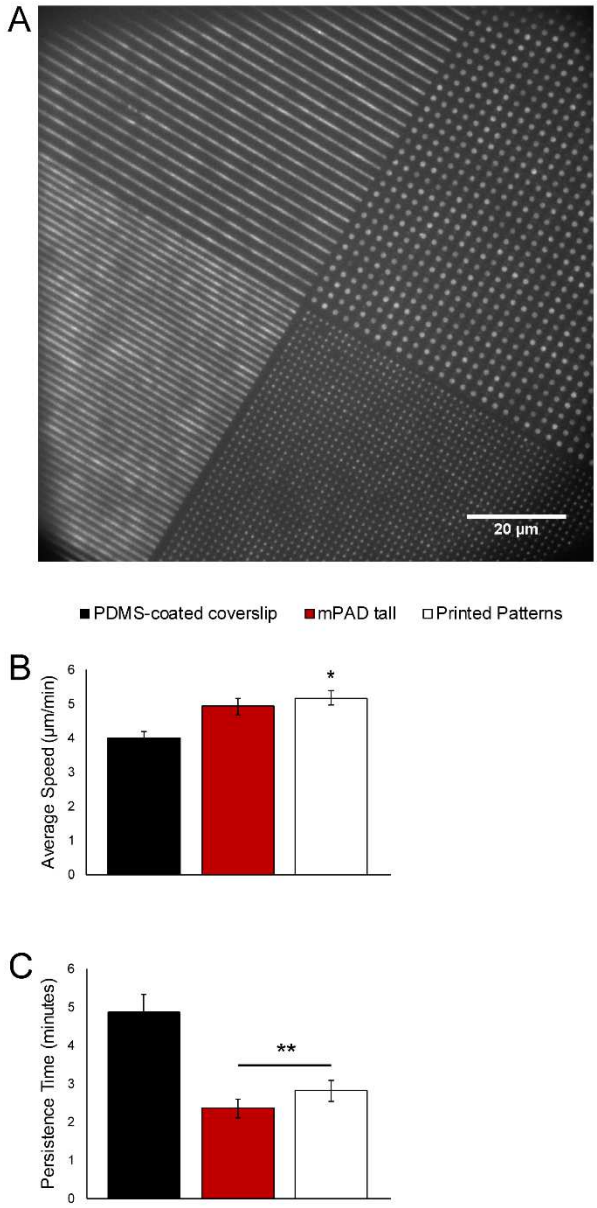


*Figure 4.5. DCs respond to geometry of printed ligand.*

A) Patterned stamps were used to transfer 488-conjugated fibronectin to PDMS-coated coverslips. Tracking was performed on the pattern located in the top right corner, which closes matches the mPAD geometry. This large dot pattern has the following dimensions: diameter of circular islands is 2 µm and centroid-to-centroid spacing is 5 µm. B) The average speed of DCs on PDMS-coated coverslips printed with islands of fibronectin is significantly greater than that on PDMS-coated coverslips printed with

continuous fibronectin, but indistinguishable from that on mPADs. C) The persistence time of DCs on both mPADs and PDMS-coated coverslips printed with islands of fibronectin is significantly lower than that on PDMS-coated coverslips printed with continuous fibronectin. Figures represent average values ± SEM, for > 650 DCs from at least three independent experiments per condition. PDMS-coated coverslip values correspond to my previous data on characterizing DC migration on PDMS surfaces (Figure 3.2). Statistical significance calculated with single factor ANOVA and post hoc Tukey test. Asterisk indicates significant difference compared to PDMS-coated coverslip. *$p<0.05$, **$p<0.01$. There are no statistically significant differences between the tall mPAD and the patterned PDMS-coated coverslips.

DCs on patterned PDMS-coated coverslips also displayed a significant difference in persistence time, matching my observations for persistence time on mPADs. These results indicate that DC migration responds to the discretization of printed ligand geometry and is not affected by the physical topography of the environment.

Finally, I wanted to know how sensitive DCs are to differences in geometry. If the mPADs used thus far allowed us to modulate how often DCs turn, I hypothesized that altering the mPAD geometry could further manipulate DC turning behavior. To test this relationship, I prepared mPADs with smaller diameter posts and interpost spacing and tracked DC migration. While the mPADs I used previously have a diameter of 1.8 μm and post-to-post spacing of ~3 μm, the new smaller mPADs have a diameter of 800 nm and post-to-post spacing of ~2 μm (Table I). With smaller feature sizes, DCs with the same area will interact with more posts on the small mPADs than they do on the larger diameter, tall mPADs. Quantification of persistence time revealed no differences in turning behavior between DCs migrating on larger and smaller diameter posts (Figure 4.6). Therefore, I conclude that migratory DCs are able to respond to large-scale differences in geometry (i.e. continuous vs. discrete ligand presentation) but are unable to discern differences in geometry on the scale of 1 μm.

*Dendritic cells sense differences in geometry through myosin contractility, intregin-based adhesions and reorganization of the actin cytoskeleton*

To gain an understanding of how the substrate geometry affects subcellular organization and signaling during DC migration, I used GFP-Lifeact DCs to visualize F-actin organization. On PDMS-coated coverslips, F-actin was highly concentrated at the

periphery of the cell, forming lamellipodia and filopodia (Figure 4.7A). When DCs were plated on mPADs, the actin

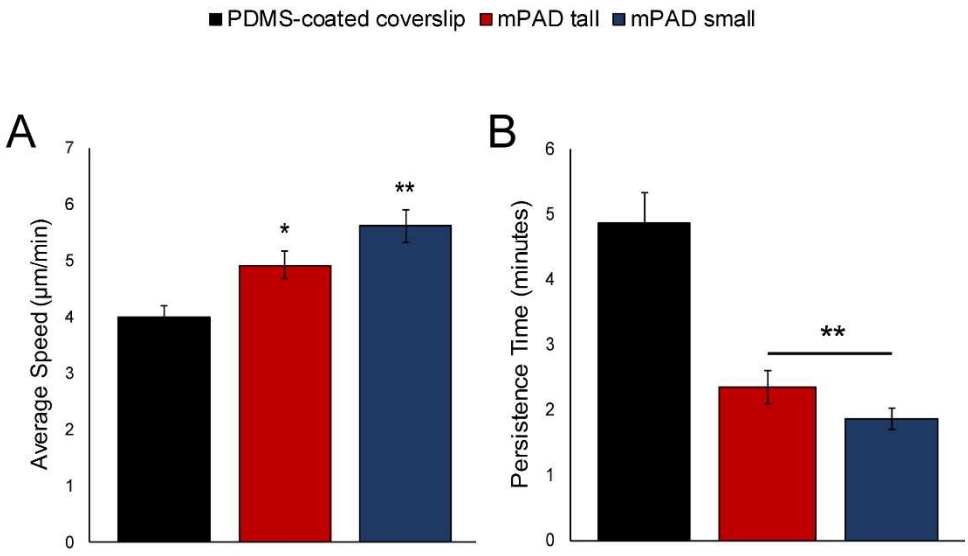


*Figure 4.6. DCs do not detect micron-scale differences in geometry.*

A) The average speed of DCs on smaller diameter mPADs is significantly greater than that on PDMS-coated coverslips, but indistinguishable from that on larger diameter mPADs. B) The persistence time of DCs on smaller diameter mPADs is significantly lower than that on PDMS-coated coverslips, but is again indistinguishable from that on larger diameter mPADs. Figures represent average values ± SEM, for > 290 DCs from at least three independent experiments per condition. PDMS-coated coverslip values correspond to my previous data on characterizing DC migration on PDMS surfaces (8). Statistical significance calculated with single factor ANOVA and post hoc Tukey test. Asterisks indicate significant difference compared to PDMS-coated coverslip. *$p<0.05$, **$p<0.01$. There are no statistically significant differences between the tall mPAD and the small mPAD.

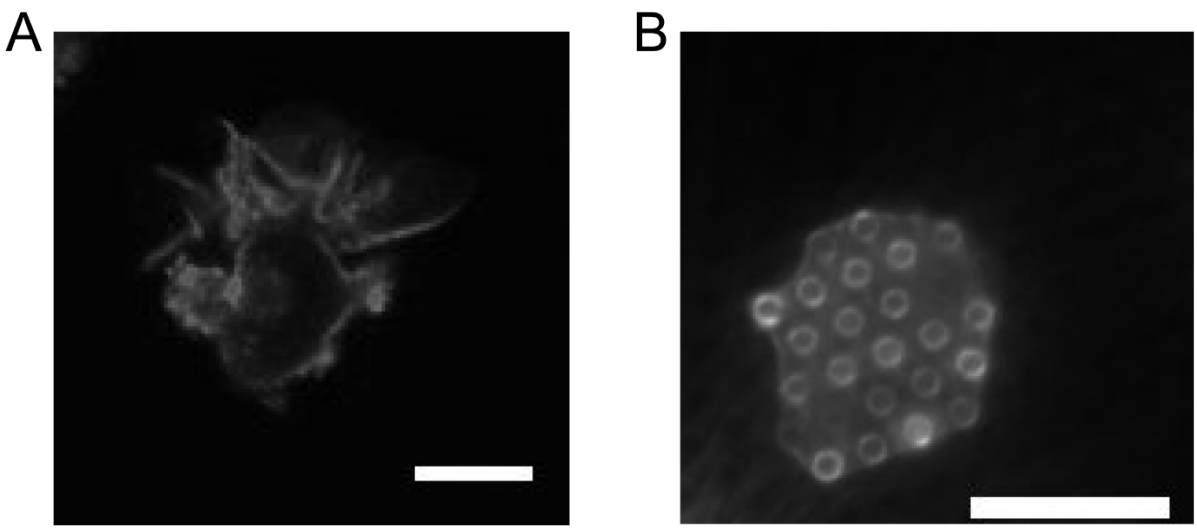


*Figure 4.7. The actin cytoskeleton is reorganized on mPADs.*

Representative GFP-LifeAct DCs plated on PDMS-coated coverslips (A) or mPADs (B and C). Cells were plated on 10 μg/mL fibronectin and stimulated with 10 nM CCL19. Scale bars represent 10 μm. A) On PDMS-coated coverslips, actin is concentrated at the periphery. B) On mPADs, actin is redistributed into rings at the periphery of engaged microposts.

showed a very different distribution, with high levels of GFP signal surrounding each engaged post under the cell body (Figure 4.7B). The process of ring formation is very dynamic, with the actin intensity in individual rings fluctuating on a time-scale of 1 minute, which is shorter than the persistence time (2.35 ± 0.25 min). The presence of these actin rings provides additional evidence that DCs detect differences in PDMS-coated coverslips and mPADs.

I next aimed to clarify the mechanisms involved in the ability of DCs to respond to discretizations in geometry through the use of small molecule inhibitors. Since I observed differences in the actin organization of DCs on PDMS-coated coverslips and mPADs, I first used CK666 to investigate actin polymerization mediated by the Arp2/3 complex (orange bars in Figure 4.8). In the next chapter, I will show that inhibition of the Arp2/3 complex led to significant reductions in average speed and had no effect on persistence time on PDMS-coated coverslips (8). Treatment with CK666 had no effect on DC morphology on either PDMS-coated coverslips or mPADs (Figure 4.8C). Addition of CK666 to DCs on mPADs led to a significant decrease in speed and had no influence on persistence time (Figure 4.8A, B). Although speed is reduced in DCs on both PDMS-coated coverslips and mPADs when CK666 is present, the significant difference is speed between DCs on mPADs and PDMS-coated coverslips remains. (Figure 4.8A, B). Thus, I conclude that while Arp2/3 complex activity is important for migratory speed during DC chemokinesis, it does not contribute to geometry sensing.

The next pathway I probed was myosin contractility, by direct inhibition of myosin with blebbistatin (blue bars in Figure 4.8). At a concentration of 2 μM, cells remained viable but displayed elongated morphology (Figure 4.8C). I saw no significant

changes in average speed or persistence time under the influence of blebbistatin on mPADs (Figure 4.8A, B). I did

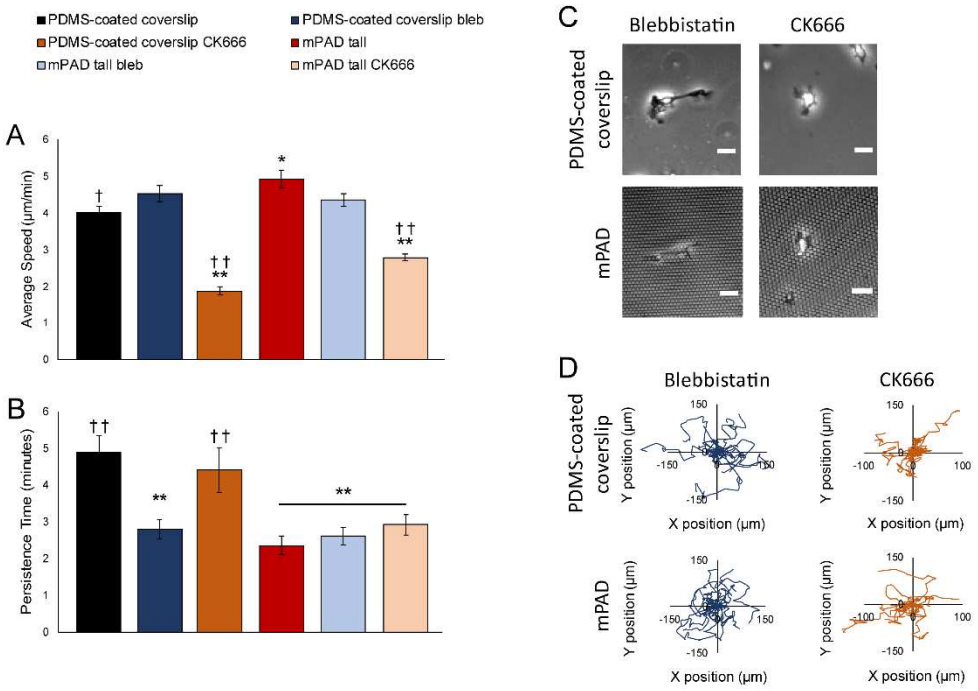


*Figure 4.8. DC response to substrate geometry is influenced by myosin contractility.*

A) The average speed of DCs on both PDMS-coated coverslips and mPADs is unaffected by myosin inhibition and is significantly reduced by inhibition of the Arp2/3 Complex. B) The persistence time of DCs on PDMS-coated coverslips is significantly reduced in the presence of the myosin inhibitor blebbistatin. Blebbistatin has no effect on DC persistence on mPADs. Arp2/3 Complex inhibition has no effect on persistence time for DCs on either PDMS-coated coverslips or mPADs. C) Sample phase contrast images of DCs inhibited with CK666 (left) or blebbistatin (right), on PDMS-coated coverslips (top) and mPADs (bottom). Colored lines indicate sample cell trajectories. Under these two inhibitor conditions DCs turn at similar frequencies. DCs were plated on 10 μg/mL fibronectin and stimulated with 10 nM CCL19. Figures represent average values ± SEM, for > 290 DCs from at least three independent experiments per condition. PDMS-coated

coverslip values correspond to my previous data on characterizing DC migration on PDMS surfaces (8). Statistical significance calculated with single factor ANOVA and post hoc Tukey test. Asterisks indicate significant difference compared to PDMS-coated coverslip without inhibitors. *$p<0.05$, **$p<0.01$. Crosses indicate significant difference compared to tall mPAD without inhibitors. †$p<0.05$, ††$p<0.01$.

however, see a significant decrease in persistence time of DCs on PDMS-coated coverslips in the presence of blebbistatin (Figure 4.8B). Indeed, the persistence time of blebbistatin-treated DCs on PDMS-coated coverslips was indistinguishable from that of untreated DCs on mPADs. This indicates that myosin contractility contributes to geometry sensing, since inhibition of this pathway eliminates the ability of DCs to sense differences in geometry between the two surfaces.

Finally, I used antibodies to impair integrin-mediated adhesions. Both of my surfaces were printed with fibronectin, so I chose to specifically block the two subunits of the major fibronectin integrin in DCs: α5 and β1. I chose antibody concentrations that would only partially block integrin function (5 μg/mL final concentration for each inhibitor, approximately 10% of the concentration I would have used for complete blocking), thus allowing for continued adhesion but reduced availability of active integrins. DCs were able to adhere and migrate on the PDMS-coated coverslip and mPAD surfaces under these conditions (Figure 4.9A). Blocking of either subunit had no effect on the average speed or persistence time of DCs on PDMS-coated coverslips (Figure 4.9A, B). In contrast, blocking either integrin subunit led to a significant decrease in average speed and significant increase in persistence time on mPADs. Indeed, treatment with either antibody effectively eliminated the geometry-induced differences in DC migration; the average speed and persistence time became indistinguishable for DCs on mPADs and PDMS-coated coverslips. Therefore, I conclude that integrin adhesion to fibronectin plays a major role in the ability of DCs to respond to discrete substrate geometry. Taken together, these results show that the

response of DCs to substrate geometry is a dynamic process mediated through myosin contractility, integrin-based adhesions and cytoskeletal reorganization.

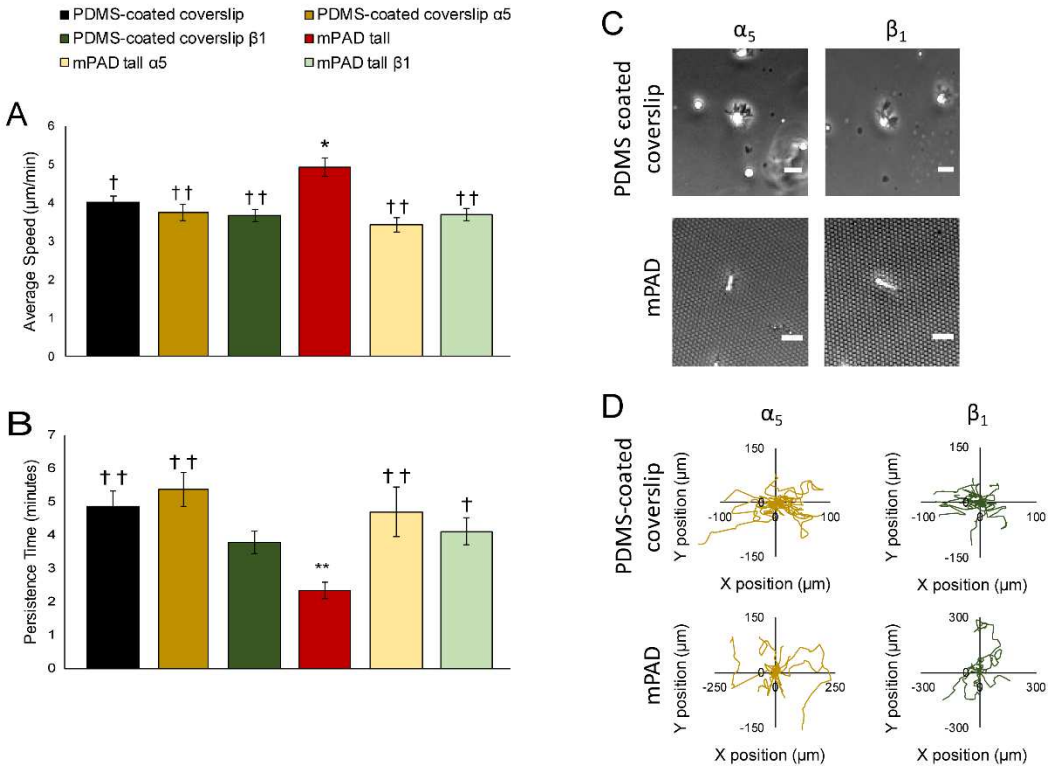


*Figure 4.9. DC response to substrate geometry is influenced by integrin-based adhesions.* A) Blocking of either integrin subunit ($\alpha_5$ or $\beta_1$) had no effect on the average speed of DCs on PDMS-coated coverslips, but significantly reduced the speed of DCs on mPADs. B) Likewise, blocking of either integrin subunit had no effect on persistence time of DCs on PDMS-coated coverslips, but significantly increased the persistence time of DCs on mPADs. C) Sample phase contrast images of DCs blocked with antibodies against $\alpha_5$ (left) or $\beta_1$ (right), on PDMS-coated coverslips (top) and mPADs (bottom). Under these two inhibitor conditions, cells persist for long periods of time on mPADs and often exhibit an elongated morphology pointed in the direction of migration. Scale bars equal 20 μm. DCs were plated on 10 μg/mL fibronectin and stimulated with 10 nM CCL19. Figures represent average values ± SEM, for > 290 DCs from at least three independent experiments per condition. PDMS-coated coverslip values correspond to my previous

data on characterizing DC migration on PDMS surfaces (8). Statistical significance calculated with single factor ANOVA and post hoc Tukey test. Indicates significant difference compared to PDMS-coated coverslip without inhibitors. *$p<0.05$, **$p<0.01$. Crosses indicate significant difference compared to tall mPAD without inhibitors. †$p<0.05$, ††$p<0.01$.

## DISCUSSION

We have previously characterized the traction forces of motile DCs using mPADs (25). During chemotaxis, DCs produce a total force with magnitude of 18 ± 14 nN/cell (25). The average force per post is on the order of half a nanoNewton, with larger forces located at the leading edge (25). Traction forces are significantly reduced when either actin polymerization or myosin motor activity are inhibited (25). In the next chapter, I will discuss the quantification of DC forces during chemokinesis and identify actin-binding proteins critical for force generation. In the present study, I used mPADs to study the dynamics of cell migration. I observed that DCs are responsive to the differences in the substrates on which they are migrating. These differences in migration are due to the geometry and of the substrate and not stiffness. Furthermore, I showed that DCs are able to sense these topographical differences through actomyosin contractility and integrin engagement.

I have previously characterized DC random migration on 2D fibronectin-coated glass and PDMS surfaces. In these settings, DCs appear to be insensitive to the level of fibronectin, the level of chemokine present and the type of underlying substrate, migrating at a consistent speed of ~4 μm/min (Ricart BG, Bendell AC unpublished results). DCs have also been shown to migrate well in 3D gels and under confinement and are capable of migrating without the use of integrins (32,33). After quantifying differences in the random migration of DCs on posts, I sought to identify whether stiffness or geometry was the causative factor. I developed a method for exploring the response of DCs to substrate stiffness while keeping the substrate geometry constant. I achieved this through the use of a set of mPADs with different post heights. Each mPAD

had the same 2D geometry, but the stiffness of the posts was inversely correlated with post height. In terms of physiological relevance, the softest mPAD (~1 kPa) is similar to the stiffness of endothelial tissue, the medium mPAD (~10 kPa) is similar to the stiffness of skeletal muscle and the stiffest mPAD (~1,000 kPa) starts to approach the compliance of rigid materials such as bone (34). Somewhat surprisingly, I discovered that DCs are insensitive to stiffness but react to differences in substrate geometry. Since DCs are present throughout the body and in a variety of different tissues, each having a characteristic stiffness, it would be useful for DCs to be able to migrate well in a variety of different environmental compliances.

After determining that DCs respond to geometry, I performed experiments to determine whether this sensitivity is due to the physical geometry or ligand patterning. Printed ligand geometry significantly affects the migration of other immune cells such as neutrophils (14), and I thought it likely to affect DC migration. When studying migration on different surfaces, multiple variables are affected, and it has often been difficult to probe the effect of the individual parameters on cell migration. For example, Frey et al. showed that 3T3 fibroblasts migrating on microposts moved faster and turned more frequently than fibroblasts on continuous surfaces (35). Even though fibronectin was adsorbed to the entire substrate, the cells preferentially migrated on the post tips and not the interpost regions (35). As a result, cells were exposed to discrete ligand and discrete substrate, and it was not determined whether the influence on migration was due to physical topography or the discrete pattern of ligand the cells encountered. In a separate study, Wójciak-Stothard et al. exposed macrophages to grooved substrates containing regularly spaced, parallel lines (12). In this environment, macrophages were shown to

migrate in straight lines, following the direction of the ridges and grooves, thus leading to a significantly increased persistence time (12). Again, it is not clear what aspect of the environment influences cell migration, as ligand patterning was restricted by the substrate structure. My approach at printing patterns on a flat substrate permitted us to separate the effect of physical geometry from ligand geometry, and allowed us to determine that DCs respond directly to ligand patterning and not substrate structure. It is unknown how sensitive DCs are to ligand patterning, but it is clear that they can robustly differentiate continuous from discrete ligand presentation.

I next asked what molecules and pathways are involved in the ability of DCs to sense geometry. Since I previously showed that myosin is necessary for interactions with post arrays and transmission of traction forces (25), it seemed likely that myosin would also be important for geometry sensing and migration. My experiments reveal that myosin inhibition reduces persistence time of DCs on flat surfaces, to levels similar to that seen for DCs on posts. However, myosin inhibition of DCs on posts is unable to further decrease persistence time. This suggests that myosin contractility is indeed important for DC migration, in particular for regulation of persistence time. The normalization of migration on flat surfaces and posts in the presence of blebbistatin has also been shown for fibroblasts (although the authors focused on normalization in terms of speed and not persistence time) (35).

My experiments with GFP-Lifeact DCs revealed that the organization of the actin cytoskeleton is affected by substrate geometry. Geometry-dependent reorganization of actin has also been observed in macrophages migrating along a series of ridges and grooves (12). In these cells, actin was highly concentrated at the boundary of the ridge

and groove interface, just as I see actin at the boundary of the post and interpost regions (12). Others have shown that the actin cytoskeleton is reorganized in cells adhered to discrete patterns of ligand (36), but unlike my observations, the actin is concentrated into solid circles over the patches and not into rings. These rings are dissimilar to other actin structures typically observed in DCs, such as podosomes, which have the appearance of punctate actin spots surrounded by a ring of adhesion protein (37). My observations suggest that actin is actively involved in the response of DCs to environmental geometry. The specific actin pathway responsible for this process has not been identified, but inhibition studies with CK666 have ruled out the Arp2/3 Complex.

A final pathway I chose to investigate was the role of integrin adhesion. Since my surfaces are coated with fibronectin, I chose to inhibit the two subunits of the main fibronectin integrin in DCs, $\alpha_5\beta_1$. While DCs in 3D environments have been shown to be capable of migrating without the use of integrins, I and others have shown that DCs migrating in 2D do indeed employ integrins (33). When I partially inhibit either integrin subunit in DCs migrating on posts I see a complete elimination of geometry dependence. Thus, integrin engagement is critical for the ability of DCs to sense geometry while migrating in 2D. Future work should be performed to identify the specific components of myosin contractility, adhesion formation and the actin cytoskeleton that are involved in responses to geometry.

ACKNOWLEDGEMENTS

DAH, JKB and ACB acknowledge support from NIH R01-GM104287. ACB acknowledges support from the NSF GRFP under Grant No. DGE-1321851.

AFM measurements were kindly performed by Daniel Blumenthal.

REFERENCES


1. Steinman RM. The Dendritic Cell System and Its Role in Immunogenicity. Annu RevImmunology. 1991;9:271–96.
2. Savina A, Amigorena S. Phagocytosis and antigen presentation in dendritic cells. Immunol Rev. 2007;219(1):143–56.
3. Banchereau J, Briere F, Caux C, Davoust J, Lebecque S, Liu Y, et al. Immunobiology of Dendritic Cells. Annu RevImmunology. 2000;18:767–811.
4. Randolph GJ, Angeli V, Swartz M a. Dendritic-cell trafficking to lymph nodes through lymphatic vessels. Nat Rev Immunol [Internet]. 2005;5(8):617–28. Available from: http://www.ncbi.nlm.nih.gov/pubmed/16056255
5. Renkawitz J, Schumann K, Weber M, Lämmermann T, Pflicke H, Piel M, et al. Adaptive force transmission in amoeboid cell migration. Nat Cell Biol [Internet]. Nature Publishing Group; 2009;11(12):1438–43. Available from: http://dx.doi.org/10.1038/ncb1992
6. Dehring DAK, Clarke F, Ricart BG, Huang Y, Gomez TS, Williamson EK, et al. Hematopoietic Lineage Cell-Specific Protein 1 Functions in Concert with the Wiskott–Aldrich Syndrome Protein To Promote Podosome Array Organization and Chemotaxis in Dendritic Cells. J Immunol [Internet]. 2011;186(8):4805–18. Available from: http://www.ncbi.nlm.nih.gov/pmc/articles/PMC3467106/
7. Ricart BG, John B, Lee D, Hunter CA, Hammer DA. Dendritic cells distinguish individual chemokine signals through CCR7 and CXCR4. J Immunol [Internet]. 2011;186(1):53–61. Available from: http://www.jimmunol.org/cgi/doi/10.4049/jimmunol.1002358

8. Bendell AC, Williamson EK, Chen CS, Burkhardt JK, Hammer DA. The Arp 2/3 Complex Binding Protein HS1 is Required for Dendritic Cell Random Migration and Force Generation. J Integr Biol. 2017;Accepted.

9. Förster R, Davalos-Misslitz AC, Rot A. CCR7 and its ligands: balancing immunity and tolerance. Nat Rev Immunol [Internet]. 2008;8(5):362–71. Available from: http://www.ncbi.nlm.nih.gov/pubmed/18379575

10. Haessler U, Pisano M, Wu M, Swartz MA, Rakesh Jain by K. Dendritic cell chemotaxis in 3D under defined chemokine gradients reveals differential response to ligands CCL21 and CCL19. Proc Natl Acad Sci USA. 2011;108(14):5614–9.

11. Charras G, Sahai E. Physical influences of the extracellular environment on cell migration. Nat Rev Mol Cell Biol [Internet]. Nature Publishing Group; 2014;15(12):813–24. Available from: http://dx.doi.org/10.1038/nrm3897%5Cn10.1038/nrm3897%5Cnhttp://www.nature.com/doifinder/10.1038/nrm3897%5Cnhttp://www.nature.com/doifinder/10.1038/nrm3897

12. Wójciak-Stothard B, Zbigniew M, Korohoda W, Curtis A, Wilkinson C. Activation of macrophage-like cells by multiple grooved substrata. Topographical control of cell behaviour. [Internet]. Cell Biology International. 1995. p. 485–90. Available from: http://doi.wiley.com/10.1006/cbir.1995.1092

13. Chen CS, Mrksich M, Huang S, Whitesides GM, Ingber DE. Geometric control of cell life and death. Science. 1997;276(5317):1425–8.

14. Henry SJ, Crocker JC, Hammer D a. Ligand density elicits a phenotypic switch in human neutrophils. Integr Biol (Camb) [Internet]. 2014;6(3):348–56. Available

from: http://www.ncbi.nlm.nih.gov/pubmed/24480897

15. Lo CM, Wang HB, Dembo M, Wang YL. Cell movement is guided by the rigidity of the substrate. Biophys J [Internet]. 2000;79(1):144–52. Available from: http://dx.doi.org/10.1016/S0006-3495(00)76279-5

16. Saez A, Ghibaudo M, Buguin A, Silberzan P, Ladoux B. Rigidity-driven growth and migration of epithelial cells on microstructured anisotropic substrates. Proc Natl Acad Sci U S A [Internet]. 2007;104(20):8281–6. Available from: http://www.pnas.org/cgi/content/abstract/104/20/8281

17. Eroshenko N, Ramachandran R, Yadavalli VK, Rao RR. Effect of substrate stiffness on early human embryonic stem cell differentiation. J Biol Eng [Internet]. 2013;7(1):7. Available from: http://www.pubmedcentral.nih.gov/articlerender.fcgi?artid=3621683&tool=pmcentrez&rendertype=abstract

18. Raab M, Swift J, Dingal PCDP, Shah P, Shin JW, Discher DE. Crawling from soft to stiff matrix polarizes the cytoskeleton and phosphoregulates myosin-II heavy chain. J Cell Biol. 2012;199(4):669–83.

19. Wan Z, Zhang S, Fan Y, Liu K, Du F, Davey AM, et al. B Cell Activation Is Regulated by the Stiffness Properties of the Substrate Presenting the Antigens. J Immunol [Internet]. 2013;190(9):4661–75. Available from: http://www.ncbi.nlm.nih.gov/pubmed/23554309

20. Connor RSO, Hao X, Shen K, Bashour K. Substrate rigidity regulates human T cell activation and proliferation. J … [Internet]. 2012;189(3):1330–9. Available from: http://www.jimmunol.org/content/189/3/1330.short

21. Jannat RA, Dembo M, Hammer DA. Neutrophil adhesion and chemotaxis depend on substrate mechanics. J Phys Condens Matter. 2010;22(19):194117.

22. Hind LE, Dembo M, Hammer D a. Macrophage motility is driven by frontal-towing with a force magnitude dependent on substrate stiffness. Integr Biol [Internet]. Royal Society of Chemistry; 2015;7:447–53. Available from: http://xlink.rsc.org/?DOI=C4IB00260A

23. Tan JL, Tien J, Pirone DM, Gray DS, Bhadriraju K, Chen CS. Cells lying on a bed of microneedles: an approach to isolate mechanical force. Proc Natl Acad Sci U S A [Internet]. 2003;100(4):1484–9. Available from: http://www.pnas.org/content/100/4/1484.full

24. Yang MT, Fu J, Wang Y-K, Desai R a, Chen CS. Assaying stem cell mechanobiology on microfabricated elastomeric substrates with geometrically modulated rigidity. Nat Protoc [Internet]. Nature Publishing Group; 2011;6(2):187–213. Available from: http://www.nature.com/doifinder/10.1038/nprot.2010.189

25. Ricart BG, Yang MT, Hunter C a., Chen CS, Hammer D a. Measuring traction forces of motile dendritic cells on micropost arrays. Biophys J [Internet]. Biophysical Society; 2011;101(11):2620–8. Available from: http://dx.doi.org/10.1016/j.bpj.2011.09.022

26. Riedl J, Flynn KC, Raducanu A, Gärtner F, Beck G, Bösl M, et al. Lifeact mice for studying F-actin dynamics. Nat Methods [Internet]. Nature Publishing Group; 2010;7(3):168–9. Available from: http://dx.doi.org/10.1038/nmeth0310-168

27. Sixt M, Lämmermann T. In Vitro Analysis of Chemotactic Leukocyte Migration in

3D Environments. In: Wells CM, Parsons M, editors. Cell Migration [Internet]. Humana Press; 2011. p. 149–65. Available from: http://dx.doi.org/10.1007/978-1-61779-207-6_11

28. Desai R a, Khan MK, Gopal SB, Chen CS. Subcellular spatial segregation of integrin subtypes by patterned multicomponent surfaces. Integr Biol (Camb). 2011;3(5):560–7.

29. Dunn GA. Characterising a kinesis response: time averaged measures of cell speed and directional persistence. [Internet]. Agents and actions. Supplements. 1983. p. 14–33. Available from: http://www.ncbi.nlm.nih.gov/pubmed/6573115

30. Henry SJ, Crocker JC, Hammer DA. Motile Human Neutrophils Sense Ligand Density Over Their Entire Contact Area. Ann Biomed Eng [Internet]. 2015; Available from: http://www.ncbi.nlm.nih.gov/pubmed/26219404

31. Mackay JL, Hammer DA. Integrative Biology through E-selectin but not P-selectin †. Integr Biol [Internet]. Royal Society of Chemistry; 2016;8:62–72. Available from: http://dx.doi.org/10.1039/C5IB00199D

32. Vargas P, Maiuri P, Bretou M, Saez PJ, Pierobon P, Maurin M, et al. Innate control of actin nucleation determines two distinct migration behaviours in dendritic cells. Nat cell Biol. 15AD;18(1):43–53.

33. Lämmermann T, Bader BL, Monkley SJ, Worbs T, Wedlich-Söldner R, Hirsch K, et al. Rapid leukocyte migration by integrin-independent flowing and squeezing. Nature [Internet]. 2008;453(7191):51–5. Available from: http://www.nature.com/doifinder/10.1038/nature06887%5Cnhttp://www.ncbi.nlm.nih.gov/pubmed/18451854

34. Cox TR, Erler JT. Remodeling and homeostasis of the extracellular matrix: implications for fibrotic diseases and cancer. Dis Model Mech [Internet]. 2011;4(2):165–78. Available from: http://dmm.biologists.org/content/4/2/165

35. Frey MT, Tsai IY, Russell TP, Hanks SK, Wang Y-L. Cellular responses to substrate topography: role of myosin II and focal adhesion kinase. Biophys J [Internet]. Elsevier; 2006;90(10):3774–82. Available from: http://dx.doi.org/10.1529/biophysj.105.074526

36. Tabdanov E, Gondarenko S, Kumari S, Liapis A, Dustin ML, Sheetz MP, et al. Micropatterning of TCR and LFA-1 ligands reveals complementary effects on cytoskeleton mechanics in T cells. Integr Biol [Internet]. Royal Society of Chemistry; 2015;7(10):1272–84. Available from: http://dx.doi.org/10.1039/C5IB00032G%5Cnhttp://pubs.rsc.org/en/content/articlepdf/2015/ib/c5ib00032g

37. Dehring DAK, Clarke F, Ricart BG, Huange Y, Gomez TS, Williamson EK, et al. Hematopoietic Lineage Cell-Specific Protein 1 Functions in Concert with the Wiskott-Aldrich Syndrome Protein to Promote Podosome Array Organization and Chemotaxis in Dendritic Cells. J Immunol. 2011;186(8):4805–18.

# CHAPTER 5 : BIOMOLECULAR COMPONENTS OF DC RANDOM MIGRATION

Adapted from: **The Arp 2/3 Complex Binding Protein HS1 is Required for Efficient Dendritic Cell Random Migration and Force Generation**

Amy C. Bendell, Edward K. Williamson, Christopher S. Chen, Janis K. Burkhardt, Daniel A. Hammer

Accepted in *The Journal of Integrative Biology*

ABSTRACT

Dendritic cell migration to the T-cell-rich areas of the lymph node is essential for their ability to initiate the adaptive immune response. While it has been shown that the actin cytoskeleton is required for normal DC migration, the role of many of the individual cytoskeletal molecules is poorly understood. In this study, I investigated the contribution of the Arp2/3 complex binding protein, haematopoietic lineage cell-specific protein 1 (HS1), to DC migration and force generation. I quantified the random migration of HS1 $^{-/-}$ DCs on 2D micro-contact printed surfaces and found that in the absence of HS1, DCs have greatly reduced motility and speed. This same reduction in motility was recapitulated when adding Arp2/3 complex inhibitor to WT DCs or using DCs deficient in WASP, an activator of Arp2/3 complex-dependent actin polymerization. I further investigated the importance of HS1 by measuring the traction forces of HS1 $^{-/-}$ DCs on micropost array detectors (mPADs). In HS1 deficient DCs, there was a significant reduction in force generation (3.96 ± 0.40 nN/cell) compared to WT DCs (13.76 ± 0.84 nN/cell). Interestingly, the forces generated in DCs lacking WASP were only slightly reduced compared to WT DCs. Taken together, these findings show that HS1 and Arp2/3 complex-mediated actin polymerization are essential for the most efficient DC random migration and force generation.

## INTRODUCTION

Dendritic cells (DCs) are potent antigen presenting cells (APCs) which possess the unique ability of linking the innate and adaptive immune responses (2,3). Immature DCs reside in a variety of tissues and continually sample their environment for antigens. Once DCs encounter a pathogen, they capture it and load antigenic fragments onto MHC molecules on their surface for presentation to other immune cells. Pathogen recognition also triggers DC maturation, which is characterized by a variety of phenotypic and functional changes (reviewed in (4,5)). Of particular interest to us is a dramatic switch from a slowly moving, tissue resident cell to a highly migratory cell (6). This increased level of migration allows DCs to exit peripheral tissues and travel via the lymphatic system to T cell rich regions of the lymph nodes, where they activate T cells and launch a specialized immune response (7).

Cell migration depends on coordinated interactions among the different components of the actin cytoskeleton (8,9). At the front of a migrating cell, rapid actin polymerization forms protrusive structures that help to push the plasma membrane forward. One such structure found in DCs is the lamellipodium (Figure 5.1A) (10), which is formed by branched actin polymerization driven by the actin related protein (Arp) 2/3 complex (Figure 5.2B) (11,12). While the Arp2/3 complex alone is a weak actin nucleator, the rate of Arp2/3 mediated actin polymerization is increased in the presence of a class of proteins known as nucleation promoting factors (NPFs) (13–16). These proteins bind to both actin and the Arp2/3 complex and enhance Arp2/3 complex-dependent nucleation of branched actin filaments. One such NPF is hematopoietic lineage cell-specific protein 1 (HS1).

HS1 (also known as HCLS1 and LckBP1) is a 75 kDa protein expressed exclusively in hematopoietic cells (17,18). HS1 is the only known class II NPF in hematopoietic cells and is

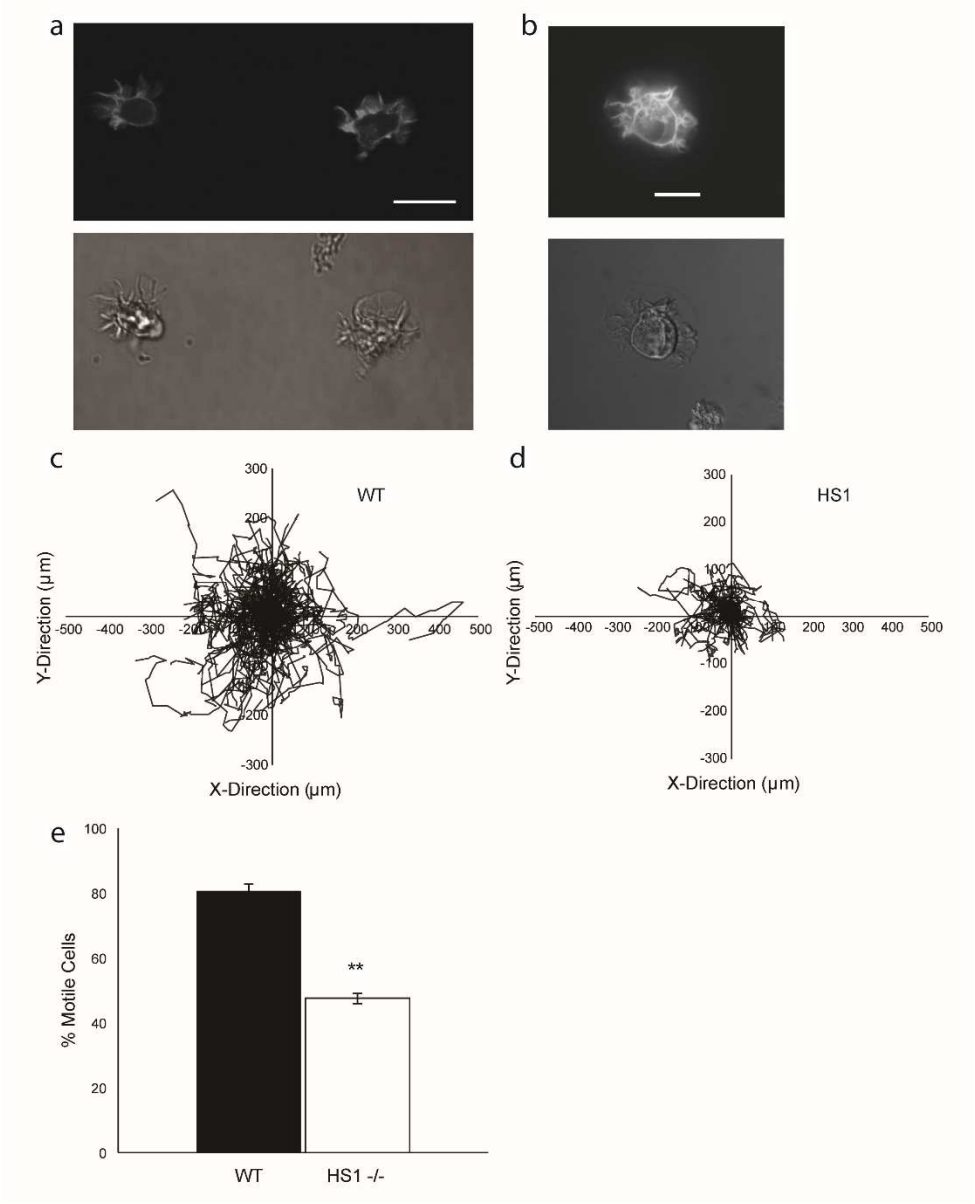


*Figure 5.1. DCs contain actin rich structures at the leading edge and show defects in migration when HS1 is eliminated.*

(A) Sample images of GFP-Lifeact DCs showing GFP-labeled actin filaments (top) and phase contrast images of the same cells (bottom). Scale bar equals 20 µm. (B) Sample images of GFP-Life-act transduced HS1 $^{-/-}$ DCs showing GFP-labeled actin filaments (top) and bright field images of the same cell (bottom). (C,D) Cell tracks for (C) WT and (D) HS1 $^{-/-}$ DCs during a representative chemokinesis experiment. ≥ 110 cells were

tracked per condition for a period of 2-3 hours. (E) Average percentage of motile cells. Figures represent average values ± SEM, for > 1000 DCs from at least three independent experiments per condition. Statistical significance calculated with single factor ANOVA and post hoc Tukey test. Indicates significant difference compared to WT DCs. *$p<0.05$, **$p<0.01$

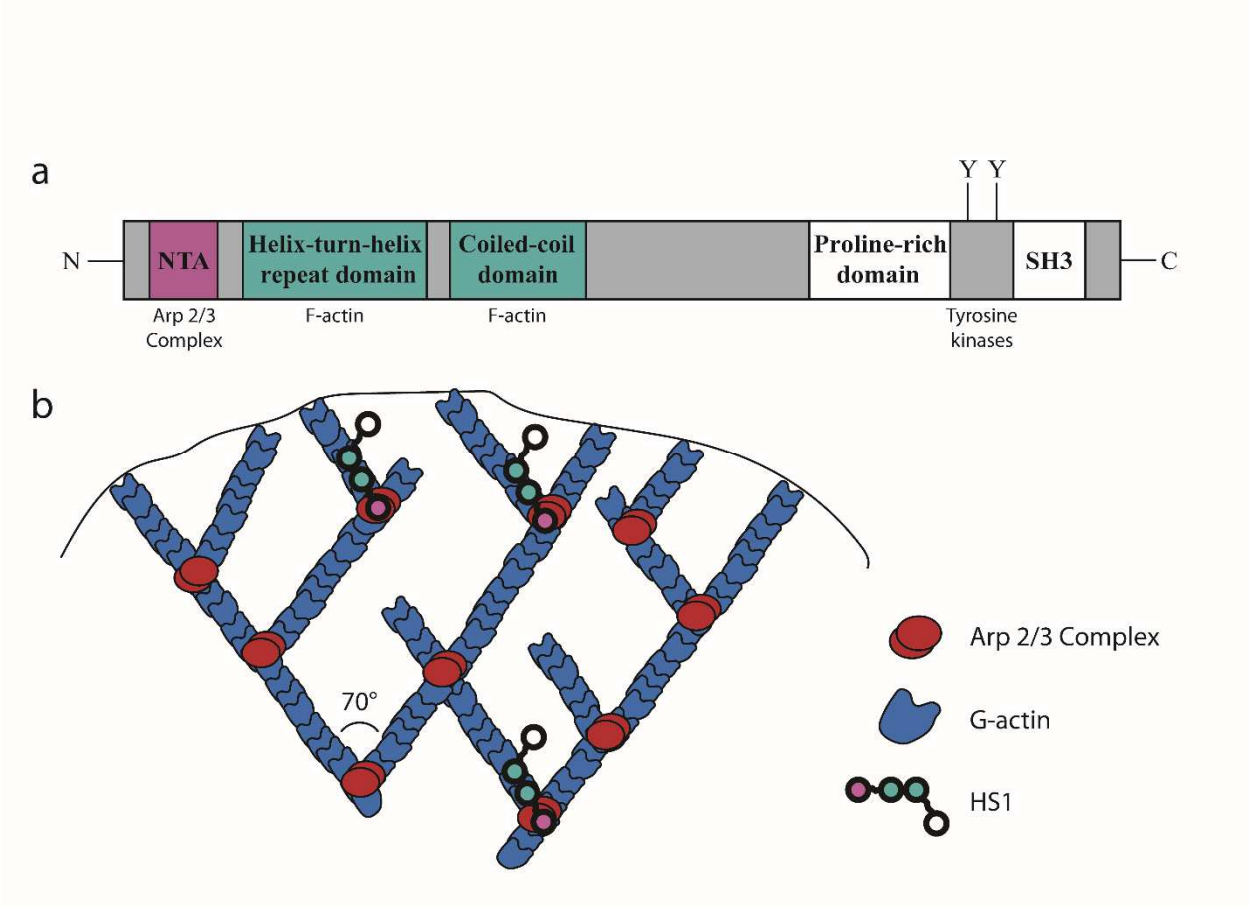


*Figure 5.2. HS1 stabilizes branched actin filaments at the leading edge of DCs.*

(A) Structure of HS1. The NTA domain, shown in red, binds to the Arp 2/3 complex. The helix-turn-helix domain and coiled-coil domains, shown in blue, bind to F-actin. A proline rich domain, SH3 domain and important tyrosine residues are located at the C-terminus. (B) Cartoon representation of branched actin structure in lamellipodia. Red represents the Arp 2/3 Complex and blue represents actin. HS1 (chain of colored circles) is thought to stabilize actin branch points by simultaneously binding the Arp 2/3 Complex and neighboring F-actin.

highly homologous with the widely studied protein cortactin (19). It contains an N-terminal acidic (NTA) region, which binds to the Arp2/3 complex, followed by a helix-turn-helix region and a coiled-coil domain, both of which bind to F-actin and are required for proper Arp2/3 complex activation and branched actin polymerization (Figure 5.2A) (15,20). HS1 has been shown to increase the rate of Arp2/3 complex mediated actin polymerization, prolong the half-life of existing branched actin filaments and regulate lamellipodial dynamics (15,20–22). It has also been shown that HS1 interacts with another NPF—Wiskott Aldrich Syndrome Protein (WASP) (23). Unlike HS1, WASP is a class I NPF, which uses its VCA domain to bind to monomeric actin and the Arp2/3 complex (24). Through its interactions with the Arp2/3 complex and WASP, HS1 is able to shape the dynamics of branched actin networks.

HS1 is expressed at high levels in mature dendritic cells (25), yet the exact role it plays in DC migration is not clear. Initial studies revealed that HS1 could be eliminated from dendritic cells without altering their morphology or viability (23,25). Nonetheless, there are a few differences in the structure and function of HS1 $^{-/-}$ DCs. HS1 $^{-/-}$ DCs adhere and spread normally, but they form disorganized and overly dynamic actin structures, such as podosomes and lamellipodia, and have defective antigen capture via receptor-mediated endocytosis (23,25). Previous work by Klos Dehring *et al.* highlighted the importance of HS1 in dendritic cell migration, in particular during chemotaxis (23). The authors found that HS1 $^{-/-}$ DCs are able to migrate across transwells in response to CCL19 or CCL21 to the same degree as WT DCs, and have unaltered expression of chemokine receptors. However, when placed in a microfluidic gradient generator, HS1 $^{-/-}$ DCs migrated significantly faster than WT DCs and were less able to persistently migrate

in the direction of the chemokine gradient. These findings reveal that the long-term ability of HS1$^{-/-}$ DCs to reach a target location is not significantly altered, but that the manner in which DCs migrate to the target is affected. Building upon this study, I sought to determine if HS1 impacts other aspects of DC migration. Using motility assays and micropost array detectors (mPADs), I quantified the random migration and force generation of HS1 $^{-/-}$ DCs, respectively. In addition, I used both Arp2/3 complex inhibitor and WASP $^{-/-}$ DCs to elucidate the molecular mechanisms through which HS1 acts. I found that HS1 is required for efficient migration and force generation, and I hypothesize that HS1 likely influences DC migration through its interaction with the Arp2/3 complex.

## MATERIALS AND METHODS

### *Reagents*

Recombinant murine CCL19 was purchased from R&D Systems (Minneapolis, MN). Lipopolysaccharide (LPS; L4516), CK-666 (Lot: 043M4606V) DMSO, Pluronics F127, silane (Trichloro(1H,1H,2H,2H-perfluorooctyl)silane) and bovine fibronectin were obtained from Sigma-Aldrich (St. Louis, MO). Penicillin-Streptomycin (10,000 U/mL), RPMI 1640 (1x, with L-Glutamine and 25 mM HEPES) and PBS were obtained from Thermo Fisher Scientific (Hampton, NH). Poly(dimethylsiloxane) (Sylgard 184 Silicone Elastomer) was purchased from Dow Corning, Midland, MI. 200 proof ethanol was obtained from Decon Laboratories (King of Prussia, PA). Fetal bovine serum was obtained from Atlanta Biologicals (Flowery Branch, GA). Recombinant GM-CSF was produced from the B78Hi/GMCSF.1 cell line provided by T. Laufer (University of Pennsylvania, Philadelphia, PA).

### *Mice*

C57BL/6J mice, WASP$^{-/-}$ mice bred on the C57BL/6J background (26) (both from Jackson Laboratories), HS1-/- mice bred on the C57BL/6J background (27) and GFP-Lifeact mice bred on the C57BL/6J background (26) were reared at Children's Hospital of Philadelphia. All mice were housed under pathogen-free conditions in the Children's Hospital of Philadelphia animal facility. All studies involving animals were reviewed and approved by the Children's Hospital of Philadelphia Institutional Animal Care and Use Committee.

*Culture of bone marrow derived DCs (BMDCs)*

Primary dendritic cells were prepared from murine bone marrow, following the protocol of Sixt and Lämmermann (28). Bone marrow was flushed from the femurs and tibiae with sterile PBS. Cells were centrifuged at 1500 rpm for 10 min at 4°C and resuspended at 2.5 x $10^6$ cells/mL in RPMI 1640 supplemented with 10% heat-inactivated fetal bovine serum and 1% penicillin and streptomycin. 1 mL cell suspension was combined with 9 mL media and 100 μL GM-CSF in a 10 cm Petri dish. On day 3, 10 mL fresh media and 100 μL GM-CSF were added, and on day 6, 100 μL GM-CSF was added after half of the media was gently replaced. 200 ng/mL LPS was added between day 7 to 9 and DCs were matured for 24 hours. After maturation, DCs were centrifuged at 1500 rpm for 10 min at 4°C and resuspended at 100,000 cells/mL for random migration experiments or 50,000 cells/mL for force measurement experiments. Cells were maintained at 37°C and 5% $CO_2$.

*Surface Preparation for Random Migration Experiments*

25 mm round glass coverslips (Thermo Fisher Scientific) were coated with a thin layer of degassed poly(dimethylsiloxane) (PDMS, 10:1 base to cure by weight) (using a Laurell spinner (4000 rpm, 1 minute). Coverslips were cured for at least three hours at 65°C. Circular holes were laser cut from the bottom of each well of a 6 well dish. The PDMS coated coverslips were affixed to the bottom of each well using 10:1 PDMS and the seal was cured overnight at 65°C. The coverslips were functionalized by microcontact printing following the protocol of Desai et al (29). Stamps for printing

were prepared by casting degassed PDMS against a flat silicon wafer. The PDMS was allowed to cure in contact with the wafer overnight at 65°C. 1 $cm^2$ square stamps were cut from the block of PDMS using a premade grid pattern as a guide. Stamps were sonicated in 200 proof ethanol for 5 minutes, rinsed twice in di$H_2O$ and gently dried with $N_2$ gas. 200 μL of a 10 μg/mL solution of fibronectin was added to each stamp and incubated at room temperature for 2 hours. Stamps were again rinsed twice in di$H_2O$ and gently dried with $N_2$ gas. The 6 well dish containing the PDMS coverslips was treated for 7 minutes with ultraviolet ozone (UVO Cleaner Model 342, Jelight, Irvine, CA) and PDMS stamps were used to transfer protein to the coverslip surface. The printed coverslips were blocked with 0.2 % Pluronic F127 for 1 hour at room temperature, rinsed twice with sterile PBS and stored at 4°C overnight.

The following day, 1 mL of mature DCs (100,000 cells/mL) were seeded on each printed coverslip. In inhibition studies, the desired concentration of CK-666 or equivalent volume of DMSO was added 1 hour prior to imaging and the cells were incubated at 37°C and 5% $CO_2$. Motility was stimulated with 10 nM CCL19 immediately before moving the plate to the microscope stage.

*Live Cell Imaging for Random Migration Experiments*

DCs were imaged at 10x by phase microscopy on a Nikon Eclipse TE300 (Nikon, Melville, NY) with custom-built Labview (National Instruments, Austin, TX) software. A motorized stage was used to capture images at multiple positions. Time-lapse experiments were performed by acquiring images every two to three minutes for up to three hours. Cells were maintained at 37°C and 5% $CO_2$ during imaging.

*Random Motility Data Analysis*

Cell migration was analyzed with the Manual Tracking plugin in ImageJ (http://rsbweb.nih.gov/ij). Cells were tracked over time by manually specifying their centroid positions in each frame. Cells that were apoptotic or completely stationary were excluded, as well as any cells in contact with other cells. The list of x- and y-coordinates obtained from ImageJ was further analyzed with a custom-written MATLAB (Mathworks, Natick, MA) script. The MATLAB script computed the MSD of the compiled list of cell tracks and used the Dunn equation $\left(\langle MSD(\tau)\rangle = 2S^2P\left[\tau - P\left(1 - exp\left(-\tau/P\right)\right)\right]\right)$ to fit speed (S) and persistence (P) (30). The random motility coefficient was calculated from the speed and persistence as follows: $\mu = \frac{1}{n}S^2P$, where n specifies the dimensionality (31).

*mPAD Preparation*

Micropost array detectors (mPADs) were prepared following the protocol of Yang et al. (32). Micropost arrays were prepared from a silicon master by replica molding. Negative molds were created by casting degassed PDMS (10:1 base to cure) against a silanized silicon master mold and curing for 12 minutes at 110°C. The negative molds were gently peeled away from the silicon master, plasma treated (SPI Supplies Plasma Prep II, West Chester, PA) for 7 seconds, and silanized overnight. PDMS (10:1 base to cure) was added to the negative molds and degassed for 30 minutes to remove any air bubbles. 25 mm round glass coverslips were cleaned with $N_2$ gas and plasma treated for 90 seconds. The molds were placed, fresh PDMS side down, onto the cleaned coverslip

and cured at 110°C for 20 hours. The mPADs were gently peeled away from the negative molds, immediately submerged in 200 proof ethanol and supercritical dried (SAMDRI-PVT-3D, Tousimis Corporation, Rockville, MD) in liquid $CO_2$. Circular holes were laser cut from the bottom of one well dishes. mPAD coverslips were secured to the bottom of the one well dishes with 10:1 PDMS and the seal was cured overnight at 65°C.

10 μg/mL fibronectin was microcontact printed onto the post tips, following the same procedure as above with minor modifications. After stamping the mPADs, 1 mL of 200 proof ethanol was added and the stamp was gently flicked off the micropost array. The ethanol was immediately diluted to 60% with di$H_2O$. The mPADs were rinsed three times with di$H_2O$ and were incubated with 1x Δ9-DiI (1,1′-dioleyl-3,3,3′,3′-tetramethylindocarbocyanine methanesulfonate; Invitrogen Carlsbad, CA) for one hour, at room temperature. To prevent photobleaching of the fluorescent label, the mPAD was covered and lights were dimmed, when possible, for the rest of the preparation process. The mPADs were gently rinsed three times with di$H_2O$. The post tips were blocked with 0.2 % Pluronic F127 for 1 hour at room temperature, rinsed three times with sterile di$H_2O$ and stored at 4°C overnight. The following day 1 mL of mature DCs (50,000 cells/mL) was seeded on the mPAD. Motility was stimulated with 10 nM CCL19 immediately before moving the dish to the microscope stage, and cells were allowed to settle on the micropost array before imaging began.

*Live Cell Imaging for Force Measurement Experiments*

DCs were imaged at 40x by phase and fluorescence microscopy on a Nikon Eclipse TE300 with custom-built Labview software. A motorized stage was used to capture images at multiple positions. Time-lapse experiments were performed by acquiring images every minute for up to an hour. Cells were maintained at 37°C and 5% $CO_2$ during imaging.

*Traction Force Analysis*

A custom MATLAB (Mathworks, Natick, MA) script was used to analyze a series of paired phase and fluorescent images. Phase images were used to manually delineate the area occupied by the cell of interest. The corresponding fluorescent image was then opened and the position of the posts in the area of interest was recorded. The script determines the ideal position of each post based on the theoretical post packing geometry. Deflection distance was calculated for the posts in the area of interest as the 2-dimensional distance between the ideal position the measured position. The deflections were then converted into vector forces using Hooke's law ($F = kx$) and the known spring constant of the micropost array (k=1.92 nN/μm) for the given post height and diameter. These forces were then used to calculate the total scalar force per cell, which was averaged over the entire ensemble of cells for each type of cell (WT, HS1 $^{-/-}$ and WASP $^{-/-}$ ).

*Statistical Analysis*

I used a one way ANOVA along with a Tukey's Post Hoc Test to determine statistical significance. Statistically significant differences at $p < 0.05$ were marked with an asterisk on plots (*) and statistically significant differences at $p < 0.01$ were marked with a double asterisk (**).

RESULTS

*HS1 is Required for Efficient DC Random Migration*

It was previously shown that HS1 contributes to DC speed and persistence during chemotaxis (23), but its role in random migration was not tested. It has been revealed in a variety of immune cell types that HS1 can have different effects on different modes of migration (33–37). Therefore, I hypothesized that I would see defects in DC chemokinesis that were absent during DC chemotaxis. To assess this, I performed parallel experiments with WT and HS1 $^{-/-}$ DCs undergoing chemokinesis. Briefly, I plated cells on PDMS surfaces that had been printed with bovine fibronectin and blocked with the Pluronic F127. I acquired time lapse images of each cell type in phase contrast and used the Manual Tracking Plugin in ImageJ to quantify cell position as a function of time.

In these low magnification, phase contrast experiments, the appearance of HS1 $^{-/-}$ DCs was qualitatively indistinguishable from that of WT DCs (Figure 5.3). HS1 $^{-/-}$ DCs were viable and still formed extensive membrane veils and protrusions. However, while HS1 $^{-/-}$ DCs retained some ability to migrate, the extent of their migration was significantly reduced. Figure 5.1C and D shows the migration patterns of representative populations of WT and HS1 $^{-/-}$ DCs. The start position of each cell was set at the origin to allow for visualization of the distance traveled by all cells in a given field of view. As expected, both WT and HS1 $^{-/-}$ DCs migrated randomly, with no directional bias. While both populations of cells were able to migrate, I saw a large difference in the area explored during migration, with HS1 $^{-/-}$ DCs restricted to a smaller region than WT DCs.

From this initial observation, it appears that HS1 is an important component of the DC migratory machinery.

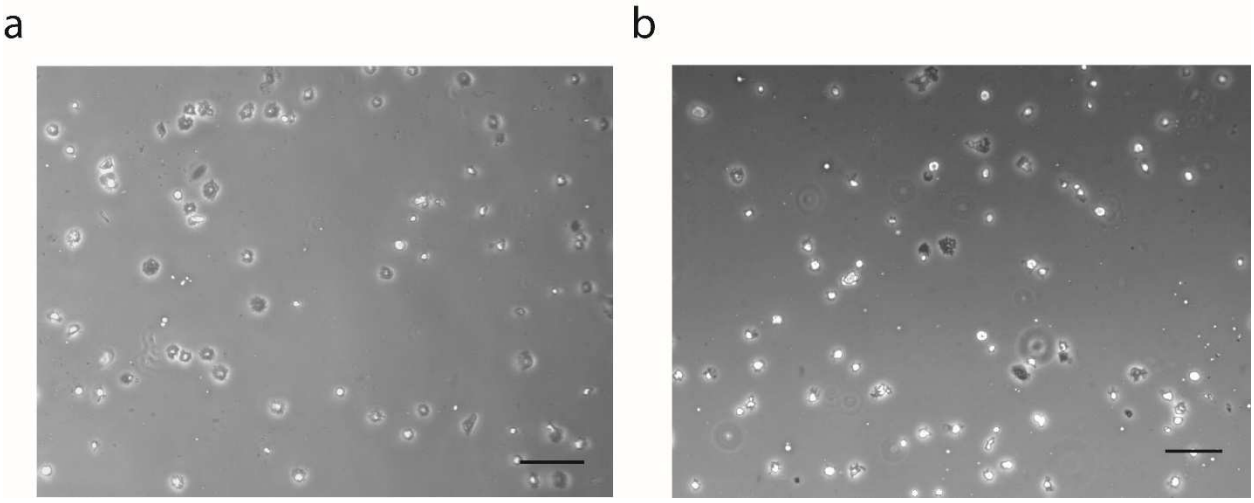


*Figure 5.3. HS1 -/- DCs are morphologically similar to WT DCs. Phase contrast images of WT DCs*

(A) and HS1 $^{-/-}$ DCs (B). Images are snapshots from longer, time course experiments. Cells are plated on 10 μg/mL fibronectin and are migrating in the presence of 10 nM CCL19. Scale bar represents 100 μm.

While some HS1 $^{-/-}$ DCs were able to move, many HS1 $^{-/-}$ DCs appeared to vacillate around a fixed point. I designated cells as "motile" if they traveled at least two cell diameters over the course of the experiment. Cells that traveled less than this were designated as "stationary." During chemokinesis, 80.45 ± 2.22 % of WT DCs were "motile," compared to only 47.61 ± 1.69% for HS1 $^{-/-}$ DCs (Figure 5.1E). This shows that HS1 $^{-/-}$ DCs have a significant defect in translocation, as compared to their WT counterparts.

I further quantified the migration of HS1 $^{-/-}$ DCs by calculating the mean squared displacement (MSD) as a function of time for both WT and HS1 $^{-/-}$ DCs (Figure 5.4A). When plotting MSD vs. time on a log-log scale, I would expect to see a slope of one for a population of cells moving randomly or diffusively. This is indeed what I observed for WT DCs. However, HS1 $^{-/-}$ DCs failed to migrate diffusively over the entire course of the experiment, as shown by an initial linear rise in MSD followed by a plateau. It has been shown that HS1 is necessary for the stability of DC lamellipodia (23) and I have observed dynamic ruffling in my HS1$^{-/-}$ DCs. I hypothesize that the decrease in migration that I observed at long times could be related to the inability of these cells to form persistent actin structures.

I next fit the curves for MSD vs. time to the Dunn equation $\left(\langle MSD(\tau)\rangle = 2S^2P\left[\tau - P\left(1 - exp\left(-{}^{\tau}/_{P}\right)\right)\right]\right)$ (30). This allowed us to calculate a variety of useful motility metrics, such as average speed (S), persistence length (the distance traveled before a cell changed direction), persistence time (P, length of time a cell traveled before changing direction) and random motility coefficient (μ). WT DCs undergoing chemokinesis moved at speeds of 4.00 ± 0.18 μm/min (Figure 5.4B). HS1 $^{-/-}$ DCs

showed a significant reduction in migration speed, traveling at only 2.31 ± 0.08 μm/min. HS1 $^{-/-}$ DCs also showed significant reductions in persistence length, but their persistence time was unaffected (Figure 4 C and D). This suggests

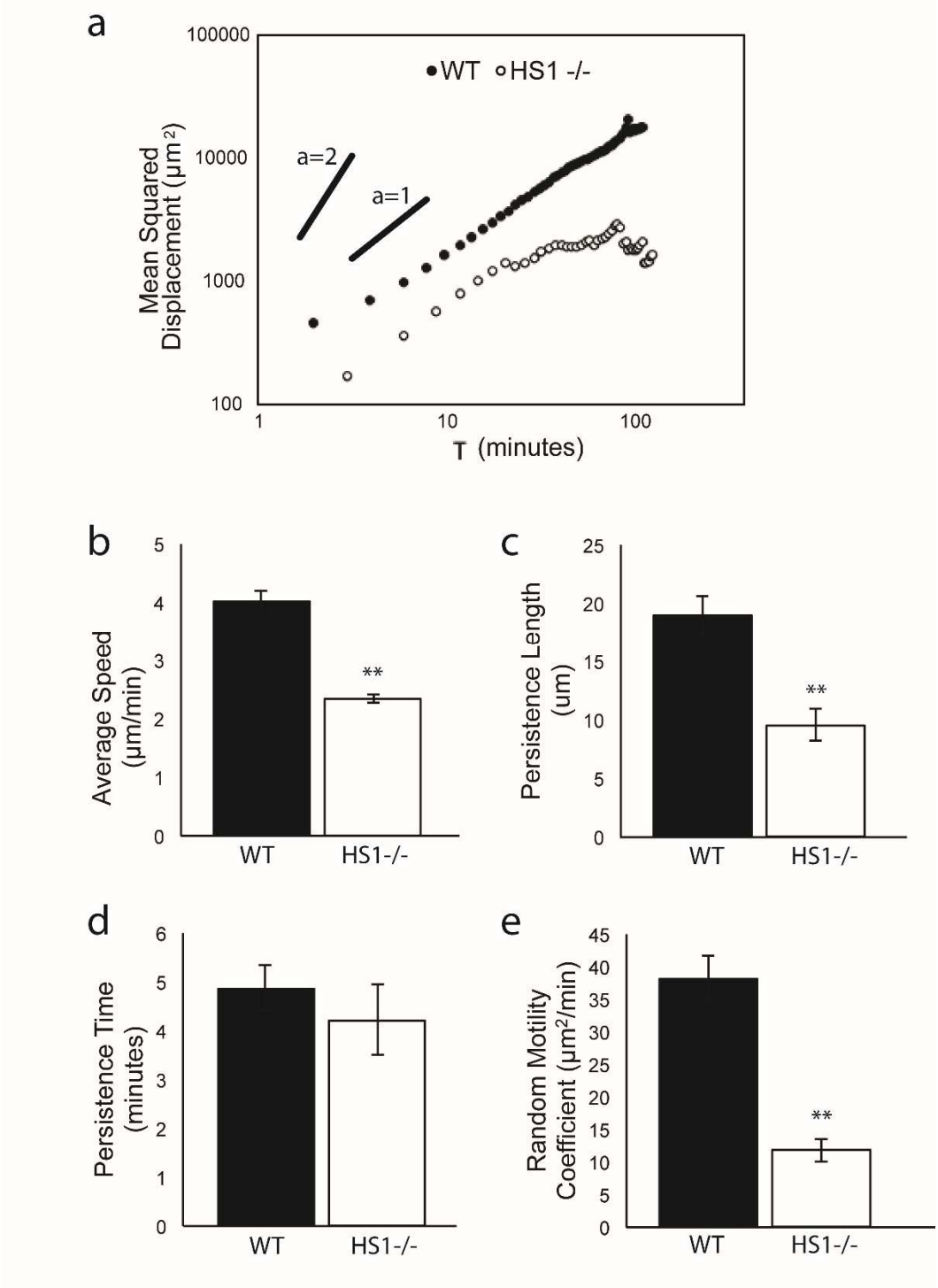


*Figure 5.4. HS1 -/- DCs exhibit multiple defects in migration during chemokinesis*

(A) MSD vs. time on log-log scale for WT and HS1 $^{-/-}$ DCs. Quantification of DC random migration: (B) average speed, (C) persistence length, (D) persistence time, (E)

random motility coefficient. Figures represent average values ± SEM, for > 1000 DCs from at least three independent experiments per condition. Statistical significance calculated with single factor ANOVA and post hoc Tukey test. Indicates significant difference compared to WT DCs. *$p<0.05$, **$p<0.01$

that HS1 $^{-/-}$ DCs were able to turn at the same frequency as WT DCs, but their reduced speed led to shorter distances traveled between subsequent turns. These effects were extended to the random motility coefficient (Figure 4E), which is a quantitative measure of cell diffusivity and is related to speed and persistence as follows: $\mu = \frac{1}{n}S^2P$. HS1 $^{-/-}$ DCs had a much lower random motility coefficient (11.80 ± 1.75 μm$^2$/min) than WT DCs (38.20 ± 3.41 μm$^2$/min). This agreed with my MSD calculation and confirmed that HS1 $^{-/-}$ DCs were less capable of diffusive migration. From these initial experiments, I conclude that HS1 expression is required for efficient DC chemokinesis.

*HS1 and the Arp2/3 Complex Work Together to Coordinate DC Random Migration*

HS1 binds to both the Arp2/3 complex and polymerized actin via its N terminus, and is thought to stabilize the branched actin network through these interactions (15,20). I hypothesize that the reduction (but not total elimination) of HS1 $^{-/-}$ DC motility could be due to the failure of HS1 $^{-/-}$ DCs to stabilize branched actin filaments. To determine how inhibition of the Arp2/3 complex compares with loss of HS1 function, I incubated WT DCs with CK-666 (Figure 5A). CK-666 is a small molecule inhibitor that binds to the Arp2/3 complex and locks it in an inactive conformation, thereby preventing actin binding and polymerization (38). I tested three different concentrations of CK-666 - 1 μM, 10 μM and 100 μM. WT DCs were added to PDMS surfaces microcontact printed with fibronectin and were incubated with CK-666 for one hour before imaging. As predicted, inhibiting Arp2/3 complex function decreased migration, and it did so in a dose dependent manner. At the highest concentration of CK-666 tested, migration was

quantitatively indistinguishable from HS1 $^{-/-}$ DC migration, as shown by reductions in average speed, persistence length and random motility coefficient (Figure 5B-D).

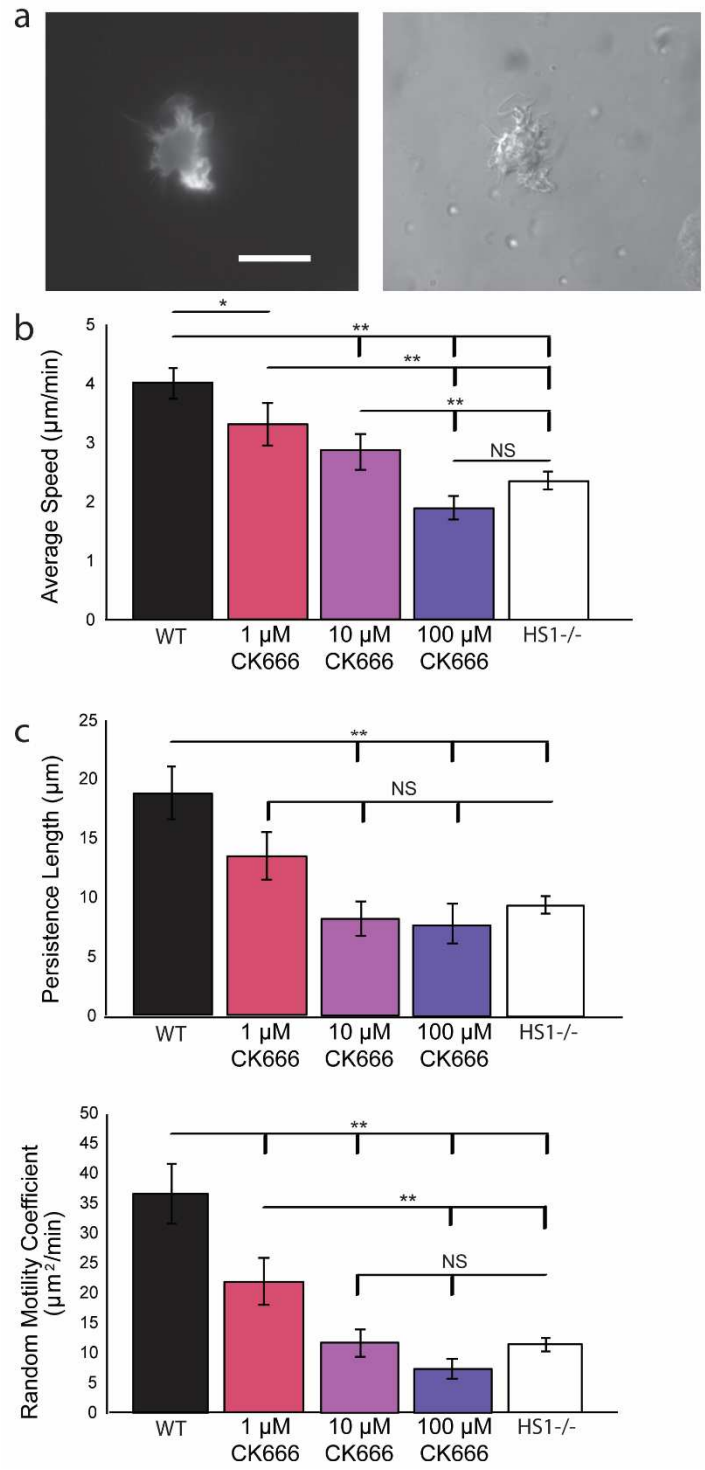


*Figure 5.5. CK666 negatively regulates DC chemokinesis.*

(A) Sample images of GFP-Life-act DC inhibited with CK-666, showing GFP-labeled actin filaments (left) and bright field images of the same cell (right). Scale bar equals 20

μm. Quantification of WT DC chemokinesis in the presence of CK-666, an Arp2/3 inhibitor (B) average speed, (C) persistence length and (d) random motility coefficient (WT and HS1 values taken from Figure 5.4 and included for reference). Three different CK-666 concentrations were used: from left to right 1 μM, 10 μM and 100 μM. Figures represent average values ± SEM, for > 290 DCs from at least three independent experiments per condition. Statistical significance calculated with single factor ANOVA and post hoc Tukey test. Indicates significant difference compared to WT DCs. *$p<0.05$, **$p<0.01$

Inhibition with CK-666 at any level did not affect the persistence time, suggesting that the Arp2/3 complex is not required for DCs to change direction at the proper frequency (data not shown). DMSO exposed cells were used as a control and showed no significant defects in persistence or random motility (Figure 5.6). To further explore the importance of the Arp2/3 Complex on DC random migration, I inhibited HS1 $^{-/-}$ DCs with 100 μM CK-666. Addition of Arp2/3 complex inhibitor to HS1 -/- DCs led to a reduction in average speed, but the persistence length and random motility coefficient were not significantly affected (Figure 5.7). Since HS1$^{-/-}$ DC migration is not greatly affected with addition of Arp2/3 complex inhibitor, this suggests that the defects observed in HS1$^{-/-}$ migration are partly due to interaction with the Arp2/3 complex.

Next I investigated the role of WASP (Wiskott-Aldrich Syndrome protein), another Arp 2/3 complex activating protein found in hematopoietic cells (39,40). Previous studies in DCs have shown that WASP is required for proper morphology and cytoskeletal organization (23,41,42), antigen processing (43), activation of the innate and adaptive immune systems (44–46), and migration (23,26,41,47). While various aspects of WASP $^{-/-}$ DC migration have been studied, to my knowledge no one has yet determined how WASP impacts the random migration of mature DCs. Since I hypothesize that defective HS1 $^{-/-}$ DC chemokinesis is due to impaired Arp2/3 complex activity and branched actin instability, I expected to observe similar defects in WASP $^{-/-}$ DC chemokinesis. As I previously observed with HS1 $^{-/-}$ DCs, WASP $^{-/-}$ DCs had significantly impaired migration, with reduced average speed, persistence length and random motility coefficient (Figure 5.8, previous HS1 $^{-/-}$ data included as a reference). The persistence length and random motility coefficient were comparable to the values

calculated for HS1 $^{-/-}$ DCs. The average speed of WASP $^{-/-}$ DCs (3.07 ± 0.15 μm/min) was significantly lower than WT DCs (4.01 ± 0.18 μm/min), but was also significantly higher than HS1 $^{-/-}$ DCs (2.35 ± 0.08 μm/min).

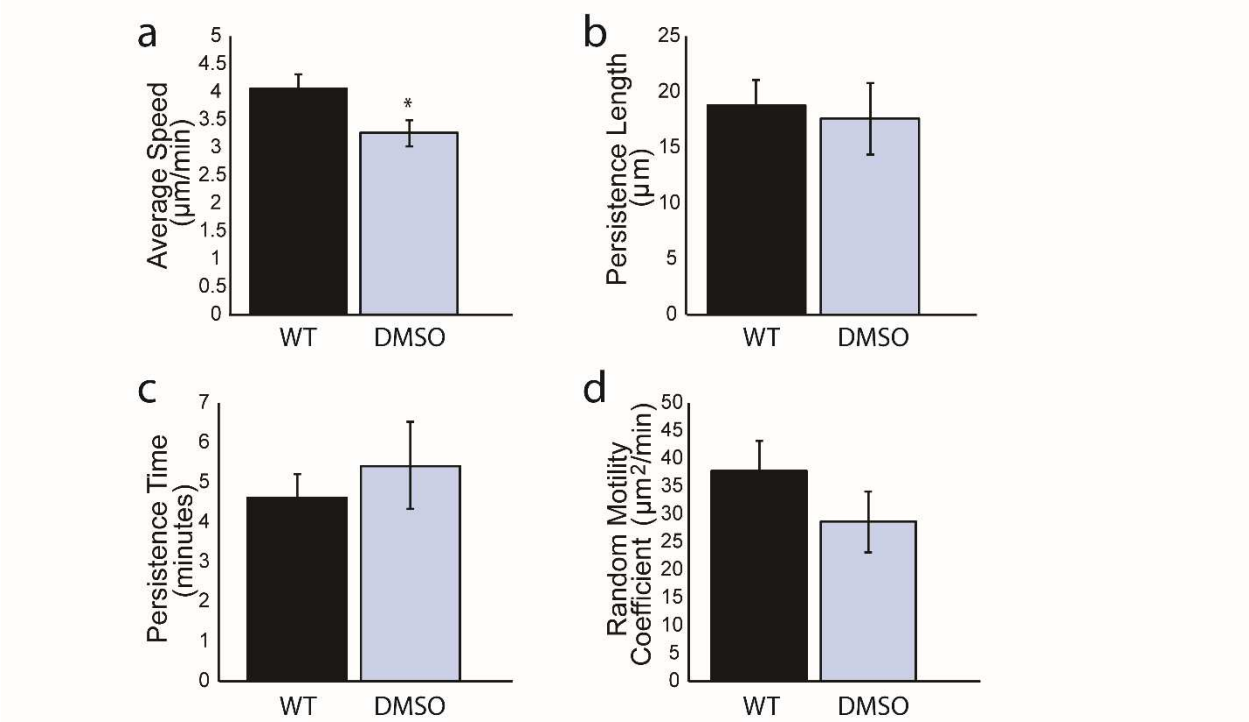


*Figure 5.6. Quantification of WT DC chemokinesis in the presence of DMSO*

(A) average speed, (B) persistence length and (C) persistence time, (D) random motility coefficient. WT values taken from Figure 5.4 and included for reference. Figures represent average values ± SEM, for > 675 DCs from at least three independent experiments per condition. Statistical significance calculated with single factor ANOVA and post hoc Tukey test. Indicates significant difference compared to WT DCs. *$p<0.05$, **$p<0.01$

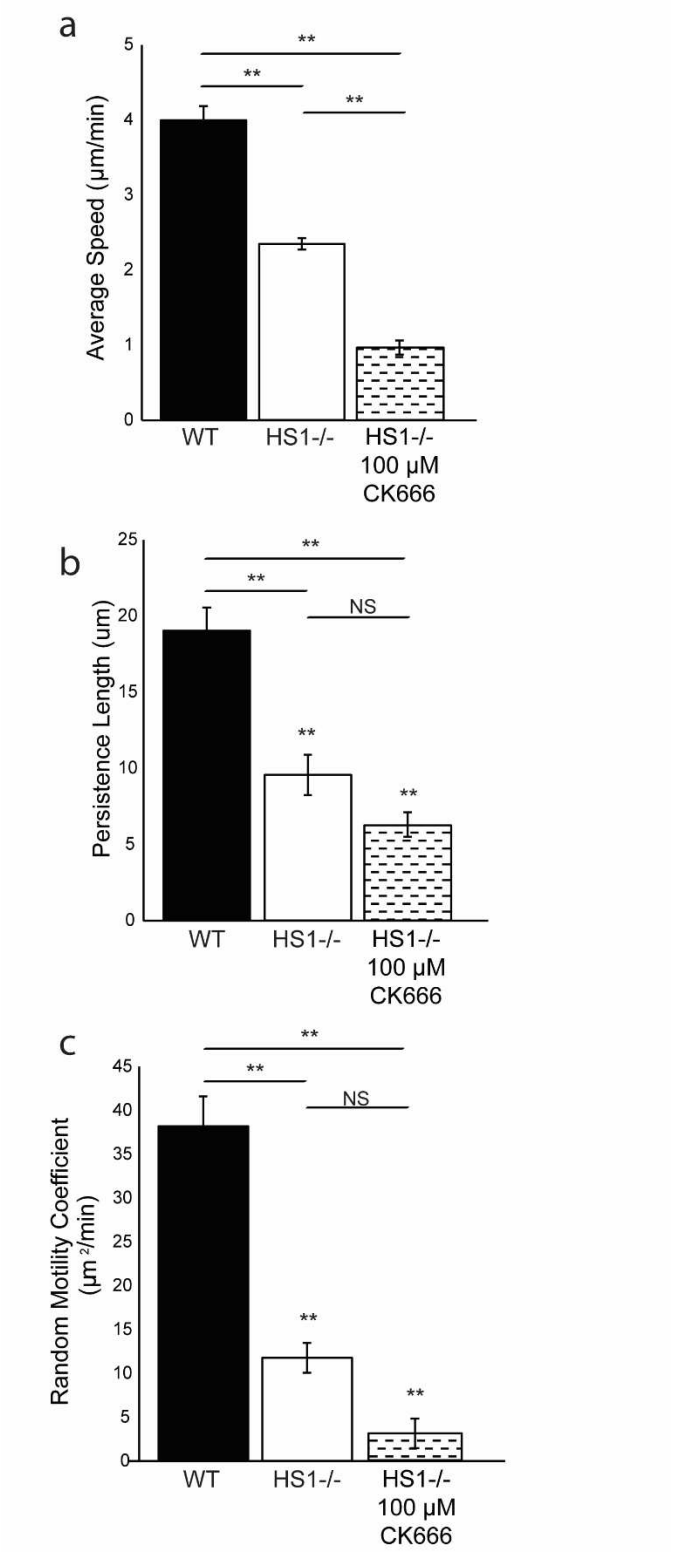


*Figure 5.7. Quantification of HS1 -/- DC chemokinesis in the presence and absence of CK-666*

(A) average speed, (B) persistence length and (C) random motility coefficient (WT and HS1 values taken from Figure 5.4 and included for reference). Figures represent average values ± SEM, for > 1000 DCs from at least three independent experiments per condition. Statistical significance calculated with single factor ANOVA and post hoc Tukey test. Indicates significant difference compared to WT DCs. *$p<0.05$, **$p<0.01$

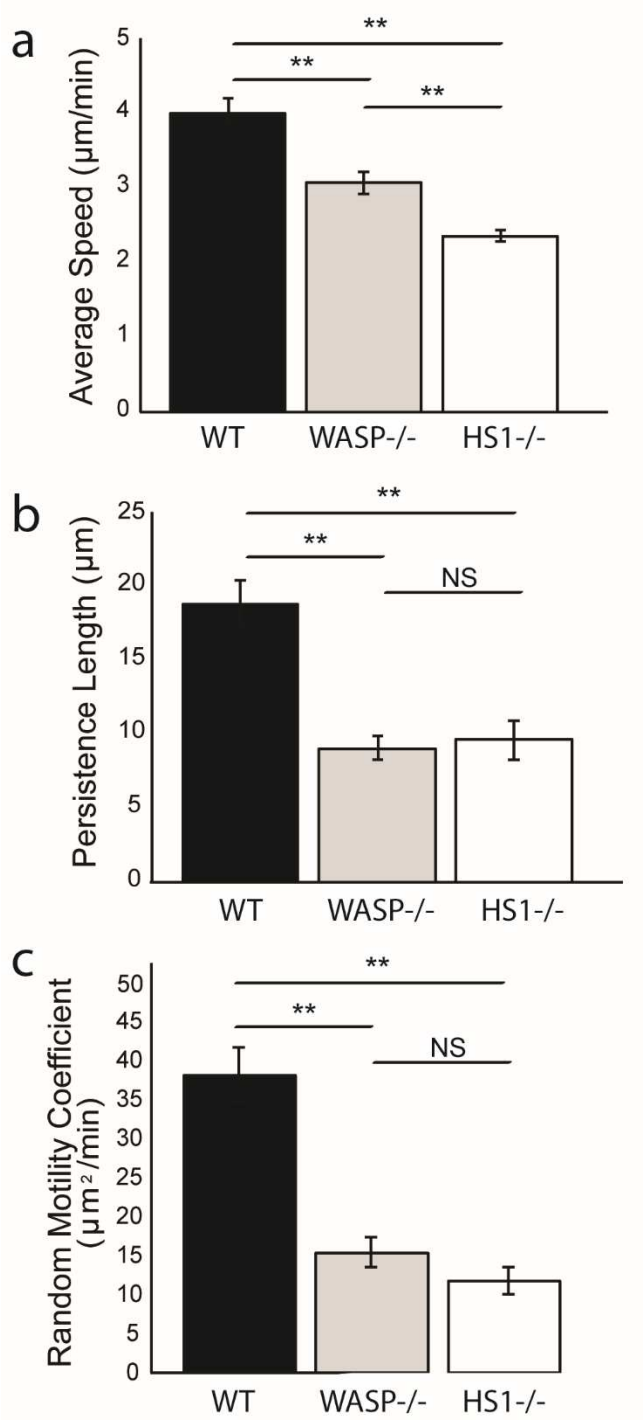


*Figure 5.8. Comparison of chemokinesis of DCs lacking WASP and HS1*

(A) average speed, (B) persistence length and (C) random motility coefficient. WASP $^{-/-}$ DCs are shown in gray. WT DCs are shown in blue and HS1 $^{-/-}$ DCs are shown in red (WT and HS1 values taken from Figure 5.4 and included for reference). Figures

represent average values ± SEM, for > 1000 DCs from at least three independent experiments per condition. Statistical significance calculated with single factor ANOVA and post hoc Tukey test. *$p<0.05$, **$p<0.01$

As with HS1 $^{-/-}$ DCs, WASP $^{-/-}$ DCs had no significant reduction in persistence time. Since HS1 and WASP have similar but non-redundant functions within the cell, it is not surprising that I observe similar but non-identical results after their knockout.

*HS1 is Required for Maximal Dendritic Cell Force Generation*

Previous work from my group has shown that inhibition of actin polymerization results in a drastic reduction in magnitude of DC traction forces (48). In that study, I used a nonspecific actin polymerization inhibitor, and it is unknown how individual actin-binding proteins are involved in DC force production. In the present study, I wanted to determine whether HS1 is involved in force generation. In the preceding sections, I have highlighted the impact of HS1 on the kinematics of DC migration. Since cell migration and force generation are intimately linked processes, I expected the impact of HS1 on random migration to correlate with a reduction in traction force strength (49). I also posited that a defect in HS1 $^{-/-}$ DC force generation would be a direct result of its interaction with the Arp2/3 complex, and would therefore extend to other proteins interacting with the Arp2/3 complex, such as WASP.

To test this hypothesis, I used micropost array detectors (mPADs) to measure the forces exerted by WT, HS1 $^{-/-}$ and WASP $^{-/-}$ DCs during chemokinesis. mPADs are arrays of elastic micropillars which are sensitive enough to measure the weak forces exerted by DCs and other amoeboid cell types (50). I used a 10:1 solution of PDMS to replica mold mPADs from silicon master molds. Before adding cells to the mPADs, I stamped the post tips with bovine fibronectin, and stained them with a lipophilic dye in order to visualize post deflection. The mPADs were also blocked with Pluronic F127 to ensure

that the cells were interacting with the post tips and not with the sides of the posts or interpost regions. I added DCs to the mPADs at a concentration of 50,000 cells/mL along with 10 nM CCL19, and allowed the cells to settle on the posts before imaging. A series of fluorescence and phase images were captured in order to record post deflections and cell position over time. A representative cell imaged in phase and fluorescence is shown in Figure 5.9A and B. The arrow in Figure 5.9B points to the location of the cell, where post deflections were observed and quantified.

Individual traction forces were calculated using a custom MATLAB code that converted post deflections into vector forces using Hooke's law, given the spring constant for the array (1.92 nN/μm). I then calculated the total force per cell, as the sum of all the scalar forces exerted on the posts by a given DC. Since there was considerable variation within each population of cells, I chose to compute an ensemble average as a function of time (Figure 5.9C). WT DCs produced traction forces on the order of 10 nN/cell, which agrees well with my previous measurements (48). I saw an initial rise in WT traction forces, followed by a plateau. I hypothesize that this initial rise in force is due to imaging shortly after adding the cells, before they had a chance to fully engage the post array. Both WASP $^{-/-}$ DCs and HS1 $^{-/-}$ DCs are capable of interacting with the mPAD array, but their force generation appeared to be lower than what I observed in WT cells.

I next performed a time and ensemble average for all three populations of DCs (Figure 5.9D). Compared to WT DCs, WASP $^{-/-}$ and HS1 $^{-/-}$ DCs produced significantly less force per cell. WT DCs produced an average force of 13.76 ± 0.84 nN/cell, whereas WASP $^{-/-}$ DCs produced an average force of 9.55 ± 0.69 nN/cell and HS1 $^{-/-}$ DCs

produced an average force of 3.96 ± 0.40 nN/cell. The force generation was most affected in HS1 $^{-/-}$ DCs, whose forces were more than 3 times lower than WT forces. While WASP $^{-/-}$ DCs produced significantly less force than WT DCs, they produced significantly greater force than HS1 $^{-/-}$ DCs. These results show

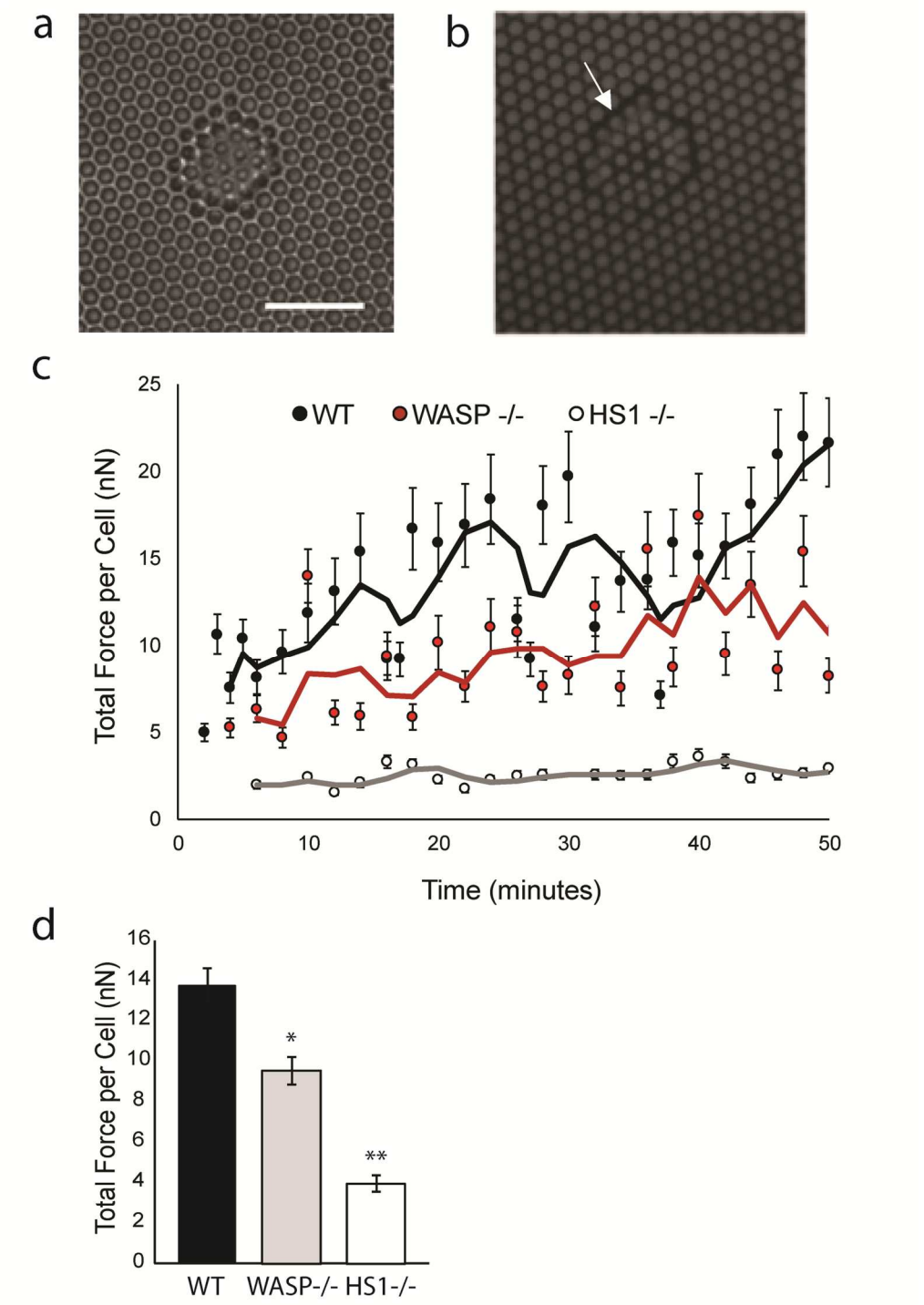


*Figure 5.9. Calculation of DC traction forces using mPADs.*

(A) Phase contrast image of DC on mPAD surface. Scale bar equals 20 μm. Fluorescent and phase images correspond to same cell and same position. (B) Sample image of fluorescent micropost tips in area occupied by DC. Post diameter and height are 1.83 μm

and 12.9 μm, respectively. (C). Average traction forces for ensemble of WT DCs, HS1 $^{-/-}$ DCs and WASP $^{-/-}$ DCs. The forces were calculated from images such as those shown in (A) and (B). Displacement of mPADs was converted to traction force using Hooke's law and known spring constant (1.92 nN/μm) for the mPAD array. The x-axis indicates time in minutes, with 0 corresponding to the start of imaging. Lines indicate 3 point moving averages for each condition. (D) Time and ensemble averages of DC traction forces, corresponding to values shown in (C). Figures represent average values ± SEM, for at least 28 DCs per condition. Statistical significance calculated with single factor ANOVA and post hoc Tukey test. Indicates significant difference compared to WT DCs. *$p<0.05$, **$p<0.01$

that both WASP and HS1 are involved in the DC force transduction pathway, but that HS1 is more important for force generation than WASP.

DISCUSSION

Due to the importance of DC migration and the involvement of the actin cytoskeleton in this process (8), I sought to identify whether the actin regulatory protein HS1 is required for DC random migration and force generation. I used microcontact printed PDMS coverslips to assess random migration and mPADs to measure cellular traction forces. I found that HS1 contributed to random migration through its effect on speed but not persistence time. HS1 $^{-/-}$ DCs migrate more slowly, and often fail to translocate over a 3 hour period, leading to a reduction in area explored during migration. One of the ways that HS1 interacts with actin is through activation of the Arp2/3 complex. This interaction appears to be important in DCs, as inhibition of the Arp2/3 complex in WT DCs or elimination of other Arp2/3 complex nucleating proteins led to similar reductions in migration. Migration and force generation are often intimately linked and I observed a concomitant reduction in force generation in HS1 $^{-/-}$ DCs along with defects in migration. Interestingly, while migration seems to have a general dependence on the Arp2/3 complex, force generation is affected to a different degree by different Arp2/3 complex activators. Since DCs need to migrate quickly and efficiently to the lymph nodes to launch an adaptive immune response (7), it is possible that defects in the Arp2/3 complex, HS1 or other similar proteins could lead to immune dysregulation. This is indeed the case for mutated WASP, which leads to the X-linked autoimmune disease Wiskott-Aldrich syndrome (WAS) (38,39). WAS leads to complete immune system dysregulation (reviewed in (40)) and is characterized by thrombocytopenia, easy bruising, frequent and prolonged bleeding, eczema and recurrent infections (41). To date, abnormalities in HS1 have been associated with both chronic

lymphocytic leukemia (51) and systemic lupus erythematosus, (52) and it is possible that HS1 will be linked to more diseases in the future.

Two parameters that describe DC random migration are cell speed and cell persistence. In DCs, I saw that HS1 does not affect the persistence time, or frequency of turning. It does, however, contribute a great deal to the speed of migration. HS1 is the hematopoietic homologue of the more widely studied NPF cortactin (19). Many of the migration results that I observe in HS1 $^{-/-}$ DCs mirror what is seen in cells expressing reduced levels of cortactin (53). Cortactin, unlike WASP or other NPFs, has the unique ability to stabilize actin branch points and prevent disassembly (54,55). I hypothesize that this stabilizing effect is responsible for the reduction in speed I observe in HS1 $^{-/-}$ DCs. WASP is still present in these cells, allowing Arp2/3 complex branch points to form, but without HS1 holding the branch point together, the structure disassembles too quickly for a cell to gain much speed.

I saw that HS1 and WASP play a role in DC random migration to different degrees. One of the first differences I observed was the extent of reduction in average speed for each type of cell. Both HS1 and WASP $^{-/-}$ DCs move more slowly, but WASP $^{-/-}$ DCs were significantly faster than HS1 $^{-/-}$ DCs. These disparate results could be explained by differences between the two proteins. WASP is a class I NPF, with a VCA domain that binds to monomeric actin and the Arp2/3 complex, while HS1 is a class II NPF with an NTA domain that binds to polymerized F actin and the Arp2/3 complex (24). Class I NPFs like WASP are thought to initiate Arp2/3 complex-mediated actin polymerization by bringing monomeric G-actin in close proximity to the Arp2/3 complex, while Class II NPFs like HS1 are thought stabilize a pre-formed branch point

by binding to both F-actin and the Arp2/3 complex. There are multiple class I NPFs in hematopoietic cells, but HS1 is the only known Class II NPF. Perhaps the speed is not affected as much in WASP $^{-/-}$ DCs due to Class I NPF redundancy, whereas elimination of HS1 rids the cell of all stabilizing Class II NPFs. Another possibility could be related to differences in downstream binding partners of the two proteins.

I expected to see similar force reductions in WASP and HS1 $^{-/-}$ DCs, since they are both known to play a role in adhesive structures, such as podosomes (23). Furthermore, the Arp2/3 complex, which is activated by both HS1 and WASP, has been shown to transiently associate with vinculin in focal complex like structures (49). Interestingly, I saw much smaller forces in HS1 $^{-/-}$ DCs than in WASP $^{-/-}$ DCs. This difference could again be explained by the slight differences in function of the two proteins. Since HS1 $^{-/-}$ DCs have unstable branched actin networks, it is possible that their actin networks disassemble before they are able to generate substantial force. It has also been shown that reducing levels of cortactin inhibits the assembly of adhesion structures (53), whereas loss of WASP $^{-/-}$ seemingly has no effect on integrin organization (6). Therefore, it is possible that adhesion and force generation are influenced by Class II NPFs (i.e. HS1) more strongly than they are by Class I NPFs (i.e. WASP).

In this study, I used CK-666 to identify whether the migration effects seen in HS1 $^{-/-}$ DCs were due to HS1's ability to activate and stabilize Arp2/3 complex mediated actin polymerization. CK-666 is a potent inhibitor of the Arp2/3 complex, with an $IC_{50}$ of 17 μM and 4 μM, for bovine and human Arp2/3 complex, respectively (56). I chose a range of concentrations surrounding these $IC_{50}$ values (1 μM, 10 μM and 100 μM), since I expected the $IC_{50}$ for murine Arp2/3 complex to lie somewhere in this range. Previous

cytotoxicity studies have indicated that concentrations up to 200 μM CK-666 with incubation times similar to ours did not negatively impact cell viability (57). I saw a graded decrease in migration as more CK-666 was added to DCs, with the highest concentration (100 μM) approximating the behavior of HS1 $^{-/-}$ DCs. I still saw low levels of migration, even at high levels of inhibitor, which is likely due to incomplete inhibition of cellular Arp2/3 complex. While the speed of HS1 $^{-/-}$ DCs is further decreased upon Arp2/3 complex inhibition, the persistence length and random motility coefficient are unaffected. Removing HS1 from DCs greatly reduces Arp2/3 complex activity without completely eliminating its ability to polymerize actin. When inhibitor is added, the remaining Arp2/3 complex activity is further reduced.

In combination with previous studies, this work reveals that HS1 is involved in various aspects of DC migration. Klos Dehring et al. showed that during chemotaxis, DCs lacking HS1 form highly dynamic lamellipodia, move well through transwells and travel through microfluidic devices with lower directionality and higher speed (23). This description of overly dynamic, unstable lamellipodia agrees well with my observations that HS1 $^{-/-}$ DCs form extensive membrane ruffles during chemokinesis and are often observed to quickly vacillate around fixed points. This suggests that new branched actin structures are actively being formed, but due to the loss of HS1, and the resultant instability of the actin network, they are often too inefficient to allow for DC translocation. During chemotaxis, HS1 $^{-/-}$ DCs are less able to migrate persistently up a gradient than WT DCs (23). Since chemokine receptor expression is unaltered by HS1 removal, and endpoint studies of HS1 $^{-/-}$ DCs show that they are able to properly respond to a gradient (transwell), this defect in directional persistence is likely due to instability

and not chemokine responsiveness (23). It is possible that HS1 $^{-/-}$ DCs, are unable to maintain protrusive actin structures at the front of the cell while traveling up a gradient. Dynamic lamellipodial protrusions at other areas of the cell body may lead to deviations in directionality. These deviations would then be corrected upon additional chemokine signaling, but the inherent actin instability would lead to more frequent missteps and lower observed persistence in HS1 $^{-/-}$ DCs. In my chemokinesis experiments, I observed no significant differences in persistence time. While this may seem contradictory, DCs behave quite differently in chemokinesis and chemotaxis. In chemokinesis, DC motion is completely random, whereas in chemotaxis, DCs are guided in a specific direction. Klos Dehring et al. showed that DCs seemed to have a higher propensity for deviations from directed migration, and in essence moved more randomly than their WT counterparts (23). Therefore, it is quite possible that in a scenario where DCs are being encouraged to migrate randomly, HS1$^{-/-}$ DCs will do so as efficiently as WT DCs.

Another major difference between my study and the work of Klos Dehring et al. is the effect of HS1 on cell speed. Klos Dehring et al observe a significant increase in speed during chemotaxis (23), while I observed a significant decrease during chemokinesis. While it is clear that HS1$^{-/-}$ DCs migrate towards a chemokine gradient during chemotaxis, the spread of HS1$^{-/-}$ DC trajectories is not identical to the spread of WT DCs trajectories (23). The cell tracks for WT DCs traveling towards a gradient in the y-direction are symmetric about the y-axis (23). However, the cell tracks for HS1$^{-/-}$ DCs traveling towards a gradient in the y-direction are biased towards the positive x-direction (23). The directional bias seen in HS1$^{-/-}$ DCs could be due to an increased susceptibility to flow in the microfluidic gradient generator. Therefore, it is possible that

the increase in HS1$^{-/-}$ DC speed during chemotaxis is due the cells being more easily pushed along by flow in the system. This is quite likely given the effect of HS1 on DC adhesive strength (defective podosomes in immature HS1-/- DCs (23) and significantly reduced traction forces in mature HS1$^{-/-}$ DCs). In the present study, I observed a significant decrease in speed, in an environment free of flow and directional cues. Therefore, it is possible that innate, random migratory speed is impaired in HS1$^{-/-}$ DCs when they are not presented with any additional stimuli, but that reductions in adhesion and subsequent susceptibility to flow could help DCs to compensate for defects in speed during chemotaxis.

While I found the Arp2/3 complex to be important for DC random migration on 2D surfaces, it appears to be dispensable for other forms of migration. Recently Vargas et al. showed that Arp2/3 complex inhibition had no effect on DC chemotaxis in confinement (58). DCs in confined channels did not form leading edge branched actin networks but instead had extensive actin cables at the cell rear. This finding does not negate my findings, since many of the experimental variables were different between their study and ours. Rather, this suggests that DCs can employ multiple methods of migration based on the characteristics of their microenvironment.

ACKNOWLEDGEMENTS

This work was supported by NIH GM104287. ACB acknowledges support from the NSF GRFP under Grant No. DGE-1321851. HS1 $^{-/-}$ DCs transduced with GFP Life-act were kindly provided by Daniel Blumenthal.

REFERENCES


1. Bendell AC, Williamson EK, Chen CS, Burkhardt JK, Hammer DA. The Arp 2/3 Complex Binding Protein HS1 is Required for Dendritic Cell Random Migration and Force Generation. J Integr Biol. 2017;Accepted.
2. Banchereau J, Briere F, Caux C, Davoust J, Lebecque S, Liu Y, et al. Immunobiology of Dendritic Cells. Annu RevImmunology. 2000;18:767–811.
3. Steinman RM. The Dendritic Cell System and Its Role in Immunogenicity. Annu RevImmunology. 1991;9:271–96.
4. Watts C, Amigorena S. Antigen traffic pathways in dendritic cells. Traffic [Internet]. 2000;1(4):312–7. Available from: http://www.ncbi.nlm.nih.gov/pubmed/11208116
5. Reis e Sousa C, Sher A, Kaye P. The role of dendritic cells in the induction and regulation immunity to microbial infection. Curr Opin Immunol. 1999;11:392–9.
6. Burns S, Hardy SJ, Buddle J, Yong KL, Jones GE, Thrasher AJ. Maturation of DC Is Associated with Changes in Motile Characteristics and Adherence. Cell Motil Cytoskeleton. 2004;57(October 2003):118–32.
7. Alvarez D, Vollmann EH, von Andrian UH. Mechanisms and consequences of dendritic cell migration. Immunity [Internet]. 2008;29(3):325–42. Available from: http://www.ncbi.nlm.nih.gov/pubmed/18799141
8. Pollard TD, Borisy GG. Cellular motility driven by assembly and disassembly of actin filaments. Cell [Internet]. 2003;112(4):453–65. Available from: http://www.ncbi.nlm.nih.gov/pubmed/12600310
9. Lauffenburger DA, Horwitz AF. Cell migration: A physically integrated molecular

process. Cell. 1996;84(3):359–69.

10. Abraham VC, Krishnamurthi V, Taylor DL, Lanni F. The actin-based nanomachine at the leading edge of migrating cells. Biophys J. 1999;77(3):1721–32.

11. Suraneni P, Rubinstein B, Unruh JR, Durnin M, Hanein D, Li R. The Arp2/3 complex is required for lamellipodia extension and directional fibroblast cell migration. J Cell Biol [Internet]. 2012;197(2):239–51. Available from: http://www.jcb.org/cgi/doi/10.1083/jcb.201112113

12. Bailly M, Ichetovkin I, Grant W, Zebda N, Machesky LM, Segall JE, et al. The F-actin side binding activity of the Arp2/3 complex is essential for actin nucleation and lamellipod extension. Curr Biol [Internet]. 2001;11(8):620–5. Available from: http://www.sciencedirect.com/science?_ob=ArticleURL&_udi=B6VRT-430G2NG-Y&_user=501045&_coverDate=04/17/2001&_rdoc=1&_fmt=high&_orig=gateway&_origin=gateway&_sort=d&_docanchor=&view=c&_acct=C000022659&_version=1&_urlVersion=0&_userid=501045&md5=35f97e5ebec

13. Mullins RD, Heuser JA, Pollard TD. The interaction of Arp2/3 complex with actin: nucleation, high affinity pointed end capping, and formation of branching networks of filaments. Proc Natl Acad Sci U S A. 1998;95(11):6181–6.

14. Yarar D, To W, Abo A, Welch MD. The Wiskott–Aldrich syndrome protein directs actin-based motility by stimulating actin nucleation with the Arp2/3 complex. Curr Biol [Internet]. 1999;9(10):555-S1. Available from: http://www.sciencedirect.com/science/article/pii/S0960982299802437

15. Uruno T, Zhang P, Liu J, Hao J-J, Zhan X. Haematopoietic lineage cell-specific protein 1 (HS1) promotes actin-related protein (Arp) 2/3 complex-mediated actin polymerization. Biochem J [Internet]. 2003;371(Pt 2):485–93. Available from: http://www.ncbi.nlm.nih.gov/pmc/articles/PMC1223309/

16. Uruno T, Liu J, Zhang P, Fan Yx, Egile C, Li R, et al. Activation of Arp2/3 complex-mediated actin polymerization by cortactin. Nat Cell Biol. 2001;3(3):259–66.

17. Takemoto Y, Furuta M, Li XK, Strong-Sparks WJ, Hashimoto Y. LckBP1, a proline-rich protein expressed in haematopoietic lineage cells, directly associates with the SH3 domain of protein tyrosine kinase p56lck. EMBO J. 1995;14(14):3403–14.

18. Kitamura D, Kaneko H, Miyagoe Y, Ariyasu T, Watanabe T. Isolation and characterization of a novel human gene expressed specifically in the cells of hematopoietic lineage. Nucleic Acids Res [Internet]. 1989;17(22):9367–79. Available from: http://www.ncbi.nlm.nih.gov/pmc/articles/PMC335138/

19. Zhan X, Hu X, Hampton B, Burgess WH, Friesel R, Maciag T. Murine cortactin is phosphorylated in response to fibroblast growth factor-1 on tyrosine residues late in the G1 phase of the BALB/c 3T3 cell cycle. J Biol Chem. 1993;268(32):24427–31.

20. Hao JJ, Zhu J, Zhou K, Smith N, Zhan X. The coiled-coil domain is required for HS1 to bind to F-actin and activate Arp2/3 complex. J Biol Chem. 2005;280(45):37988–94.

21. Gomez TS, McCarney SD, Carrizosa E, Labno CM, Comiskey EO, Nolz JC, et al.

HS1 Functions as an Essential Actin-Regulatory Adaptor Protein at the Immune Synapse. Immunity [Internet]. 2006;24(6):741–52. Available from: http://www.sciencedirect.com/science/article/pii/S1074761306002603

22. Muzio M, Scielzo C, Frenquelli M, Bachi A, De Palma M, Alessio M, et al. HS1 complexes with cytoskeleton adapters in normal and malignant chronic lymphocytic leukemia B cells. Leukemia [Internet]. 2007;21(9):2067–70. Available from: http://dx.doi.org/10.1038/sj.leu.2404744

23. Dehring DAK, Clarke F, Ricart BG, Huang Y, Gomez TS, Williamson EK, et al. Hematopoietic Lineage Cell-Specific Protein 1 Functions in Concert with the Wiskott–Aldrich Syndrome Protein To Promote Podosome Array Organization and Chemotaxis in Dendritic Cells. J Immunol [Internet]. 2011;186(8):4805–18. Available from: http://www.ncbi.nlm.nih.gov/pmc/articles/PMC3467106/

24. Goley ED, Welch MD. The ARP2/3 complex: an actin nucleator comes of age. Nat Rev Mol Cell Biol [Internet]. 2006;7(10):713–26. Available from: http://www.nature.com/doifinder/10.1038/nrm2026

25. Huang Y, Biswas C, Dehring DAK, Sriram U, Williamson EK, Li S, et al. The actin regulatory protein HS1 is required for antigen uptake and presentation by dendritic cells. J Immunol [Internet]. 2011;187(11):5952–63. Available from: http://www.ncbi.nlm.nih.gov/pmc/articles/PMC3221870/

26. Snapper SB, Meelu P, Nguyen D, Stockton BM, Bozza P, Alt FW, et al. WASP deficiency leads to global defects of directed leukocyte migration in vitro and in vivo. J Leukoc Biol. 2005;77(June):993–8.

27. Taniuchi I, Kitamura D, Maekawa Y, Fukuda T, Kishi H, Watanabe T. Antigen-

receptor induced clonal expansion and deletion of lymphocytes are impaired in mice lacking HS1 protein, a substrate of the antigen-receptor-coupled tyrosine kinases. EMBO J [Internet]. 1995;14(15):3664–78. Available from: http://www.ncbi.nlm.nih.gov/pmc/articles/PMC394441/

28. Sixt M, Lämmermann T. In Vitro Analysis of Chemotactic Leukocyte Migration in 3D Environments. In: Wells CM, Parsons M, editors. Cell Migration [Internet]. Humana Press; 2011. p. 149–65. Available from: http://dx.doi.org/10.1007/978-1-61779-207-6_11

29. Desai R a, Khan MK, Gopal SB, Chen CS. Subcellular spatial segregation of integrin subtypes by patterned multicomponent surfaces. Integr Biol (Camb). 2011;3(5):560–7.

30. Dunn GA. Characterising a kinesis response: time averaged measures of cell speed and directional persistence. [Internet]. Agents and actions. Supplements. 1983. p. 14–33. Available from: http://www.ncbi.nlm.nih.gov/pubmed/6573115

31. Henry SJ, Crocker JC, Hammer DA. Motile Human Neutrophils Sense Ligand Density Over Their Entire Contact Area. Ann Biomed Eng [Internet]. 2015; Available from: http://www.ncbi.nlm.nih.gov/pubmed/26219404

32. Yang MT, Fu J, Wang Y-K, Desai R a, Chen CS. Assaying stem cell mechanobiology on microfabricated elastomeric substrates with geometrically modulated rigidity. Nat Protoc [Internet]. Nature Publishing Group; 2011;6(2):187–213. Available from: http://www.nature.com/doifinder/10.1038/nprot.2010.189

33. Scielzo C, Bertilaccio MTS, Simonetti G, Dagklis A, ten Hacken E, Fazi C, et al.

HS1 has a central role in the trafficking and homing of leukemic B cells HS1 has a central role in the trafficking and homing of leukemic B cells. Blood. 2010;116(18):3537–46.

34. Cavnar PJ, Mogen K, Berthier E, Beebe DJ, Huttenlocher A. The Actin Regulatory Protein HS1 Interacts with Arp2/3 and Mediates Efficient Neutrophil Chemotaxis. J Biol Chem [Internet]. 9650 Rockville Pike, Bethesda, MD 20814, U.S.A.: American Society for Biochemistry and Molecular Biology; 2012;287(30):25466–77. Available from: http://www.ncbi.nlm.nih.gov/pmc/articles/PMC3408136/

35. Butler B, Kastendieck DH, Cooper JA. Differently phosphorylated forms of the cortactin homolog HS1 mediate distinct functions in natural killer cells. Nat Immunol [Internet]. Nature Publishing Group; 2008;9(8):887–97. Available from: http://dx.doi.org/10.1038/ni.1630

36. Lettau M, Kabelitz D, Janssen O. SDF1α-induced interaction of the adapter proteins Nck and HS1 facilitates actin polymerization and migration in T cells. Eur J Immunol [Internet]. 2015;45(2):551–61. Available from: http://doi.wiley.com/10.1002/eji.201444473

37. Mukherjee S, Kim J, Mooren OL, Shahan ST, Cohan M, Cooper J a. Role of Cortactin Homolog HS1 in Transendothelial Migration of Natural Killer Cells. PLoS One [Internet]. 2015;10(2):e0118153. Available from: http://dx.plos.org/10.1371/journal.pone.0118153

38. Hetrick B, Han MS, Helgeson L a, Nolen BJ. Small molecules CK-666 and CK-869 inhibit actin-related protein 2/3 complex by blocking an activating conformational change. Chem Biol [Internet]. Elsevier Ltd; 2013;20(5):701–12.

Available from:
http://www.sciencedirect.com/science/article/pii/S1074552113001245

39. Higgs HN, Blanchoin L, Pollard TD. Influence of the C terminus of Wiskott-Aldrich syndrome protein (WASp) and the Arp2/3 complex on actin polymerization. Biochemistry [Internet]. 1999;38(46):15212–22. Available from: http://www.ncbi.nlm.nih.gov/pubmed/10563804

40. Blanchoin L, Amann K, Higgs H, Marchand J, Kaiser D, Pollard T. Direct observation of dendritic actin complex and WASP / Scar proteins. Nature. 2000;171(1994):1007–11.

41. Binks M, Jones GE, Brickell PM, Kinnon C, Katz DR, Thrasher a J. Intrinsic dendritic cell abnormalities in Wiskott-Aldrich syndrome. Eur J Immunol [Internet]. 1998;28(10):3259–67. Available from: http://www.ncbi.nlm.nih.gov/pubmed/9808195

42. Burns S, Thrasher AJ, Blundell MP, Machesky LM, Jones GE. Configuration of human dendritic cell cytoskeleton by Rho GTPases, the WAS protein, and differentiation. Blood. 2001;98(4):1142–9.

43. Westerberg L, Wallin RP a, Greicius G, Ljunggren H-G, Severinson E. Efficient antigen presentation of soluble, but not particulate, antigen in the absence of Wiskott-Aldrich syndrome protein. Immunology [Internet]. 2003;109(3):384–91. Available from: http://www.pubmedcentral.nih.gov/articlerender.fcgi?artid=1782978&tool=pmcentrez&rendertype=abstract

44. Borg C, Abdelali J, Laderach D, Maruyama K, Wakasugi H, Charrier S, et al. NK

Cell Activation by Dendritic Cells (DC) Require The Formation of a Synapse leading to IL-12 Polarization in DC. Blood [Internet]. 2004;104(10):3267–76. Available from: http://www.ncbi.nlm.nih.gov/entrez/query.fcgi?cmd=Retrieve&db=PubMed&dopt=Citation&list_uids=15242871

45. Bouma G, Burns S, Thrasher AJ. Impaired T-cell priming in vivo resulting from dysfunction of WASp-deficient dendritic cells. Blood. 2007;110(13):4278–84.

46. Pulecio J, Tagliani E, Scholer A, Prete F, Fetler L, Burrone OR, et al. Expression of Wiskott-Aldrich syndrome protein in dendritic cells regulates synapse formation and activation of naive CD8+ T cells. J Immunol. 2008;181(2):1135–42.

47. de Noronha S, Hardy S, Sinclair J, Blundell MP, Strid J, Schulz O, et al. Impaired dendritic-cell homing in vivo in the absence of Wiskott-Aldrich syndrome protein. Blood [Internet]. 2005;105(4):1590–7. Available from: http://www.ncbi.nlm.nih.gov/pubmed/15494425

48. Ricart BG, Yang MT, Hunter C a., Chen CS, Hammer D a. Measuring traction forces of motile dendritic cells on micropost arrays. Biophys J [Internet]. Biophysical Society; 2011;101(11):2620–8. Available from: http://dx.doi.org/10.1016/j.bpj.2011.09.022

49. DeMali K a., Barlow C a., Burridge K. Recruitment of the Arp2/3 complex to vinculin: Coupling membrane protrusion to matrix adhesion. J Cell Biol. 2002;159(5):881–91.

50. Tan JL, Tien J, Pirone DM, Gray DS, Bhadriraju K, Chen CS. Cells lying on a bed of microneedles: an approach to isolate mechanical force. Proc Natl Acad Sci U S

A [Internet]. 2003;100(4):1484–9. Available from: http://www.pnas.org/content/100/4/1484.full

51. Frezzato F, Gattazzo C, Martini V, Trimarco V, Teramo A, Carraro S, et al. HS1, a lyn kinase substrate, is abnormally expressed in B-chronic lymphocytic leukemia and correlates with response to fludarabine-based regimen. PLoS One. 2012;7(6):1–11.

52. Sawabe T, Horiuchi T, Koga R, Tsukamoto H, Kojima T, Harashima S, et al. Aberrant HS1 molecule in a patient with systemic lupus erythematosus. Genes Immun. 2003;4(2):122–31.

53. Bryce NS, Clark ES, Leysath JL, Currie JD, Webb DJ, Weaver AM. Cortactin promotes cell motility by enhancing lamellipodial persistence. Curr Biol. 2005;15(14):1276–85.

54. Weaver AM, Karginov A V., Kinley AW, Weed S a., Li Y, Parsons JT, et al. Cortactin promotes and stabilizes Arp2/3-induced actin filament network formation. Curr Biol [Internet]. 2001;11(5):370–4. Available from: http://www.sciencedirect.com/science/article/pii/S0960982201000987

55. Egile C, Rouiller I, Xu XP, Volkmann N, Li R, Hanein D. Mechanism of filament nucleation and branch stability revealed by the structure of the Arp2/3 complex at actin branch junctions. PLoS Biol. 2005;3(11):1902–9.

56. Nolen BJ, Tomasevic N, Russell a, Pierce DW, Jia Z, McCormick CD, et al. Characterization of two classes of small molecule inhibitors of Arp2/3 complex. Nature [Internet]. Nature Publishing Group; 2009;460(7258):1031–4. Available from: http://dx.doi.org/10.1038/nature08231

57. Ilatovskaya D V, Chubinskiy-Nadezhdin V, Pavlov TS, Shuyskiy LS, Tomilin V, Palygin O, et al. Arp2/3 complex inhibitors adversely affect actin cytoskeleton remodeling i the cultured murine kidney collecting duct M-1 cells. Cell Tissue Res. 2013;354(3):783–92.

58. Vargas P, Maiuri P, Bretou M, Saez PJ, Pierobon P, Maurin M, et al. Innate control of actin nucleation determines two distinct migration behaviours in dendritic cells. Nat cell Biol. 15AD;18(1):43–53.

# CHAPTER 6 : CONCLUSIONS AND FUTURE WORK

SPECIFIC AIMS

The research presented in this thesis shows that I was able to characterize DC chemokinesis on PDMS surfaces and identify several key biophysical and biomolecular factors that regulate this process. The specific aims of this work were as follows:

Aim 1: Quantify DC chemokinesis on PDMS-coated coverslips and mPADs

Aim 2: Identify biophysical factors involved in regulating DC chemokinesis

Aim 3: Identify biomolecular factors required for efficient DC random migration

## SPECIFIC FINDINGS

### *DC Chemokinesis on PDMS Surfaces*

In Chapter 3, I thoroughly characterized DC random migration on PDMS-coated coverslips through calculation of the MSD, average speed, persistence time, persistence length and random motility coefficient. While the speed of DCs has been characterized on a variety of surfaces (1–3), the other parameters have only recently been measured (4). This is the first measurement of these values on PDMS-coated surfaces and my observations support the use of PDMS surfaces for the study of DC migration. Since many cell types behave differently on different surfaces (5), and past DC chemokinesis experiments were performed on glass (4), this work provides an important baseline for unperturbed DC chemokinesis on my engineered substrates. I found that fibronectin provides a good ECM protein for anchoring DCs to the substrate and that the protein could be readily transferred through microcontact printing. DC chemokinesis was stable across a variety of fibronectin and chemokine concentrations. My values for average speed agree well with other measurements in the literature, suggesting cellular speed is a very robust property of DC migration (2,6). Furthermore, my values for speed and persistence are inversely correlated and fit a well-established trend seen in a variety of cell types undergoing chemokinesis (7). Finally, I used mPADs to calculate traction forces of randomly migrating DCs. Previous DC force measurements were performed during chemotaxis, and this work provides the first in-depth analysis of the forces of random motility. Collectively these experiments provide a complete biomechanical description of DC chemokinesis

*Biophysical Components of DC Chemokinesis*

Up to this point, I have used two different substrates—PDMS-coated coverslips for quantification of random motility parameters and mPADs for traction force measurements. These two surfaces are quite different from one another in terms of both stiffness and geometry. It has been shown that the physical properties of the extracellular environment can affect a variety of cell properties (5). Of particular interest, it has been shown in other immune cells that stiffness and geometry can greatly impact cell migration (8–11). This topic had not been addressed in DCs and was the focus of the study described in Chapter 4. I began by asking ourselves how DC migration differed on the two surfaces (PDMS-coated coverslips and mPADs). I ran motility assays on mPADs instead of PDMS-coated coverslips and observed significant differences in migration. I next engineered multiple substrates to independently investigate the effects of stiffness and geometry on DC random migration. First, I used a series of different mPADs with different stiffnesses and identical 2D geometry and determined that DCs are insensitive to substrate stiffness. This also suggested to us that DC migration was influenced by geometry. To test this directly, I held stiffness constant while varying geometry of printed ligand on PDMS-coated coverslips. These experiments revealed that DC migration was nearly identical on patterned PDMS-coated coverslips and mPADs and confirmed my hypothesis that DC chemokinesis is regulated by substrate geometry. After these initial experiments, I performed a variety of small molecule inhibitor studies to identify the signaling pathways involved in geometry sensing. I identified three key pathways—organization of the actin cytoskeleton, myosin contractility and integrin engagement. Through this work, I provide the first description of how DCs respond to

environmental stiffness and geometry and highlight some of the key cell signaling molecules involved in this process.

*Biomolecular Components of DC Chemokinesis*

In Chapter 5, I investigated the specific contributions of two actin regulatory proteins to DC chemokinesis. It has long been understood that polarization of a cell's cytoskeleton is a crucial first step in locomotion (12). Two proteins involved in organization of actin at the leading edge are HS1 and WASP, which act with the Arp 2/3 complex to form branched actin networks (13). I quantified random motility of DCs lacking each of these proteins individually and determined that they are both critical for regulating cellular speed but had no effect on persistence. It seems likely to us that their influence on migration is mediated through their interaction with the Arp2/3 complex, as direct inhibition of this protein complex yielded similar defects in motility. While the importance of WASP in DCs has been clearly established, only two studies of HS1 deficient DCs exist (14–17). This study provides the first insight into how HS1 is involved in DC chemokinesis and complements previous findings of how WASP influences DC migration. I further characterized the random migration of HS1 $^{-/-}$ and WASP $^{-/-}$ DCs through quantification of traction forces. I found that both proteins contribute to the strength of DC interactions with their surroundings, but that HS1 is much more critical for this process than WASP. These are the first traction force measurements reported for HS1 and WASP deficient DCs. Overall, these experiments provide considerable insight into how DCs organize their cytoskeletal machinery and interact with their surroundings as they migrate.

# FUTURE WORK

## *Filopodial Control of Environmental Sensing and Directional Commitment*

A striking feature of dendritic cells is the intricate network of filopodial extensions at the cell periphery (Figure 6.1). Several studies have been performed to identify the importance of these structures in DCs, and it is widely accepted that they are involved in exploring the cell's environment. For example, filopodia seem to assist DCs in the lymph node as they search for cognate T cells, improving the ability of DCs to probe the surrounding cells and providing increased surface area for the formation of cell-cell contacts (18,19). It has also been shown in other cell types that filopodia interact with chemical and topographical signals in the microenvironment (20,21). My observations of migrating DCs seem to indicate that filopodia preferentially form at the front of the cell, but it has not been firmly established whether these structures are actively involved in DC directional decision making. Answering this question would greatly enhance my understanding of DC migration, particularly how DCs reorganize their migration machinery and make decisions about where they would like to go. I propose acquiring long time courses of migrating GFP-Lifeact DCs and computing a correlation coefficient for direction of motion and filopodial positions. If a correlation does exist, one could develop a model for predicting DC migration based on filopodial distribution. Another interesting component of this study would be determining the force profile of filopodia. In other cell types, it has been shown that adhesive structures exist along the base of filopodia (22). I have previously shown that the strongest traction forces in DCs during chemotaxis are concentrated at the leading edge (23). It would be

interesting to spatially resolve the force distribution at the leading edge to determine if these strong pulling forces occur under the cell body or the filopodia.

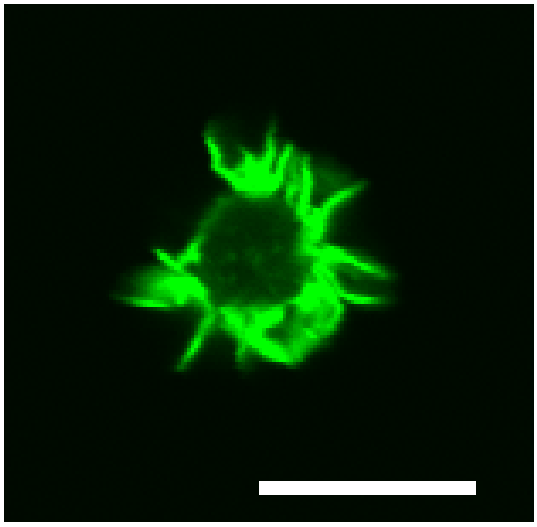

*Figure 6.1. DCs form numerous filopodia that extend from the plasma membrane*

Mature GFP-Lifeact DC. Scale bar equals 20 μm.

*Understanding the Biomechanics of Cell Turning*

Another interesting topic for future study would be understanding how DCs turn. While movement up a chemoattractant gradient plays an important role in DC function, DCs must also be able to reassess their surroundings and change direction. This process of changing directions or turning is quite physiologically relevant. For example, before DCs commit to a specific direction, they often dance around between two adjacent lymphatic vessels (24). This concept has also been recapitulated in vitro by studying competing chemokine gradients (3,25). Another example is random migration in the lymph nodes, in which DCs are constantly changing direction in their search for cognate T cells (19,26). Although the ability to change directions is important, the exact mechanisms through which DCs turn are unclear. While this is an interesting problem, it is technically challenging. A previous study by Liu et al. used a microfluidic approach to examine turning dynamics in a neutrophil-like cell line (27). One could use this approach with DCs, but they are weakly adherent and are subject to drift in the presence of even small amounts of flow. Therefore, I believe this experiment would be best carried out in a flow free environment. From these experiments one could determine how long it takes DCs to respond to a reversal in stimulus and the path a DC takes as it turns. One could imagine two possible scenarios for how a cell might turn. It could stop in its tracks and flip the front and rear with no actual displacement, or its front could remain its front the entire time as the whole cell follows a circuitous path to realign in the direction of attractant. Another component of this study would be determining the force distribution of a turning DC, which may shed some light on the internal reorganization that is occurring. The results discussed in Chapter 4 may be of some use for a study in cell

turning. Adding pattered surfaces (either mPADs or printed islands) would give the cells a stimulus for turning. The hierarchy between soluble chemoattractant and ligand patterning is unknown, and could also be an interesting avenue to explore.

*Quantifying Adhesive Strength and Organization of Podosomes on mPADs*

In all of the work discussed in this thesis I described the migration and force generation of mature DCs. I chose to use mature DCs because they are known to be more motile (28). While immature DCs are less motile, they do possess an interesting actin structure (the podosome), which is absent from mature DCs (29). Podosomes are composed of an actin rich core surrounded by a ring of adhesion molecules (30). The exact function of podosomes in DCs is not clear, but it has been suggested that they may play a role in adhesion, migration and mechanosensing (30,31). Because immature DCs contain these structures and mature DCs do not, I would expect the force profiles to be quite different depending on the maturation state of the DC. Ideally one would isolate the force per podosome, but depending on their distribution, it may be difficult to resolve using the standard DC force measurement setup (1.83 μm post diameter, 3 μm spacing). If resolution becomes an issue, I propose using the smaller diameter mPADs (800 nm diameter, 2 μm spacing). In Chapter 4 I showed that there were no differences in DC migration between these two mPADs. The effective spring constant of the two mPADs is also quite similar, so the compliance of either should be well suited to DC force measurement. Another interesting aspect of this study would be examining the actin structures in immature DCs on microposts. When mature DCs engage the microposts, I see the formation of artificial actin ring structures. These rings are unlike podosomes,

and are not found in mature DCs on continuous, printed surfaces. I hypothesize that these actin rings are involved in mechanosensing. However, in immature DCs, which already possess mechanosensing machinery in the form of podosome arrays, it is unknown how the cell's actin cytoskeleton will respond to the mPAD. It is possible that no rings will form, if the podosomes are sufficient for mechanosensing. It is also possible that podosomes will be replaced with these actin rings or some hybrid structure will be formed.

## FINAL THOUGHTS

Without dendritic cells, my immune systems would be in complete disarray. The importance of DCs in fighting disease and infection has led to their use in a variety of clinical trials as well as an FDA approved vaccine. Migration is essential for the function of DCs, and improper trafficking of DCs manifests itself in severe autoimmunity and an inability to fight off disease. As such, characterizing all aspects of DC migration is crucial to improving my understanding of immunity and perfecting future treatments. In this thesis, I build upon existing knowledge through the use of PDMS surfaces to characterize random migration and identify several key biomolecular and biophysical parameters. I hope that this work will motivate future scientists to continue uncovering new information about this complex and exciting cell type.

REFERENCES


1. Vargas P, Maiuri P, Bretou M, Saez PJ, Pierobon P, Maurin M, et al. Innate control of actin nucleation determines two distinct migration behaviours in dendritic cells. Nat Cell Biol. 2016;8(1):43–55.
2. Lämmermann T, Bader BL, Monkley SJ, Worbs T, Wedlich-Söldner R, Hirsch K, et al. Rapid leukocyte migration by integrin-independent flowing and squeezing. Nature [Internet]. 2008;453(7191):51–5. Available from: http://www.nature.com/doifinder/10.1038/nature06887%5Cnhttp://www.ncbi.nlm.nih.gov/pubmed/18451854
3. Ricart BG, John B, Lee D, Hunter CA, Hammer DA. Dendritic cells distinguish individual chemokine signals through CCR7 and CXCR4. J Immunol [Internet]. 2011;186(1):53–61. Available from: http://www.jimmunol.org/cgi/doi/10.4049/jimmunol.1002358
4. Ricart BG. Dendritic Cell Migration and Traction Force Generation in Engineered Microenvironments. University of Pennsylvania Scholarly Commons. 2010.
5. Charras G, Sahai E. Physical influences of the extracellular environment on cell migration. Nat Rev Mol Cell Biol [Internet]. Nature Publishing Group; 2014;15(12):813–24. Available from: http://dx.doi.org/10.1038/nrm3897%5Cn10.1038/nrm3897%5Cnhttp://www.nature.com/doifinder/10.1038/nrm3897%5Cnhttp://www.nature.com/doifinder/10.1038/nrm3897
6. Pulecio J, Tagliani E, Scholer A, Prete F, Fetler L, Burrone OR, et al. Expression of Wiskott-Aldrich syndrome protein in dendritic cells regulates synapse formation

and activation of naive CD8+ T cells. J Immunol. 2008;181(2):1135–42.

7. Lauffenburger DA, Linderman J. Receptors: Models for Binding, Trafficking, and Signaling. Oxford; 1996.

8. Hind LE, Dembo M, Hammer D a. Macrophage motility is driven by frontal-towing with a force magnitude dependent on substrate stiffness. Integr Biol [Internet]. Royal Society of Chemistry; 2015;7:447–53. Available from: http://xlink.rsc.org/?DOI=C4IB00260A

9. Mackay JL, Hammer DA. Integrative Biology through E-selectin but not P-selectin †. Integr Biol [Internet]. Royal Society of Chemistry; 2016;8:62–72. Available from: http://dx.doi.org/10.1039/C5IB00199D

10. Jannat RA, Dembo M, Hammer DA. Neutrophil adhesion and chemotaxis depend on substrate mechanics. J Phys Condens Matter. 2010;22(19):194117.

11. Henry SJ, Crocker JC, Hammer DA. Motile Human Neutrophils Sense Ligand Density Over Their Entire Contact Area. Ann Biomed Eng [Internet]. 2015; Available from: http://www.ncbi.nlm.nih.gov/pubmed/26219404

12. Pollard TD, Borisy GG. Cellular motility driven by assembly and disassembly of actin filaments. Cell [Internet]. 2003;112(4):453–65. Available from: http://www.ncbi.nlm.nih.gov/pubmed/12600310

13. Uruno T, Zhang P, Liu J, Hao J-J, Zhan X. Haematopoietic lineage cell-specific protein 1 (HS1) promotes actin-related protein (Arp) 2/3 complex-mediated actin polymerization. Biochem J [Internet]. 2003;371(Pt 2):485–93. Available from: http://www.ncbi.nlm.nih.gov/pmc/articles/PMC1223309/

14. Bouma G, Burns S, Thrasher AJ. Impaired T-cell priming in vivo resulting from

dysfunction of WASp-deficient dendritic cells. Blood. 2007;110(13):4278–84.

15. Bouma G, Mendoza-naranjo A, Blundell MP, Falco E De, Parsley KL, Burns SO, et al. Cytoskeletal remodeling mediated by WASp in dendritic cells is necessary for normal immune synapse formation and T cell priming. Blood. 2011;118(9):2492–501.

16. Dehring DAK, Clarke F, Ricart BG, Huang Y, Gomez TS, Williamson EK, et al. Hematopoietic Lineage Cell-Specific Protein 1 Functions in Concert with the Wiskott–Aldrich Syndrome Protein To Promote Podosome Array Organization and Chemotaxis in Dendritic Cells. J Immunol [Internet]. 2011;186(8):4805–18. Available from: http://www.ncbi.nlm.nih.gov/pmc/articles/PMC3467106/

17. Huang Y, Biswas C, Dehring DAK, Sriram U, Williamson EK, Li S, et al. The actin regulatory protein HS1 is required for antigen uptake and presentation by dendritic cells. J Immunol [Internet]. 2011;187(11):5952–63. Available from: http://www.ncbi.nlm.nih.gov/pmc/articles/PMC3221870/

18. Nikolic DS, Lehmann M, Felts R, Garcia E, Blanchet FP, Subramaniam S, et al. HIV-1 activates Cdc42 and induces membrane extensions in immature dendritic cells to facilitate cell-to-cell virus propagation. Blood. 2011;118(18):4841–52.

19. Miller MJ, Hejazi AS, Wei SH, Cahalan MD, Parker I. T cell repertoire scanning is promoted by dynamic dendritic cell behavior and random T cell motility in the lymph node. Proc Natl Acad Sci U S A [Internet]. 2004;101(4):998–1003. Available from: http://www.pubmedcentral.nih.gov/articlerender.fcgi?artid=327133&tool=pmcentrez&rendertype=abstract%5Cnhttp://www.ncbi.nlm.nih.gov/pubmed/14722354%5

Cnhttp://www.pubmedcentral.nih.gov/articlerender.fcgi?artid=PMC327133

20. Dalby MJ, Gadegaard N, Riehle MO, Wilkinson CDW, Curtis ASG. Investigating filopodia sensing using arrays of defined nano-pits down to 35 nm diameter in size. Int J Biochem Cell Biol. 2004;36(10):2015–25.

21. Mattila PK, Lappalainen P. Filopodia: molecular architecture and cellular functions. Nat Rev Mol Cell Biol [Internet]. 2008;9(6):446–54. Available from: http://www.nature.com/doifinder/10.1038/nrm2406

22. Schäfer C, Borm B, Born S, Möhl C, Eibl EM, Hoffmann B. One step ahead: Role of filopodia in adhesion formation during cell migration of keratinocytes. Exp Cell Res [Internet]. Elsevier Inc.; 2009;315(7):1212–24. Available from: http://dx.doi.org/10.1016/j.yexcr.2008.11.008

23. Ricart BG, Yang MT, Hunter C a., Chen CS, Hammer D a. Measuring traction forces of motile dendritic cells on micropost arrays. Biophys J [Internet]. Biophysical Society; 2011;101(11):2620–8. Available from: http://dx.doi.org/10.1016/j.bpj.2011.09.022

24. Weber M, Hauschild R, Schwarz J, Moussion C, de Vries I, Legler DF, et al. Interstitial dendritic cell guidance by haptotactic chemokine gradients. Sci (New York, NY) [Internet]. 2013;339(6117):328–32. Available from: http://www.sciencemag.org/content/339/6117/328.long%5Cnpapers://99cf836b-0208-4bf7-a35c-5506d5268000/Paper/p18255

25. Haessler U, Pisano M, Wu M, Swartz MA, Rakesh Jain by K. Dendritic cell chemotaxis in 3D under defined chemokine gradients reveals differential response to ligands CCL21 and CCL19. Proc Natl Acad Sci USA. 2011;108(14):5614–9.

26. Bousso P, Robey E. Dynamics of CD8+ T cell priming by dendritic cells in intact lymph nodes. Nat Immunol. 2003;4(6):579–85.

27. Liu Y, Sai J, Richmond A, Wikswo JP. Microfluidic switching system for analyzing chemotaxis responses of wortmannin-inhibited HL-60 cells. Biomed Microdevices. 2008;10(4):499–507.

28. Vargas P, Maiuri P, Bretou M, Saez PJ, Pierobon P, Maurin M, et al. Innate control of actin nucleation determines two distinct migration behaviours in dendritic cells. Nat cell Biol. 15AD;18(1):43–53.

29. Burns S, Hardy SJ, Buddle J, Yong KL, Jones GE, Thrasher AJ. Maturation of DC Is Associated with Changes in Motile Characteristics and Adherence. Cell Motil Cytoskeleton. 2004;57(October 2003):118–32.

30. Linder S. Podosomes at a glance. J Cell Sci [Internet]. 2005;118(10):2079–82. Available from: http://jcs.biologists.org/cgi/doi/10.1242/jcs.02390

31. Albiges-Rizo C, Destaing O, Fourcade B, Planus E, Block MR. Actin machinery and mechanosensitivity in invadopodia, podosomes and focal adhesions. J Cell Sci [Internet]. 2009;122(17):3037–49. Available from: http://jcs.biologists.org/cgi/doi/10.1242/jcs.052704